drones

MDPI

Article

Conceptual Development of Terminal Airspace Integration Procedures of Large Uncrewed Aircraft Systems at Non-Towered Airports †

Tim Felix Sievers [1,2,*], Jordan Sakakeeny [3,*], Husni Idris [3], Niklas Peinecke [1], Vishwanath Bulusu [4], Enno Nagel [1] and Devin Jack [5]

[1] Institute of Flight Guidance, German Aerospace Center (DLR), 38108 Braunschweig, Germany; niklas.peinecke@dlr.de (N.P.); enno.nagel@dlr.de (E.N.)
[2] Institute of Aeronautics and Astronautics, Technical University of Berlin, 10587 Berlin, Germany
[3] Aviation Systems Division, NASA Ames Research Center, Moffett Field, CA 94035, USA; husni.r.idris@nasa.gov
[4] Crown Innovations, Inc., NASA Ames Research Center, Moffett Field, CA 94035, USA; vishwanath.bulusu@nasa.gov
[5] Adaptive Aerospace Group, NASA Langley Research Center, Hampton, VA 23681, USA; devin.p.jack@nasa.gov
* Correspondence: tim.sievers@dlr.de (T.F.S.); jordan.a.sakakeeny@nasa.gov (J.S.)
† This paper is an extended version of our papers published in Sievers, T.F.; Peinecke, N. Navigating the Uncertain: Integrating Uncrewed Aircraft Systems at Airports in Uncontrolled Airspace. In Proceedings of the 2024 Integrated Communications, Navigation and Surveillance Conference (ICNS), Herndon, VA, USA, 23–25 April 2024, and in Sievers, T.F.; Sakakeeny, J.; Idris, H.; Peinecke, N.; Bulusu, V.; Nagel, E.; Jack, D. A Concept for Procedural Terminal Area Airspace Integration of Large Uncrewed Aircraft Systems at Non-Towered Airports. In Proceedings of the First US-Europe Air Transportation Research & Development Symposium (ATRDS2025), Prague, Czech Republic, 24–27 June 2025.

Highlights

What are the main findings?

- Analyzing the interaction of several quantitative measures (e.g., average traffic density, flight time, and flight distance) in different altitude bands provides an initial picture to structure crewed flight behavior at non-towered airports.
- Holding options above the airport traffic pattern may present feasible integration solutions for UAS, but holding altitudes vary significantly based on the airport's surrounding topography, airspace classes, present aircraft types, and crewed flight behavior.

What are the implications of the main findings?

- A variety of factors influence the development of an internationally harmonized "one size fits all" approach for UAS integration, including advancements related to UAS flight rules, DAA capabilities, and UAS traffic management solutions.
- The development of standards and regulations is crucial to derive "ideal" solutions for the integration of UAS, determining where, when, and how to integrate UAS with crewed traffic in and around traffic patterns of non-towered airports.

Abstract

Uncrewed aircraft systems are expected to revitalize traffic activities at under-utilized airports. These airports are often located in uncontrolled airspace and do not have an operating control tower to provide separation services for approaching aircraft. This presents unique challenges for the integration of uncrewed aircraft at non-towered airports. This paper offers a methodology to systematically assess traffic activities and quantify flight behaviors of crewed aircraft using historical flight data. To integrate uncrewed traffic in high-density traffic scenarios or during off-nominal flight situations, this paper assesses

check for updates

Academic Editor: Pablo Rodríguez-Gonzálvez

Received: 21 October 2025
Revised: 26 November 2025
Accepted: 27 November 2025
Published: 13 December 2025

Citation: Sievers, T.F.; Sakakeeny, J.; Idris, H.; Peinecke, N.; Bulusu, V.; Nagel, E.; Jack, D. Conceptual Development of Terminal Airspace Integration Procedures of Large Uncrewed Aircraft Systems at Non-Towered Airports. *Drones* **2025**, *9*, 858. https://doi.org/10.3390/drones9120858

the concept of a holding stack above the traffic pattern airspace to handle increased traffic uncertainty and to provide safe integration procedures. Twelve non-towered airport environments, relevant for initial uncrewed cargo operations across Germany, California, and Texas, are investigated to assess concept feasibility and real-world implementation. Based on the interaction of various quantitative measures, results are presented on the feasibility of holding stacks in the terminal airspace and the influence of crewed aircraft's historical flight behavior on different integration procedures for uncrewed aircraft. The analysis of various measures suggests that six airports are comparatively suitable candidates for holding layers above the airport traffic pattern, with holding altitudes to start between 2500 and 3500 feet above the ground.

Keywords: UAS; regional air mobility; non-towered airport; traffic pattern; holding stack

1. Introduction

Uncrewed Aircraft Systems (UAS) offer many benefits, such as flexible asset utilization, the ability for a Remote Pilot (RP) to operate one or more aircraft from anywhere, and improved economics compared to aircraft flying with an onboard pilot [1]. Among the many use cases enabled by this technology (e.g., firefighting, inspection work, and public safety), previous work has shown that the cargo use case in the Regional Air Mobility (RAM) realm is one of the most likely initial use cases for remotely piloted aircraft [2,3]. A significant proportion of current regional air cargo flights use airports without an operational control tower. Note that in this work, the more colloquial "non-towered" descriptor will be used to describe airports and airfields without an operational control tower. These non-towered airports are commonly located in uncontrolled airspace, and aircraft pilots following Visual Flight Rules (VFR) do not receive Air Traffic Control (ATC) separation services when approaching these airports. In addition, non-towered airports are expected to play an increasingly important role in future air mobility concepts [3,4]. Larger, fixed-wing regional cargo UAS with a Maximum Takeoff Weight (MTOW) of up to 25 tonnes (note that throughout the paper metric tonnes (t) are used as a weight measurement) are expected to take advantage of the less busy non-towered airports throughout the world [1].

In both Europe and the United States (US), thousands of non-towered airports are currently under-utilized [2,5,6]. They are expected to be leveraged as part of new and emerging air traffic concepts. However, it remains to be determined how UAS can be integrated at non-towered airports, given that crewed traffic behavior is less predictable compared to operations at towered airports [7]. Pilots under VFR individually decide how to integrate into the terminal airspace of non-towered airports based on ongoing traffic activities, wind conditions, and personal preferences. This variability makes the prediction of VFR traffic intent around non-towered airports more uncertain compared to operations under Instrument Flight Rules (IFR), which require filing a flight plan prior to their flight. Furthermore, there are limited data on operating schemes, traffic behaviors, and VFR intent prediction at non-towered airports [8]. Therefore, a common operating environment for large UAS flying under IFR or "new" flight rules will be needed in and around non-towered airports.

This research aims to answer the following questions:

- First, how could UAS be procedurally integrated into the terminal airspace of non-towered airports, especially with crewed aircraft in the airport vicinity?
- Second, how might crewed aircraft track history inform UAS flight planning and UAS procedural integration options at non-towered airports?

This work expands upon Refs. [9,10] and proposes a concept for procedural terminal airspace integration of large UAS at non-towered airports, whereby, where appropriate, a holding stack over the airport with different holding layers is implemented, providing the UAS with space in which to loiter when the traffic uncertainty in the terminal airspace exceeds a pre-determined threshold. In the holding stack, UAS could safely monitor ongoing terminal airspace activities of crewed aircraft before integrating into the standard Traffic Pattern (TP) of the airport. The exact means of this monitoring are outside the scope of this paper.

The paper will provide an overview of current crewed integration procedures and integration hurdles for UAS at non-towered airports in Section 2. Section 3 will propose the foundational concept of this paper, a holding stack concept for UAS in terminal airspaces to safely integrate UAS at non-towered airports. Accordingly, a methodology is introduced for systematically analyzing the terminal airspace of non-towered airports. Using that methodology, Section 4 will derive quantitative measures and assess historical crewed aircraft activities at twelve airports and discuss implications for potential UAS integration procedures. Section 5 presents the concluding remarks.

2. Background: Airborne Integration at Non-Towered Airports

This paper maintains a scope similar to the authors' previous work, as Germany, California, and Texas are considered to be regions with high potential relevant for the deployment of initial regional cargo UAS operations in Europe and the US [2]. UAS vehicle types, such as electric Vertical Takeoff and Landing (eVTOL) aircraft, are not explicitly out of scope for regional cargo UAS operations, though the focus is primarily on larger fixed-wing UAS (e.g., Cessna 208 Caravan retrofitted for uncrewed flights). UAS for regional cargo operations are likely to fall into the "certified" category, which is defined by the European Union Aviation Safety Agency (EASA) as operations with the highest safety risk and require certification of the UAS operator, the UAS, and the RP [11]. Note that there are currently no "certified" civilian UAS operations. It is assumed (see previous work [2]) that initial larger UAS operations are likely to replace current regional air cargo operations and that such operations will be "certified". Further, it is assumed that these UAS are only allowed to operate under IFR.

2.1. Current Terminal Airspace Integration Procedures of Crewed Aircraft

Current integration procedures for crewed aircraft at non-towered airports depend on a few important factors, namely the flight rules under which the aircraft is flying, the meteorological conditions, and the presence of an appropriate Instrument Approach Procedure (IAP) for the active runway end(s) [12]. Note that, although there may be slight differences between operations in the US and Germany, the general rules described herein apply to flights in both countries.

2.1.1. Flight Rules and Meteorological Conditions

The flight rules under which an aircraft is operating govern the flight. There are two main sets of flight rules: IFR and VFR. Under IFR, it is incumbent upon ATC to separate IFR aircraft from other IFR aircraft. In general, in the US, this separation is achieved at non-towered airports via the procedural paradigm of "one-in/one-out", whereby ATC will only clear one IFR aircraft into a terminal airspace at a time. Note that it is incumbent upon the pilot on board the aircraft flying under IFR to "see and avoid" and remain "well clear" of other traffic [13], especially aircraft operating under VFR. Under VFR, communication with ATC is generally not required, and the pilot on board must still "see and avoid".

If aircraft under IFR are allowed to approach a non-towered airport, they must generally follow published procedures and communicate their positions and intents at specific points in the airport's terminal airspace. In Germany, however, flights under IFR are not common in uncontrolled airspace. To accommodate IFR flights at non-towered airports, Germany has established Radio Mandatory Zones (RMZs) around 27 non-towered airports (including a heliport, Donauwoerth (EDPR)) out of 151 publicly accessible non-towered airports [2]. Typically, an RMZ covers the terminal airspace with a size of $\sim 10 \times 20$ km and extends from the ground up to 1000 ft ($\sim$300 m) Above Ground Level (AGL) to the above bordering controlled airspace Class E. Within an RMZ, all aircraft (flying under IFR or VFR) are required to establish a Very High Frequency (VHF) radio link to the ground and to listen to any communication on a designated RMZ radio frequency. Flight entries and exits must be communicated via the radio link. An entry or exit clearance by ATC is not required [14].

In addition to an RMZ, two German non-towered airports, Egelsbach (EDFE) and Magdeburg–Cochstedt (EDBC), operate an Aerodrome Traffic Zone (ATZ), and Egelsbach (EDFE) operates an additional Transponder Mandatory Zone (TMZ) to support IFR integration in uncontrolled airspace. An ATZ is established to allow only aircraft that intend to land or depart via specific routes to or from a non-towered airport. Additionally, a TMZ requires aircraft to carry an active transponder on board [14].

For IFR approaches at non-towered airports in the US as well as in Germany within a dedicated airspace environment, pilots must file a flight plan and follow an IAP. The IAP commonly consists of several three-dimensional Waypoints (WPs), which indicate the IFR flight route towards a runway end via an Initial Approach Fix (IAF) and Final Approach Fix (FAF) [12,14].

The two meteorological conditions, Visual Meteorological Conditions (VMC) and Instrument Meteorological Conditions (IMC), will also dictate which flight rules can be utilized. Under IMC, only flights operating under IFR are allowed. Under VMC, flights can operate under VFR or IFR, the latter assuming that the pilot is rated for IFR operations and the aircraft has the necessary equipment for IFR operations.

2.1.2. Integration of Crewed Aircraft Under IMC

At non-towered airports under IMC, the integration problem for an IFR aircraft is trivial, assuming the presence of an appropriate IAP. In the US, ATC will procedurally allow only one IFR aircraft at a time into the terminal environment, and VFR aircraft are not a concern, given that they may not operate under IMC. In this scenario, the crewed aircraft will fly the IAP down to the appropriate altitude, at which point the pilot on board visually identifies the runway and continues to land.

2.1.3. Integration of Crewed Aircraft Under VMC

At non-towered airports under VMC, however, the integration problem for an aircraft operating under IFR becomes significantly more complex, given the presence of VFR aircraft. The pilot on board an IFR aircraft must still "see and avoid" VFR aircraft in the vicinity; however, IFR traffic usually has no priority over VFR traffic in the TP. As soon as the IFR aircraft has entered the TP, it is subject to the same right-of-way rules as VFR traffic. Generally, the pilot of the IFR aircraft has three options: to continue under IFR using the IAP, to continue under IFR using a visual approach, or to cancel IFR and continue under VFR. According to verbal discussions with current regional air cargo pilots in the US, the second and third options are commonplace in their operations. For the second and third options, the pilot will then integrate into the non-towered terminal environment using the standard TP for the airport. The airport TP is located at an altitude above the

airport (typically 1000 ft (∼300 m) AGL [15]) that allows pilots to visually assess ongoing traffic activities before safely descending towards the airport runway.

The altitude of the TP and the TP integration procedures can vary for different airspace environments, depending on the airport layout, the surrounding topography of the airport and the individual skills and preferences of the pilot [14,15]. As seen in Figure 1, there are several methods of entry into a standard TP. Before a VFR pilot enters a TP, the pilot must be able to assess the traffic in the TP and in the vicinity, as well as the wind conditions. Ideally, the pilot should fly at an altitude above that of the non-towered airports TP so that the pilot does not interfere with airspace users entering the TP. TPs are usually flown at an altitude of 1000 ft (∼300 m) AGL counterclockwise at a distance of at least 1.5 km from the runway so that the left-seated pilot can keep the runway in view throughout the airport approach.

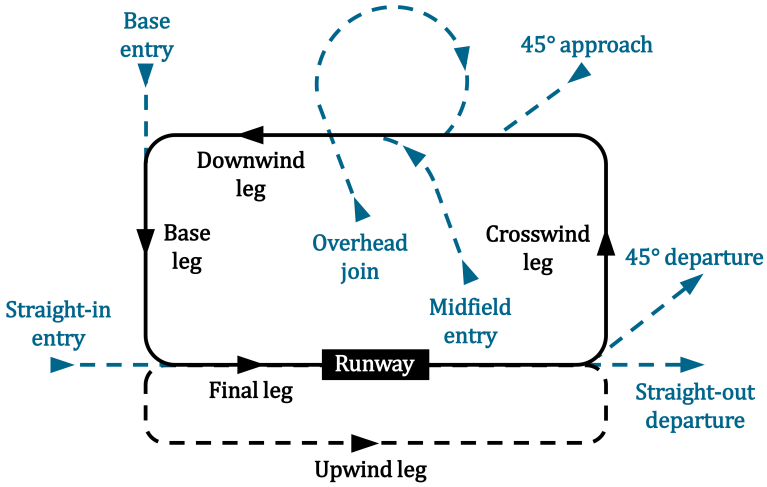

Figure 1. Standard airport TP scheme [16]; own depiction.

Although TPs have standardized TP legs, TP sizes can vary from airport to airport. Typically, VFR pilots enter the TP at the beginning of the downwind leg (e.g., via a 45° approach; see Figure 1) at the required TP altitude (TPA) with appropriate aircraft speed and flight heading, and descend steadily throughout the downwind leg, base leg, and final leg before landing the aircraft on the runway. If the pilot is unable to approach the runway during the base and final leg, the pilot usually flies upwind parallel to the runway and rejoins the downwind leg via the crosswind leg. As a general rule, the flight maneuver from the end of the downwind leg over the base leg to the final leg should take about one minute. In addition to the downwind entry of the TP, pilots can also fly directly into the base leg as part of a base entry or enter the final leg of the TP as part of a straight-in approach. Alternatively, midfield entries or overhead joins are also a possibility for pilots to integrate into the TP. In this case, if the pilot approaches from the upwind side, the pilot flies above the TP orthogonally to the runway (∼500–1000 ft (∼150–300 m) above the TPA) and joins the downwind leg directly or in the course of a loop [14,15].

The dimensions of the TP are usually not strictly defined and allow VFR pilots to make flexible adjustments depending on the conditions of the terminal airspace environment. Non-towered airport TPs offer a relatively high degree of flexibility for pilots, creating a dynamic airspace environment that is dependent on current air traffic, pilot skills and aircraft capabilities, wind conditions, and requirements such as those prescribed in a German Visual Operation Chart (VOC); see Figure 2. It can be concluded that the higher the VFR traffic volume in the airspace around a non-towered airport, the more unpredictable the pilot behavior and TP integration procedures, and the greater the overall uncertainty in the terminal airspace.

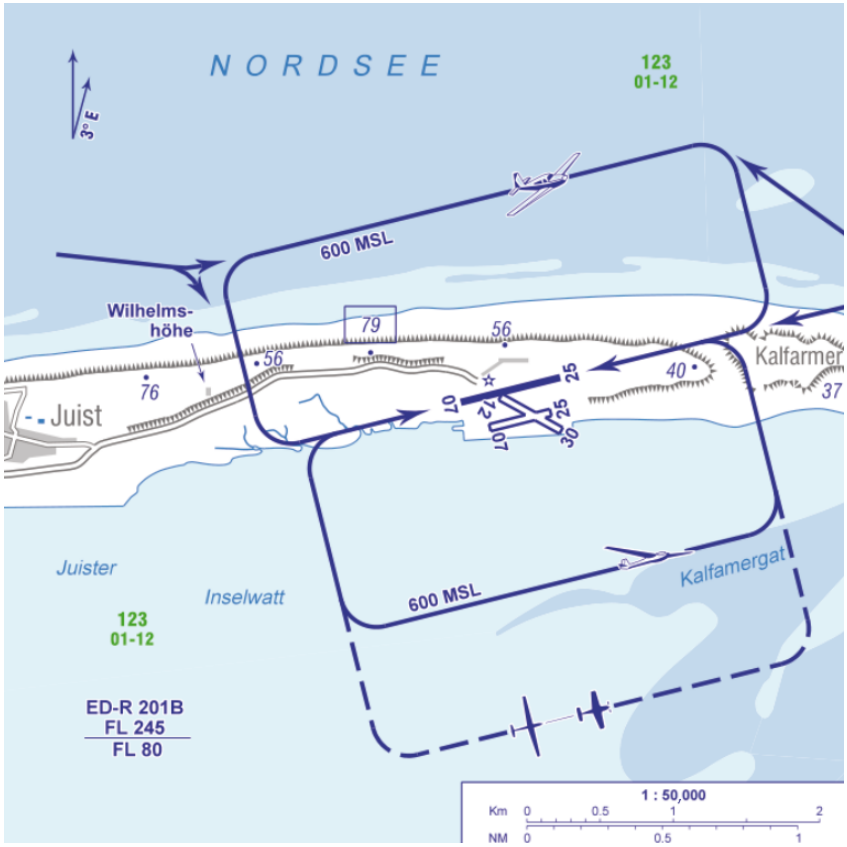

Figure 2. VOC of the terminal airspace of Juist (EDWJ) [17].

The Federal Aviation Administration (FAA) suggests using the 45° approach or the overhead join approach at non-towered airports, depending on the direction from which the aircraft is approaching [15]. In the US, a generic TP, per appropriate regulations and guidance, applies at most non-towered airports. In contrast, in Germany, a VOC prescribes more directly the integration of crewed aircraft. VOCs are usually published for VFR approaches, which show a standardized TP with the corresponding information. For example, the VFR pilot can obtain information on the recommended side for the airport approach and TP entry together with the required flight altitudes and geographic information; see Figure 2. In general, however, these two TP integration layouts follow the same procedures as described above. The UAS integration concept presented in this paper will assume VMC, in which traffic largely relies on TP integration procedures, and represents the most complex integration environment at non-towered airports.

2.2. Initial Terminal Airspace Integration Concepts to Enhance Efficiency

2.2.1. High Traffic Volume Operational Concepts

From 2001 to 2006, the US National Aeronautics and Space Administration (NASA) conducted the Small Aircraft Transportation System (SATS) program to enable efficient self-sequencing of crewed air traffic at non-towered airports with high traffic volumes under IMC. The goal of the program was to solve the "one-in/one-out" paradigm, which states that under IMC, in the US, only one IFR aircraft at a time can be on approach or departure or on a runway of a non-towered airport. The SATS concept was based on a Self-Controlled Area (SCA), which enabled pilots to take over the separation in the terminal airspace under their own responsibility. An Airport Management Module (AMM) was designed to automatically coordinate the sequencing and provide information for approaches and departures under IMC, without conventional ground-based surveillance or ATC sequencing instructions. Additionally, pilots were required to have completed special training and

carry aircraft equipment such as an Automatic Dependent Surveillance-Broadcast (ADS-B) transponder, a cockpit display for traffic information, and special software for conflict detection to be allowed to operate in an SCA. The operational procedure required pilots to request clearance to enter the SCA via the AMM over a data link communication. The AMM then automatically calculated the separation and sequencing information based on the aircraft performance and vehicle position. If compliant with the SCA requirements, the AMM then issued clearance to the pilot by providing associated approach or departure information and airport meteorology for the operation in the SCA [18,19].

The operational concept of the SCA at SATS airports intended that aircraft approach fixed points arranged in the shape of a T, called Initial Approach Fixes (IAF) (see Figure 3). An IAF served as an entry point into the SCA on both sides of the T, IAF-L and IAF-R. If the aircraft was outside the SCA under ATC control, it had to wait at 4000 ft (∼1220 m) AGL. The holding areas within the SCA were located at 2000 ft (∼610 m) AGL and 3000 ft (∼910 m) AGL and served as an IAF. Based on the decisions of the AMM, aircraft entered the IAF either vertically or laterally. If the aircraft approached the IAF vertically, it remained at 3000 ft (∼910 m) AGL until it descended to 2000 ft (∼610 m) AGL. If the AMM decided on a lateral entry, the aircraft approached the IAF directly at 2000 ft (∼610 m) AGL. If the AMM gave the signal for a landing approach, the pilot continued to the Intermediate Fix (IF) and from there via the FAF to the runway. As a result, the SATS operational concept allowed for four simultaneous self-organized aircraft approaches under IMC at non-towered airports [20,21].

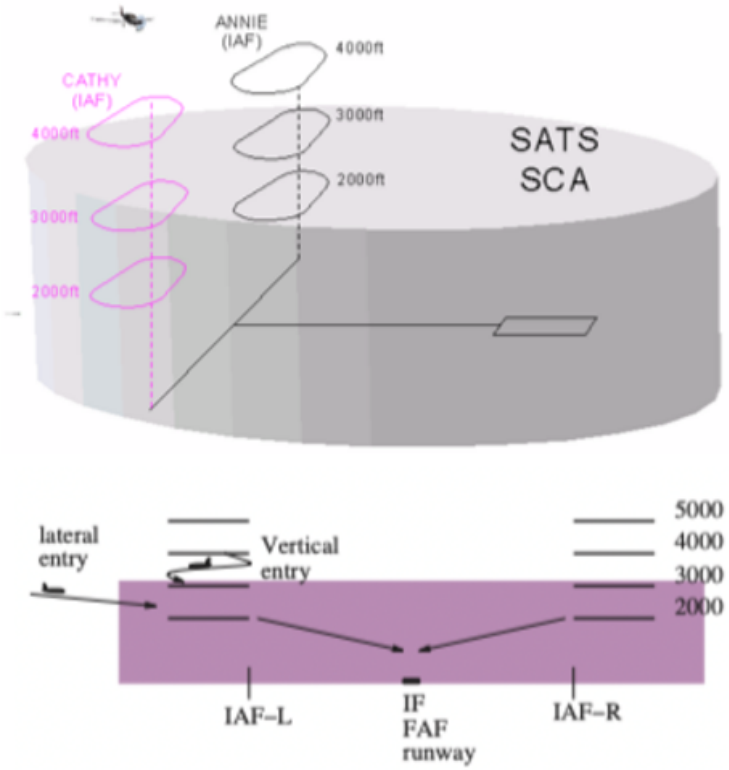

Figure 3. SCA at a non-towered airport [19,20].

Despite proven operational efficiency, the SATS program was not realized because the technological hurdles of carrying specific aircraft equipment and requirements, such as special pilot training, were too high at the time. There were also doubts as to whether SATS would compete with road transportation [22].

2.2.2. Initial Terminal Airspace Integration Concepts for UAS

The integration of UAS into airspace has been the subject of ongoing discussion and research for several years. With the development of UAS with different operational requirements and capabilities, concepts must be developed for how to integrate UAS cooperatively with existing air traffic in different terminal airspace environments around airports. This integration with existing air traffic is recognized to be one of the greatest challenges in UAS airspace integration [4,23–25].

There are different concepts and approaches that address the integration of UAS into controlled terminal airspaces. In 2013, Ref. [23] introduced an initial concept to handle multiple fixed-wing UAS in the terminal airspace of a towered hub airport. An airport-based ground control station was intended to navigate UAS and enable dual threshold operations on a single runway. This concept was intended to be applicable to any towered airport with a parallel runway layout.

In 2022, the European SESAR Joint Undertaking research project INVIRCAT proposed a Concept of Operations (ConOps) for the integration of UAS into controlled terminal airspaces of towered airports under IFR [26]. Different technical and operational aspects for a seamless integration of UAS into controlled terminal airspaces were investigated, followed by simulations to validate the concept. The ConOps included aspects like system latency regarding Command and Control (C2) link and voice communication link, automatic takeoff and landing, handover of UAS control between different RPs and impact on ATC, and contingency procedures such as Lost C2 Link (LC2L) (i.e., the C2 link is severed) [27]. However, most of the research in this area has focused on integrating UAS at major towered airports under ATC supervision with the help of defined IFR approach procedures. It can be assumed that the integration of UAS at towered airports with published IFR procedures is likely to occur relatively seamlessly, with UAS following the already standardized procedures for crewed aviation. Today, Standard Terminal Arrival Routes (STAR) and Standard Instrument Departure Routes (SID) guide IFR aircraft to and from the en-route airspace via initial approach fix points to separate traffic based on checkpoints that restrict flight levels and speeds. The integration of UAS at airports becomes much more complex when there are few, if any, IFR procedures and VFR aircraft operate in the airspace around the airport. Due to the presence of these less predictable VFR aircraft, there is greater uncertainty in airspace environments of non-towered airports, with only "see and avoid" principles and schematic TPs (rather than instrument procedures) being common separation procedures for today's airspace users.

As emerging, larger UAS operations (e.g., fixed-wing regional cargo) will increasingly occur at smaller under-utilized airports, the uncertainty of VFR traffic intent must be given greater consideration. To date, few studies have analyzed VFR data in the context of UAS airspace integration. Ref. [7] is the only published recent research investigating VFR traffic intent uncertainty and its potential impact on UAS operational capacities at a regional US airport, Fort Worth Alliance (KAFW). Ref. [7] analyzes one month of traffic data in the terminal airspace of Fort Worth Alliance (KAFW) to generate spatial-temporal occupancy maps to analyze the interaction probability of UAS with VFR traffic. Ref. [7] emphasizes that the characterization of VFR traffic intent uncertainty is an important step towards strategic and tactical air traffic flow management for efficient UAS integration.

In addition to limited research on VFR traffic intent uncertainty, few concepts investigate integration procedures of UAS at non-towered airports. In Refs. [24,28], a concept proposes a UAS holding pattern above the TP of non-towered airports. In this concept, UA RPs must resolve potential conflicts with VFR traffic by going to a safety altitude. UAS wait in a holding pattern above the TP before the RP decides to descend and enter the TP of the non-towered airport.

In Refs. [24,28], the UAS holding pattern is defined above the highest point of the TP to allow the RP of the UAS to decide when and how to enter the traffic circuit and, if necessary, to establish radio contact with other airspace users. The holding pattern consists of five WPs, which, depending on wind direction and traffic, can enable the RP to approve an omnidirectional landing. The four outer WPs represent the entry into the holding pattern and allow the UAS to enter the holding pattern (via the entry WPs) in a clockwise or counterclockwise direction; see Figure 4. The outer WPs also serve as exit WPs, from which the UAS descends into the beginning of the downwind leg at TP height.

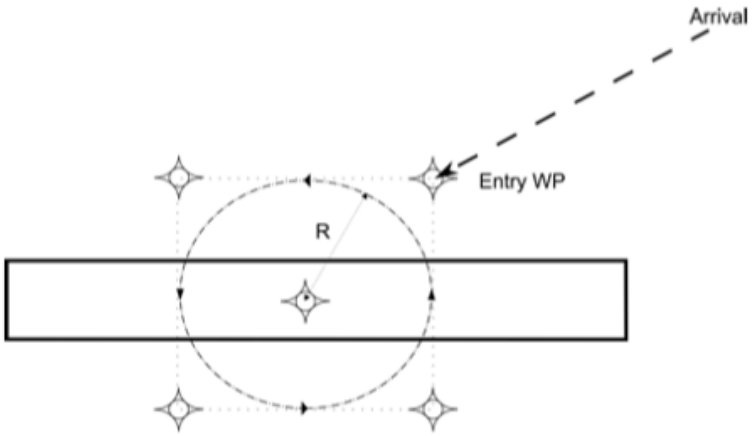

Figure 4. UAS holding pattern above the airport TP [24].

In addition to a UAS holding pattern above the TP of the non-towered airport, Refs. [24,28] propose to place UAS holding patterns at the TP level next to the downwind leg before UAS enter the base leg; see Figure 5. These holding patterns next to the downwind leg are intended to enable UAS to maintain sufficient separation from the aircraft ahead. These downwind leg holding patterns could also give way to other aircraft that choose the base entry or straight-in entry of the TP, for example, or to aircraft that fly a TP in the opposite direction [28].

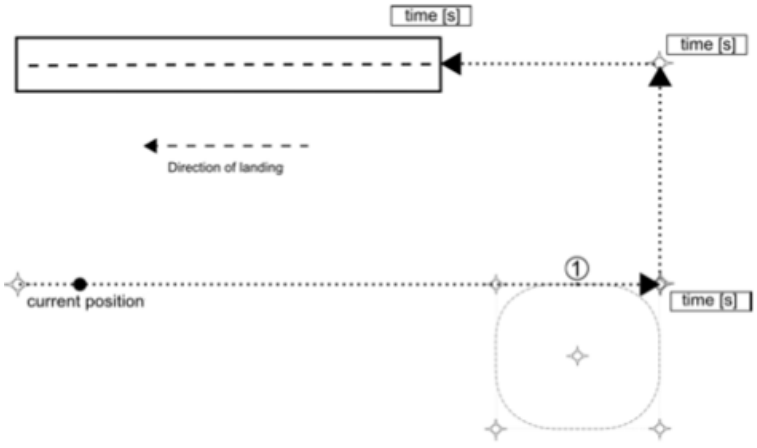

Figure 5. UAS holding pattern at the end of the downwind leg [24].

However, these concepts raise several questions. First, UAS are largely confronted with non-cooperative VFR traffic around non-towered airports, which leads to increased traffic intent uncertainty in the TP and in the terminal airspace. It remains to be clarified how UAS or the RP will predict and detect the intent of VFR traffic in-flight and resolve potential conflicts. No consideration is given to Detect and Avoid (DAA) requirements on board the UAS or uncrewed traffic management concepts to enable cooperative interaction

practices between UAS and crewed aircraft. Second, there is a significant lack of data on existing and forecast traffic activities to assess concept feasibility at the locations where these UAS holding patterns are to be established. Third, these concepts have not been applied to realistic airport environments to assess potential real-world implementation.

2.3. Hurdles for Terminal Airspace Integration of UAS

2.3.1. Landing

At present, there are limited options for large, fixed-wing UAS to integrate at non-towered airports, and none of these options is currently approved for widespread, nominal usage. Military UAS, such as the MQ-9 Reaper, typically will execute a long, straight-in approach, the type of approach that the FAA, in Advisory Circular 90-66C, explicitly recommends against when traffic is present in the pattern [29]. Additionally, currently certified civilian automatic landing systems found on some airliners generally necessitate an appropriate landing guidance system (e.g., Instrument Landing System (ILS)) and associated IAP, which often has a straight-in component. For smaller aircraft, such as those used for regional air cargo, the only currently certified automatic landing system is for use in emergency only (i.e., the Garmin automatic landing system [30]). Although not currently certified, there have been advances made in autopilot and automatic landing systems that do not require an expensive landing guidance system [2,31]. For the purpose of the concept presented in this paper, it is assumed that such a system will be certified in the future and that such a system can fly a conventional TP with no other traffic in the pattern, confirm runway occupancy, and perform an automated landing. However, this assumption does not imply that the UAS can merge and space with other traffic in a TP, only that it can fly a TP and execute a landing in an automated fashion.

2.3.2. See and Avoid

As discussed above, the pilot on board a crewed aircraft needs to "see and avoid" other traffic, especially traffic operating under VFR. A UAS, by nature, does not have a pilot on board. Therefore, it may only fly under IFR, and systems such as Airborne Collision Avoidance System X (ACAS X) provide DAA and Collision Avoidance (CA) capabilities to the RP such that the RP can keep the UAS "DAA well clear" of other traffic [32,33]. For the purpose of this concept, it is assumed that the UAS contains a certified onboard system, such as an ACAS X variant, and that such a system functions correctly in the more demanding terminal environment. Note that the development of such a system is still an area of active research, especially at lower altitudes. Additionally, a Ground-Based Surveillance System (GBSS) could be used as a local low-altitude radar to provide information about aircraft, especially non-cooperative aircraft without a transponder.

In summary, it is imperative that the RP has sufficient knowledge of the traffic at the airport. Nonetheless, absent a robust merging and spacing integration capability, it is likely that there will be levels of traffic at a non-towered airport at which a UAS cannot be safely integrated, even if the RP has sufficient knowledge of said traffic. To further support UAS airspace integration in complex airspace environments, it can be expected that safe and efficient separation of UAS from VFR traffic (i.e., merging and spacing) in non-towered airport environments will be achieved through the provision of a digitalized airspace ecosystem such as U-space.

U-space is Europe's uncrewed traffic management system that defines technical and operational requirements within a regulatory framework for future UAS operations [34]. UAS operations within U-spaces must utilize U-space services (e.g., UAS flight authorization service, traffic information service, network identification service, and geo-awareness service) that are provided by one or more U-space Service Providers (USSP).

Additionally, all airspace users in U-space airspaces will have to be electronically visible to the ground and to other U-space users (e.g., broadcasting their current position via certified ADS-B out to a USSP), also referred to as "e-conspicuity" obligation for crewed aircraft entering U-space airspace [35].

Accordingly, U-space airspaces around non-towered airports in uncontrolled airspace will allow for cooperative air traffic only, as crewed airspace users must broadcast their flight information by means of being e-conspicuous. Thus, UAS obligated to receive U-space services will be informed about the flight information and position of crewed and uncrewed traffic. However, crewed traffic will not necessarily be aware of UAS flight information. Crewed traffic will only be required to broadcast their flight position. In addition, it can be assumed that UAS receiving U-space traffic information services will give right-of-way to VFR traffic and that UAS will adapt their flight procedures according to the position of VFR traffic. To allow for a seamless terminal airspace integration of initial UAS operations, it is expected that UAS should interfere with flight patterns of crewed airspace users as little as possible while still maintaining operational efficiency and safety.

A first regulatory sandbox for a U-space airspace around a non-towered airport is being set up in Germany at Magdeburg-Cochstedt (EDBC), which also serves as the German National Experimental Test Center for UAS and is operated by the German Aerospace Center (DLR) [36].

2.3.3. Lost C2 Link

The RP operates the UAS via the C2 link, through which the RP can upload commands and receive telemetry. However, in the event of an LC2L, the RP is no longer able to operate the UAS, and the UAS will execute an LC2L procedure. In an LC2L procedure, the UAS is expected to follow the procedure automatically, only deviating if there is a DAA alert, which is assumed to be resolved automatically. The development of such procedures, especially for non-towered airport environments, is ongoing, and procedures are not yet certified. To that end, RTCA, Inc. has published DO–400, "Guidance Material: Standardized Lost C2 Link Procedures for Uncrewed Aircraft Systems" [37]. Two recommendations from DO–400, Recommendations #13 and #14, discuss the need to define arrival, approach, and landing LC2L procedure guidelines and to "…investigate the potential need to separate UA [(Uncrewed Aircraft)] holding patterns from traditionally piloted aircraft holding patterns" [37] (p. 52). This work aims to address these two recommendations for the non-towered airport environment.

2.4. Theoretical Integration Procedures of UAS

An IFR-flying UAS, as discussed in Section 2.1.3, is generally assumed to fly an IAP. However, many IAPs are straight-in approaches for landing and, if there is traffic in the pattern, a straight-in approach for landing is not recommended [15]. Further, a visual or VFR approach is often preferred for operational efficiency. It is assumed that, if a UAS is not able to land or integrate into the TP, the UAS will need to hold somewhere until it is safe to land.

Recalling the assumption that, for certain low levels of traffic, the RP can successfully integrate the UAS into the TP (here called a "visual-like" approach), these assumptions lead to five theoretical scenarios for UAS integration in VMC; see Table 1. It is assumed that a UAS in an LC2L state is incapable of executing a "visual-like" approach. Although novel flight rules have been proposed in literature (see [38,39]), no novel flight rules are assumed in this work. These five theoretical scenarios indicate the need to measure the complexity of traffic in and around the airspace of the TP, as well as the need for some sort of holding maneuver. Consequently, this work proposes a holding maneuver to be applied in Sce-

nario 3. A holding maneuver may also apply in Scenario 5, though a further distinction based on the phase of flight is an area of future research. Inherent in the five scenarios is the assumption that traffic in the pattern can be detected and complexity assessed, and that there exist certain safety thresholds at which the UAS moves from one scenario to the next.

Table 1. Theoretical scenarios for UAS integration in the terminal airspace of non-towered airports.

Scenario	C2 Link	Traffic in Terminal Airspace	Anticipated UAS Behavior
1	Nominal	None	Execute IAP or "visual-like" approach
2	Nominal	Minimal	Execute "visual-like" approach
3	Nominal	Saturated	Execute holding maneuver
4	Lost	None	Execute IAP
5	Lost	Any	Execute holding maneuver

Especially important is the determination of when the UAS should execute the proposed holding maneuver. In this work, however, these five scenarios are purely conceptual and a step towards a robust, real-world implementation. Although historical data are used to give a glimpse at what traffic might look like at a non-towered airport, it is crucial that, for a real-life application of this concept, some type of real-time traffic monitoring (e.g., a GBSS or U-space) be implemented.

Further, without a rigorous safety analysis of that real-time data and without internationally harmonized frameworks to structure and assess collision risk management [40], these safety thresholds are difficult to ascertain. However, metrics of complexity in the airspace of TPs can nonetheless be applied to assist in stepping towards future safety analyses and testing integration concepts. In the following, this work will discuss quantitative measures and the implications that they might have for the integration of UAS into non-towered environments.

3. UAS Holding Stack Concept and Methodology

Increased uncertainty and complexity in an airport environment can be caused by temporary factors such as poor weather conditions, runway unavailability, traffic congestion, or contingencies. In these cases, especially at major hub airports, ATC might set up holding patterns in a multilayer holding stack to queue one IFR aircraft per layer over time until congestion has been cleared or the missed approach has been terminated, for example. These holding patterns are commonly referred to as standard holding patterns with a published holding fix and directions to the fix, entry and exit procedures, integration altitudes, flight speeds, and turn rates [41]. A prominent example is London Heathrow (EGLL), one of the busiest airports in the world, where four fixed multilayer holding stack locations are used in the vicinity of the airport to systematically separate arriving IFR aircraft [42].

3.1. Terminal Airspace and Procedure Design

Generally, the structural design of a terminal airspace, also referred to as Terminal Control Area (TCA) or Terminal Maneuvering Area (TMA) in controlled airspace environments, is particularly important to protect arriving and departing IFR flights at airports with high traffic densities. Terminal airspaces in controlled airspace commonly contain "significant points" that specify arrival and departure routes to and from runway ends [43,44]. Here, the International Civil Aviation Organization (ICAO) has provided extensive documentation on how to design a terminal airspace (e.g., Annex 2, Annex 11, Doc. 4444, Doc. 9426, Doc. 8186 and Doc. 9368). Based on these ICAO documents, EUROCONTROL has

provided a step-by-step guideline on how to develop a ConOps for the design of terminal airspaces and the procedures contained therein.

The first two steps, capacity assessment and traffic flow analysis, are intended to investigate existing and forecast traffic activities by considering traffic density, flow complexity, type of aircraft operations and local conditions and/or restrictions, to name a few [43]. In the further steps of the ConOps, STARs and SIDs are designed to effectively accommodate traffic flows from and to en-route airspace. The final steps of the guideline include validation, implementation, and monitoring activities. The guideline highlights that "each individual [airspace] area must be seen to be unique in its own way. . . . Airspace structures have evolved with time. This evolution will continue and will need to take account of new generations of aircraft with improved performance ability. . . . Therefore it is necessary for continuous reassessment of existing airspace structures based upon future requirements and the development of aviation technology" [43] (p. 162).

To meet the ongoing advancements of aviation technologies and related air mobility concepts, this research provides terminal airspace and procedure design implications on how emerging UAS operations might integrate into today's terminal airspace of non-towered airports. To this end, a holding stack concept for UAS to safely and systematically integrate into the terminal airspace of a non-towered airport in case of increased traffic uncertainties and complexities is proposed.

The proposed UAS holding stack concept builds on traffic management approaches and operational concepts discussed in Section 2. The operating principles of the UAS holding stack concept are based on NASA's SATS self-sequencing system with vertical holding areas, the framework of the INVIRCAT project, such as the role of the RP and C2 link data flows to and from the UA in the terminal airspace, and the current IFR holding principles set by ATC.

The holding stack concept presented in this paper is intended to provide a space for UAS to loiter in a safe manner in the terminal airspace, for example, due to traffic in the TP, runway blockage, an LC2L, or a combination thereof. To identify feasible altitude bands for holding stack locations and respective UAS integration procedures from holding into the TP of an airport, this paper focuses on deriving implications for the first two steps of the EUROCONTROL ConOps guideline for terminal airspace and procedure design: capacity assessment and traffic flow analysis of existing traffic activities.

The traffic management of the UAS holding stack, such as UAS integrating into the holding stack or from the holding stack into the airport TP, especially in high-density traffic scenarios, and highly automated merging and spacing with other airspace users, could be managed by digital traffic services within an U-space ecosystem (see Section 2.3.2) or by supplemental data service providers outside of U-space, for example. The location of the holding stack should be sufficiently separated from other traffic, while nonetheless being close enough to the TP that integration is feasible given the inherent uncertainty and complexity of the non-towered environment. Additionally, the holding stack should be close to the airport of interest so that the UAS can divert to the holding stack in the event of a safety threshold, discussed in the previous section, being exceeded without adding excessive distance and time to the flight. To meet these requirements, the proposed location of the holding stack is placed above historically flown TPs of a non-towered airport, as depicted in Figure 6.

For a UAS to enter holding, similar to NASA's SATS program, it is expected that the UAS will approach fixed points (i.e., entry waypoints) above the airport's individual TP and wait at conflict-free altitudes until the UAS can descend into lower holding areas or approach the runway directly from initial holding. While in the SATS program, aircraft communicated via an AMM on the ground of the airport that assigned aircraft to holding

altitudes and provided sequencing information, UAS are expected to communicate within a digital ecosystem, such as U-space, in the proposed concept and separate according to onboard DAA functions and/or conflict management services provided by data service providers, when such a system is active. In the absence of such a system, the RP will communicate with traffic via a VHF radio link, like a pilot of a crewed aircraft. The detailed interaction of UAS traffic management systems with UAS and crewed aircraft is beyond the scope of this paper but can be explored in more detail in Refs. [38,45].

For the proposed UAS holding stack concept, in line with the operating framework of the INVIRCAT project, the RP is responsible for the safety of flight operation according to ICAO Annex 2 – Rules of the Air [26,46]. For flights in controlled airspace, for example, prior to entering a non-towered airport environment in uncontrolled airspace, the RP is expected to follow the same clearance and separation instructions issued by ATC as crewed aircraft. For a detailed overview of the RP's responsibilities in flight planning, monitoring, and decision-making, as well as navigating and communicating, see Ref. [26].

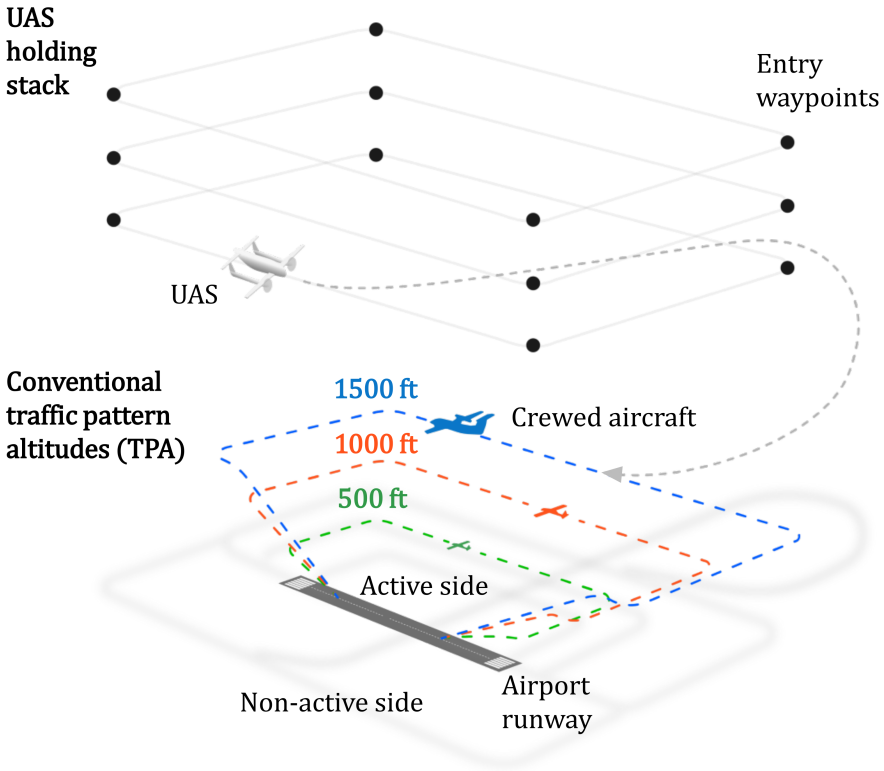

Figure 6. Conceptual scheme of the UAS holding stack above conventional TPA with UAS overhead join from holding into TPA.

Although it is unlikely that there will be a "one size fits all" approach to placing a holding stack at a non-towered airport, there are some general limitations: (1) The bottom of the holding stack will need to be vertically separated from the top of historical TPs at the airport; see Figure 7b. (2) The number of holding stack layers and the top of the holding stack is limited by overhead traffic streams (see Figure 7b) and relevant UAS performance characteristics, such as climbing and descending capabilities. (3) If multiple UAS are allowed in the holding stack simultaneously, some means of holding stack management (i.e., entry, exit, and flight direction) will need to be developed.

Limitations 1 and 2 will be addressed in this paper to assess the feasibility of the concept. Limitation 3 will need to be explored in future work following the assessment of feasibility and the establishment of metrics for the quantitative description of the airspace around a non-towered airport.

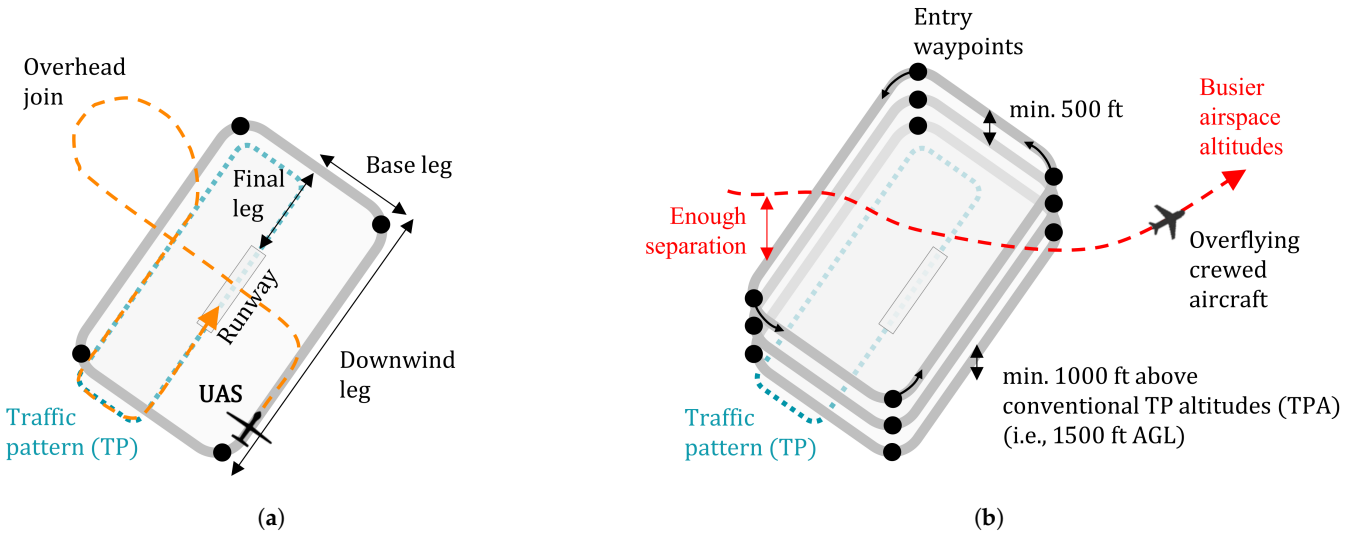

Figure 7. Conceptual design of the UAS holding stack above conventional TPA according to the dimension of the airport-specific TP (top view): (**a**) UAS holding stack design with one layer (gray rectangle) with UAS overhead join approach from holding into TP towards runway (orange-dashed line). (**b**) UAS holding stack design with vertical layers (gray rectangles).

A holding stack location above the TP is anticipated to be safer than placing it next to the TP, as lower traffic densities can be expected above conventional TP integration altitudes, and UAS are able to enter the holding stack from any direction without crossing conventional TP integration altitudes. Conventional TP integration altitudes are standard altitudes where a crewed aircraft is recommended to integrate into the TP. Although some non-towered airports have specific assigned TP integration altitudes, crewed aircraft are commonly expected to integrate into the TP at 1000 ft (∼300 m) AGL [15]. Depending on the performance characteristics of different aircraft, higher-performance aircraft (e.g., jet aircraft) are expected to integrate into the TP at an altitude of 1500 ft (∼460 m) AGL, whereas lower-performance aircraft (e.g., piston aircraft) may be expected to integrate into the TP at a lower altitude, as low as 500 ft (∼150 m) AGL. The concept expects UAS to integrate from the holding stack into the TP at a conventional TP integration altitude based on the performance characteristics of the UAS (higher UAS performance, higher TP integration altitude) using recommended TP entry procedures (i.e., overhead join approach into the downwind leg).

The size of the UAS holding stack is proposed to be based on the size of the historically flown TP and will vary by airport. The size of the historically flown TP can be determined by assessing the airspace segments with the highest historical traffic densities. Based on the airspace segments with the highest historical traffic densities, the length of the TP legs can be determined, such as the downwind leg and base leg.

For airports with only one TP, the legs of the UAS holding stack will be determined by the legs of the TP and extended towards the non-active side of the airport by doubling their size, see Figure 7a, subject to applicable terrain and airspace restrictions. Extending the holding stack towards the non-active side of the airport is considered important to allow UAS sufficient time and space to integrate from the holding stack with crewed aircraft coming from the non-active side of the airport. In short, it is expected that the holding stack will be twice the size of the historically flown TP to give the UAS more space to loiter and integrate with crewed traffic from holding.

Airports with TPs on both sides of the runway are treated slightly differently. For example, Juist (EDWJ) is a non-towered airport located on one of the islands in the German

North Sea. It has two recommended active TPs: north of the runway for motorized aircraft and south of the runway for non-motor-driven aircraft (e.g., gliders), which can be seen in its VOC in Figure 2. The traffic density heatmap of historical flight track data at Juist (EDWJ) shows that the southern TP has a higher traffic density than the northern TP over an exemplary altitude band of 0–3000 ft AGL (∼910 m) (see Figure 8). In the case of two active TPs, the length of the UAS holding stack legs is determined by the TP on the same side of the runway, which in turn is determined according to the highest historical traffic density, as explained earlier in this paper. In other words, the UAS holding stack is not simply double the size of the busier historically flown TP but is an overlap of both TPs.

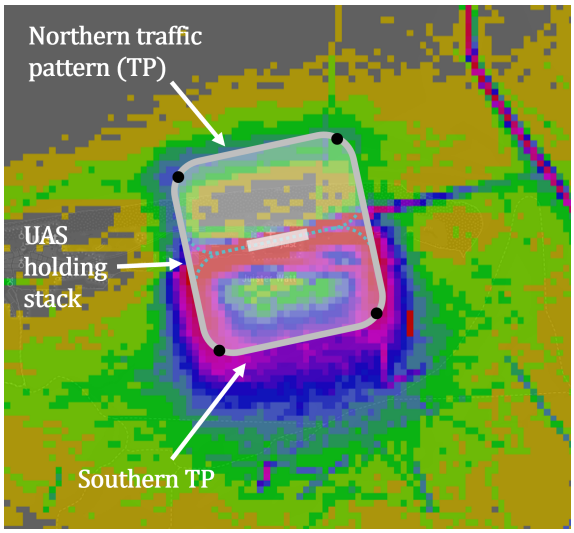

Figure 8. Traffic density heatmap of Juist (EDWJ) with two active TPs (north and south of the runway) and UAS holding stack (gray rectangle) in conventional TPA 0–1500 ft (∼460 m) AGL. The southern TP shows significantly higher TP activities (darker colors) than the northern TP (lighter colors).

A holding stack for UAS is proposed to consist of different vertical layers, similar to ATC stacking arriving IFR aircraft in holding stacks at major hub airports; see Figure 7b. The lowest altitude at which the UAS holding stack can begin will vary by airport, but generally will start at 2500 ft (∼760 m) AGL. The highest conventional TPA, that of a jet aircraft (see Figure 6), is at 1500 ft (∼460 m) AGL. The recommended overhead join approach is 500 ft (∼150 m) above that, or at 2000 ft (∼610 m) AGL. Another 500 ft (∼150 m) above that altitude is needed as a safety buffer to comply with separation minima [16].

The number of levels in the holding stack, as well as the upper altitude limit of the holding stack, will depend on the traffic and UAS demand at the airport of interest. For example, a holding stack upper altitude might be limited by the presence of a low-altitude airway (e.g., Victor airway in the US) above the airport. Finally, each holding stack layer will be separated by 500 ft (∼150 m), in accordance with separation minima [16].

Entry into the holding stack is notionally designated at the corners of each level. A UAS exiting from the holding stack should join with a standard overhead join approach into the downwind leg of the TP, leaving the lateral dimensions of the holding stack; see Figure 6.

Initially, it can be expected that one UAS will be assigned per holding layer, similar to how ATC today stacks one IFR aircraft per holding layer. For example, if the first UAS is assigned to the first holding layer (bottom of the holding stack) and the second UAS is assigned to the second holding layer (above the initial bottom layer), a third UAS is expected to enter the holding stack at a third layer on top of the first two holding layers. The third UAS might exit the holding stack towards the TP from its initial entry layer (third layer of the holding stack) or transition through the lower first and/or second holding layer

once the first and second UAS have transitioned from their holdings into the TP. For most cases, it is not expected that a UAS will need to travel through multiple empty holding stack layers before integrating into the TP. Generally, the queuing of UAS in the holding stack will be managed by "first-in/first-out" principles. Additionally, different holding stack layers could be used to sort UAS by flight mission priorities or aircraft capabilities (e.g., aircraft flying similar holding speeds) in high traffic density scenarios. However, as mentioned earlier, holding stack management (i.e., entry, exit, and flight direction) and the coordination of simultaneous UAS in the holding stack will not be further explored in this paper.

The FAA Airplane Flying Handbook (FAA-H-8083-3C) recommends single-engine airplanes to integrate into the TP of non-towered airports flying 70–90 knots (kn) indicated airspeed [15]. Similar speeds are expected to be used by UAS in layers of the holding stack. Although the concept proposed in this work currently addresses UA powered by a piston or turboprop engine, it is expected that larger aircraft or crewed/uncrewed eVTOL aircraft, similar to today's helicopters, which also integrate into TPs at lower altitudes (500 ft ($\sim$150 m) AGL) [47], will also utilize this concept.

The UAS holding stack concept proposes that the dimension of the holding stack depends on the size of the historically flown TP, varying by airport. For an airport with two active TPs, such as Juist (EDWJ), the UAS holding stack is proposed to be the dimension of an overlap of both historically flown TPs, the northern and southern TP (see Figure 8). According to the UAS holding stack dimension of Figure 8, the northern and southern TP of Juist (EDWJ) have a combined perimeter of $\sim$12 km, which is used in the following as an initial reference for calculating the circuit time that a UAS needs to travel through an entire holding layer. For this exemplary calculation, the performance characteristics of a Cessna 208 Caravan aircraft are chosen. Companies such as Reliable Robotics and Merlin Labs are currently working to convert this aircraft type from a crewed aircraft to a remotely piloted UAS, with plans to convert larger aircraft for remotely piloted cargo operations in the future [48,49]. Therefore, it is assumed that an aircraft (i.e., Cessna 208 Caravan) will hold with an average speed of 90 kn in the layer of a UAS holding stack. Note that for lower-performance single-engine aircraft, such as the Cessna 172, the average speed may be lower, leading to an increase in the time spent in the holding stack. Accordingly, a Cessna 208 Caravan UAS needs $\sim$4.32 min to fly through every leg of the holding stack layer of Juist (EDWJ) (proposed perimeter of $\sim$12 km), which corresponds to the nominal circuit time of an IFR aircraft of about four minutes in a standard holding pattern set up by ATC [41].

Building on these assumptions for an exemplary holding layer circuit time, the descent time of a UAS from the lowest layer of a holding stack into the recommended TPA of Juist (EDWJ), which is also expected to be used by UAS to enhance the predictability of the UAS flight path by other aircraft in the vicinity of the UAS, will be considered in the following:

$\mathrm{VD}_{\mathrm{transfer}}$: Vertical Distance (VD) from holding into TPA, 1900 ft ($\sim$580 m),

r_{ROD} : Assumed Rate of Descent (ROD), 800 ft ($\sim$240 m) per min,

v_{avg} : Assumed indicated airspeed of an aircraft, 90 kn ($\sim$2.78 km per min).

Equation (1) gives the time that a UAS needs to vertically transfer from a holding layer into a TP, while Equation (2) gives the Horizontal Distance (HD) that the UAS has to cover during the vertical descent:

$$t_{\mathrm{transfer}} = \frac{\mathrm{VD}_{\mathrm{transfer}}}{r_{\mathrm{ROD}}} \quad \text{in} \quad \text{min.} \tag{1}$$

$$\mathrm{HD}_{\mathrm{transfer}} = v_{\mathrm{avg}} \cdot t_{\mathrm{transfer}} \quad \text{in} \quad \text{km.} \tag{2}$$

The TPA of Juist (EDWJ) is at ∼600 ft (∼180 m) AGL [17]. Recalling that the lowest holding layer altitude is proposed to be at 2500 ft (∼760 m) AGL, this results in a minimum vertical transfer distance of 1900 ft (∼580 m). For this distance, a UAS with a given descent rate of a Cessna 208 Caravan would take ∼2.38 min, traveling ∼6.6 km (∼4.1 miles (mi) or ∼3.6 nautical miles (NM)) horizontally. This distance can probably be flown on a relatively straight trajectory, while longer distances will likely have to be flown in a spiral descent to avoid spreading out too far horizontally. For a vertical transfer distance of 1900 ft (∼580 m), a relatively straight trajectory from holding into TP with a horizontal distance of ∼6.6 km (∼4.1 mi or ∼3.6 NM) can be considered operationally feasible, since the downwind leg of Juist (EDWJ), for example, already has a length of ∼6 km (∼3.7 mi or ∼3.2 NM) with the downwind leg of the holding layer proposed to be on top of the downwind leg of the TP; see Figure 7a.

3.2. Conceptual Operating Scheme of UAS Flight Planning at Non-Towered Airports

To better understand how operational processes of UAS integration at non-towered airports intertwine, Figure 9 provides an overview of the key process steps considered for the concept in this work (see blue boxes). This paper focuses on a three-step methodology to identify and assess historically flown TPs and their surrounding traffic activities at airports. This intends to provide insight as to where, when, and how crewed and uncrewed traffic might have to interact in the future, which airspace segments could be utilized for the proposed UAS holding stack concept, and how UAS are expected to integrate into the TP of an airport using various metrics and illustrative analyses of real airport environments.

1. **Assessment of airspace environment of non-towered airports**
   The first step for integrating UAS into non-towered environments is the assessment and spatial definition of the main operating environment (Section 4.1), namely the volume of the airspace that surrounds historically flown TPs, referred to as "TP airspace" in the following.
2. **Assessment of flight behaviors of airspace users**
   Second, after systematically identifying the bounds of where crewed traffic has historically flown the TP (i.e., TP airspace), flight behaviors are assessed using different quantitative measures (Section 4.2).
3. **Assessment of locations for UAS holding stack**
   Third, after investigating crewed flight metrics and traffic densities, locations in and above the TP airspace are investigated to derive potential UAS holding stack locations, exemplified for different airports of interest (Section 4.3).

All three steps impact the UAS behavior on where, when, and how to integrate into the TP of an airport. Additionally, the conceptual operating scheme provides five TP integration cases for UAS based on the implications of the proposed three-step methodology and the current traffic situation of an airport, which will be discussed at the end of this paper.

The current real-time traffic situation of an airport, which, for example, could be provided to the RP via GBSS and/or digital services from U-space, will determine if it is required for a UAS to transfer into a holding stack or not. "No current traffic" will not require a UAS to execute a holding maneuver to monitor current ongoing traffic activities. Similarly, "minimal current traffic" (e.g., one or two crewed aircraft) in the terminal airspace might not necessitate the UAS to transfer into holding, since the UAS might simply follow the preceding aircraft into the TP, depending on the location of all present aircraft.

However, reaching a level of "saturated current traffic" in the terminal airspace might require the UAS to transfer into holding until the intent uncertainty of current traffic activities has been resolved, and it is safe for the UAS to integrate into the TP. Note that

the size of an airport's terminal airspace will normally exceed the size of an airport's TP airspace. For this research, the terminal airspace of non-towered airports can be considered to be the size of ~200 km^2 (~77 mi^2), which is the common size of an RMZ, for example. With both airspaces normally centered according to the runway coordinates, the TP airspace is a subset of the terminal airspace with sizes ranging between ~20–100 km^2 (~8–39 mi^2), which is based on the airports of interest in this paper.

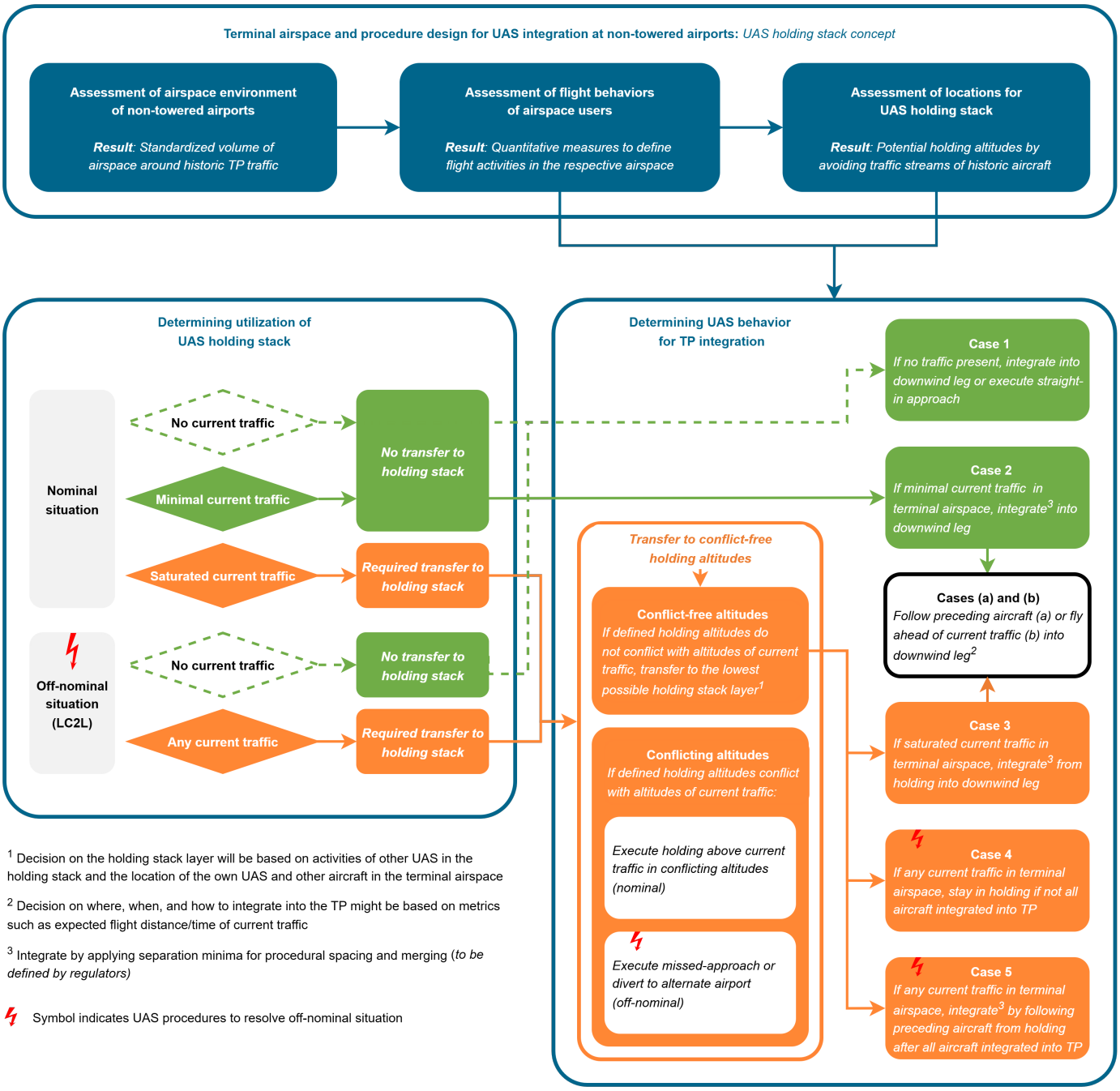

Figure 9. Conceptual operating scheme for UAS integration at non-towered airports.

Different entities, such as regulatory authorities, ATC and/or USSP, or the UAS operator itself, could be responsible for determining the levels of traffic and associated safety thresholds for transfer into holding. In addition to safety thresholds, the requirement to transfer into holding could be based on additional factors such as the level of DAA equipage on board the UAS and/or the availability of automatic landing systems.

Furthermore, UAS integration decisions depend on whether the UAS is operating in a nominal or off-nominal situation, such as during an LC2L. However, this work does not provide safety thresholds to distinguish between different levels of traffic (i.e., between "minimal current traffic" and "saturated current traffic", see Figure 9), which is subject to ongoing safety regulations as discussed in Section 2.4. Additionally, concepts and regulations for contingency and emergency procedures need to be developed to safely guide UAS during off-nominal situations. For this concept, if a UAS is not able to integrate into a holding pattern above the airport, for example, the UAS is likely to execute a missed approach or divert to an alternate airport. However, this paper will not focus on off-nominal situations due to a lack of standards and procedural contingency/emergency regulations.

The three-step methodology for the terminal airspace and procedure design applying holding stacks for UAS integration at non-towered airports, as seen in Figure 9, will be covered in the following section using various quantitative measures and in-depth analyses for different exemplary non-towered airports.

4. Analysis of Flight Track Data Around Non-Towered Airports

4.1. Assessment of Airspace Environment of Non-Towered Airports

Despite best practices and, in the case of German airports, VOCs suggesting the "ideal" TP in terms of integration altitude and distance of the downwind leg from the runway, the historical traffic at non-towered airports is nevertheless distributed, both vertically and horizontally, beyond the "ideal" pattern. Therefore, it is vital to identify the bounds of this spread to properly define the TP airspace as the volume around the non-towered airport and to analyze historical traffic behavior within this volume.

4.1.1. Data Selection

Historical data on air traffic are obtained from two sources. For the German airports, flight data from Flightradar24 covering one year of data for the latest year available (2022) are used to analyze speed, heading, and four-dimensional WPs indicating the longitude, latitude, altitude, and time of every aircraft in the airspace [50]. Flightradar24 uses ground-based ADS-B receivers that collect data every second from aircraft in their vicinity that are equipped with an ADS-B transponder. Furthermore, these are complemented by data from multilateration (MLAT) and data collected from the Open Glider Network utilizing commercial FLARM transponders. Similar data are examined for US airports, using Sherlock Data Warehouse to access flight track data for the latest year available (2023) from terminal airspaces [51]. Using these historical data, the TP airspace can be defined.

Data were analyzed using internal DLR software to filter and sort flight track data and to visualize traffic density heatmaps with QGIS (v3.38.0). All other data processing and visualization were performed in MATLAB R2025b.

Note that not all airspace users within the investigated airspace segments might have transmitted flight data in the respective year. A European survey has shown that 78% of crewed aircraft flying in uncontrolled airspace carry some kind of e-conspicuity system (e.g., ADS-B) on board their aircraft to transmit flight data to other airspace users and ground-based systems [52]. Therefore, the data sets analyzed have to be considered of an indicative but not comprehensive quality.

4.1.2. Vertical Bounding of the TP Airspace

At each airport, the Average Number of Simultaneous Flights per Square Kilometer (ASFK) is calculated [53]. The ASFK is a measure of the density of historical operations. For each 0.01 km^2 spatial cell, the time spent in that cell by historical flights during a given time period (i.e., one year) is recorded in flight seconds. This sum is then divided by the

area of the airspace cell (i.e., 0.01 km^2) and the overall recording time to provide the average density for a single airspace cell, as provided in Equation (3). Figures 10 and 11 show the ASFK across different altitude bands for Watsonville (KWVI) and Juist (EDWJ).

$$\text{ASFK} = \frac{t_{\text{cell}}}{A_{\text{cell}} \cdot T_{\text{period}}} \quad \text{in} \quad \frac{\text{flights}}{\text{km}^2}. \tag{3}$$

t_{cell}: Flight time [s] spent by flights in the cell over the observation period,

A_{cell}: Area of the spatial cell [km^2], e.g., 0.01 km^2,

T_{period}: Duration of the observation period [s], e.g., one year = 31,536,000 s.

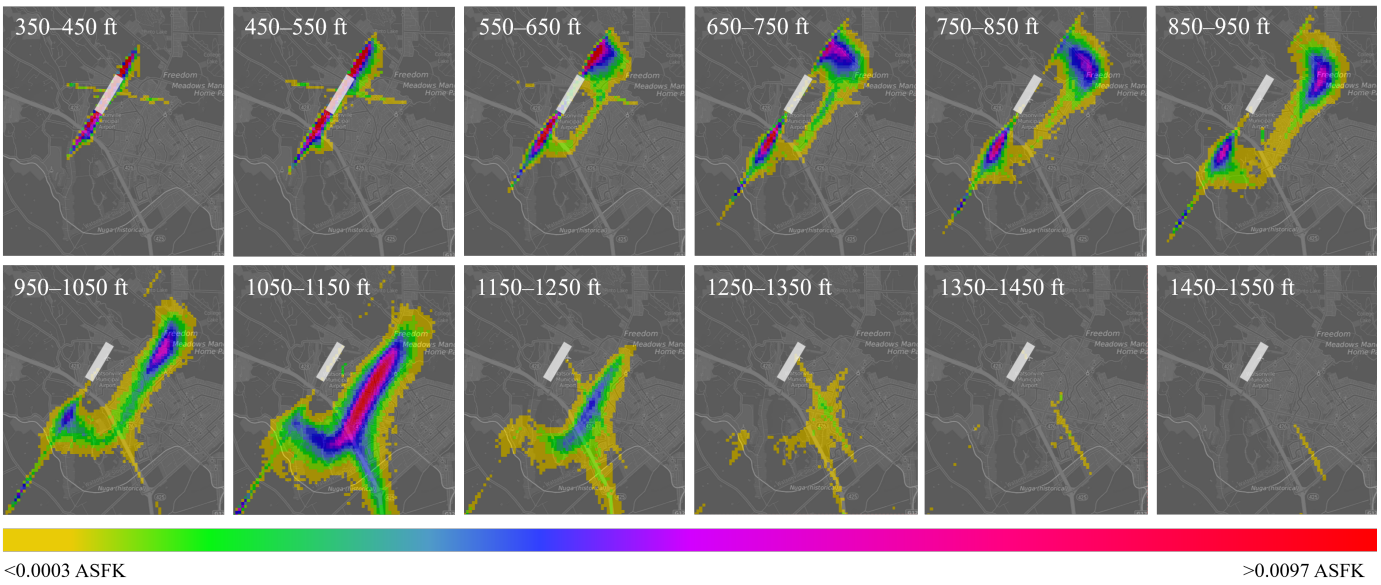

Figure 10. Traffic densities in altitude bands of Watsonville (KWVI). Altitude band 1050–1150 ft (∼335–350 m) AGL shows the highest traffic density in the downwind leg (∼0.0097 ASFK).

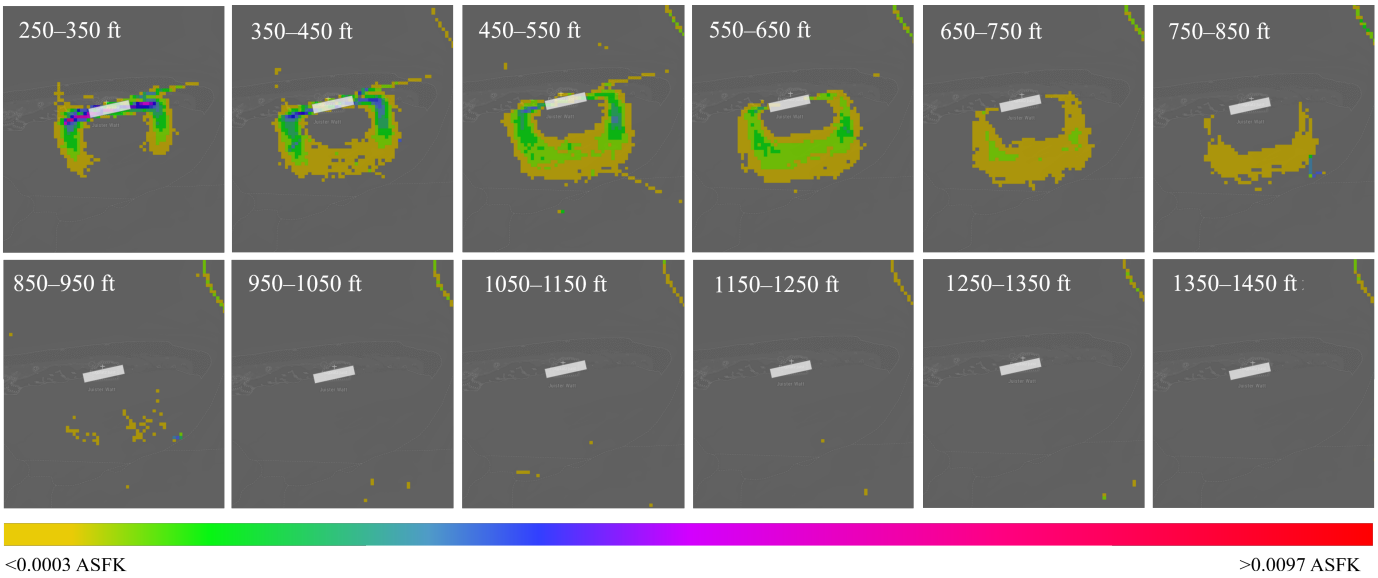

Figure 11. Traffic densities in altitude bands of Juist (EDWJ). Altitude band 550–650 ft (∼170–200 m) AGL shows the highest traffic density in the downwind leg (∼0.0010 ASFK).

As discussed previously, it is anticipated that most traffic would integrate into the TP at conventional TPA between 500–1500 ft (∼150–460 m) AGL. This can also be seen by looking at Figure 10, with most traffic integrating into the TP downwind leg of Watsonville

(KWVI) between 1050–1150 ft (∼335–350 m) AGL. This also appears to be close to the recommended TPA of Watsonville (KWVI), which is 1000 ft (∼300 m) AGL [54].

For Juist (EDWJ), the highest downwind leg density (∼0.0010 ASFK) can be observed between 550–650 ft (∼170–200 m) AGL, with 600 ft Mean Sea Level (MSL) being the recommended TPA of Juist (EDWJ); see Figure 2. Note that the airport runway of Juist (EDWJ) is at an elevation of only 8 ft MSL. For Watsonville (KWVI), almost no TP activities occur above ∼1500 ft (∼460 m) AGL. For Juist (EDWJ), TP traffic densities have already become low between ∼850–950 ft (∼260–290 m) AGL.

Since traffic can still integrate into conventional TPA from above 1500 ft (∼460 m) AGL, 3000 ft (∼910 m) AGL was chosen as an upper bound to the TP airspace. Assessment of several non-towered airports indicated that the density of historical operations above 1500 ft (∼460 m) AGL was significantly lower; however, traffic used the airspace above conventional TPA before integrating into the TP. These traffic activities above conventional TPA are likely to have an impact on the decision on the feasibility of the holding stack location and the number of holding stack layers. A discussion of the differences in traffic densities in different altitude bands of the TP airspace at airports of interest and the implications of these differences will follow in Section 4.2.

4.1.3. Horizontal Bounding of the TP Airspace

In the next step, as indicated in Figure 12c, the horizontal bounds of the TP airspace are drawn around all airspace cells that represent an airspace density of at least $8 \cdot 10^{-4}$ ASFK (light green on the given scale). This bounding threshold implies that, over the course of the year, a total of ∼2500 flight seconds ($7 \cdot 10^{-1}$ flight hours) were spent within the 0.01 km^2 spatial cell.

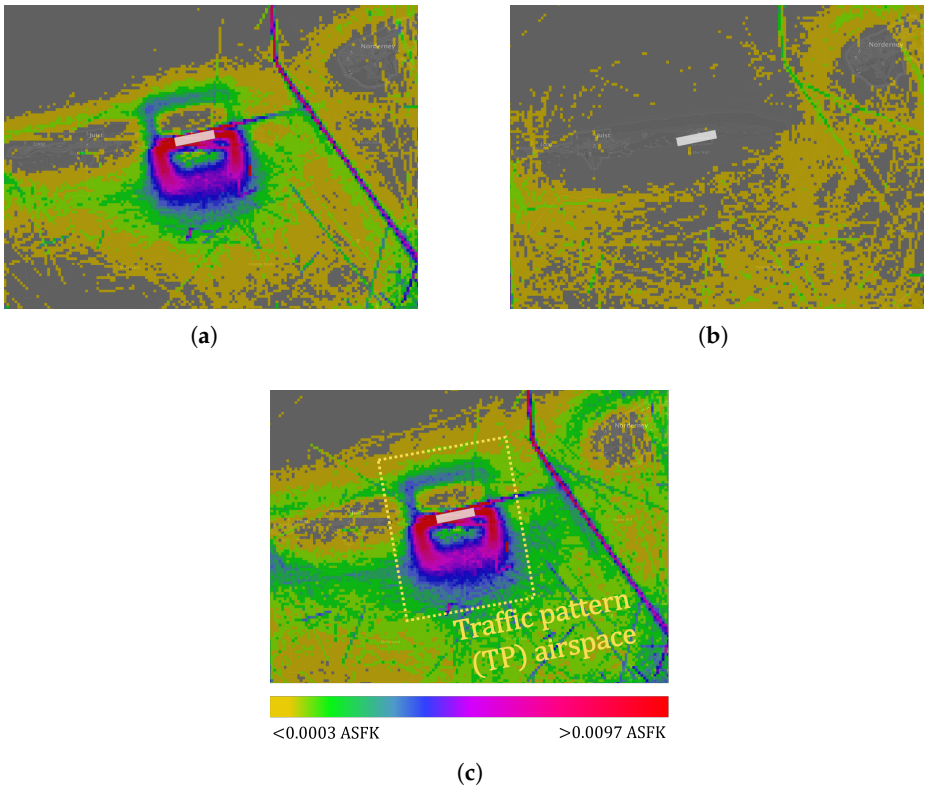

(**a**) (**b**) (**c**)

Figure 12. Visualization of traffic densities in altitude bands at Juist (EDWJ) to identify the TP airspace (yellow-dashed bounding box): (**a**) Traffic densities in conventional TPA 0–1500 ft (∼460 m) AGL. (**b**) Traffic densities above conventional TPA 1500–3000 ft (∼460–910 m) AGL. (**c**) Traffic densities in the TP airspace 0–3000 ft (∼910 m) AGL.

For this research, the proposed bounding threshold of $8 \cdot 10^{-4}$ ASFK is based on a preliminary assessment of historical traffic at the airports of interest. As seen in Figure 12c, the proposed bounding threshold covers the flight track data of aircraft flying the airport's individual TP. However, future work will apply further mathematical rigor to refine and better scale this bounding threshold. In summary, every TP airspace is vertically bound at 3000 ft (∼910 m) AGL but has individual horizontal bounds based on the density of the TP at each non-towered airport.

4.2. Assessment of Flight Behaviors of Airspace Users

Flight operations can vary significantly from one non-towered airport to the next. To gain a better quantitative understanding of operations at non-towered airports, this paper proposes several metrics to describe operations. These metrics will be applied to twelve example airports (see Figure 13). It is intended that these metrics can be utilized to design scenarios and simulations that will help define the undefined safety thresholds discussed in Section 2.4. As mentioned previously, the actual definition of these safety thresholds is beyond the scope of the present work. A discussion of how these metrics might impact the integration of UAS into non-towered airports will follow.

Twelve different airports, four each from Germany, California, and Texas, were chosen as airports of interest. Different regions were chosen to provide a varied and international view of non-towered airports. These three regions were previously identified as regions where UAS are likely to be introduced for use in the regional air cargo use case [2].

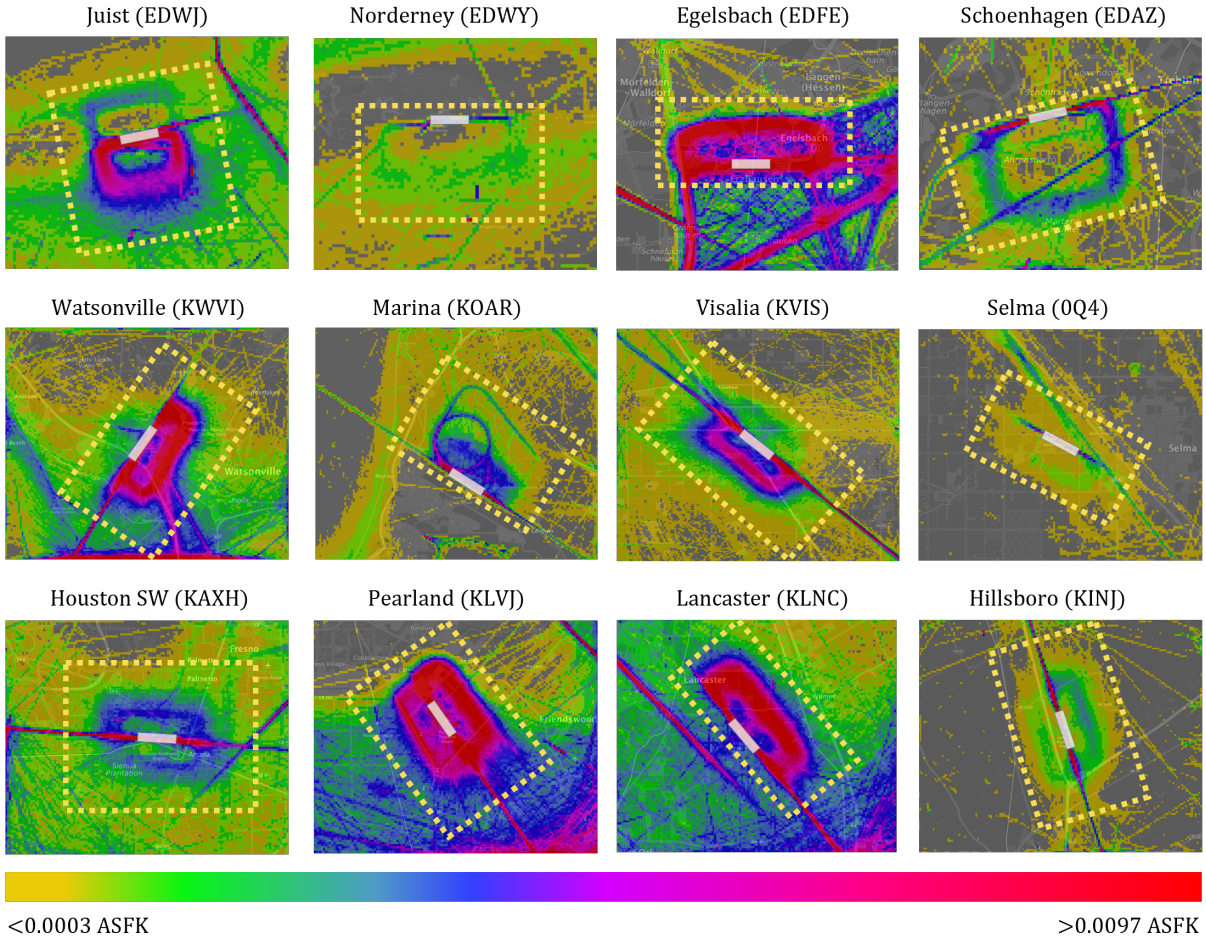

Figure 13. Identification of TP airspaces (yellow-dashed bounding boxes) at airports of interest. Traffic densities are visualized in an altitude band of 0–3000 ft (∼910 m) AGL. Airports and their TPs are not to scale.

The historical traffic density at each airport of interest, as well as the identified TP airspace for each non-towered airport, is shown in Figure 13. Flight data are extracted from the identified TP airspaces, which are aligned with the runway center-line of the respective airport and are shown in Figure 13 as the yellow-dashed bounding box. For airports with multiple runways, the TP airspace was aligned with the busier runway.

The twelve airports were selected due to their strategic location for initial regional cargo UAS operations. Locations considered relevant for the initial deployment of highly automated regional cargo operations are suburban areas (e.g., Watsonville (KWVI), Marina (KOAR), Visalia (KVIS), and Hillsboro (KINJ)), hard-to-reach areas such as rural regions or islands (e.g., Juist (EDWJ) and Norderney (EDWY)), and areas close to main airports or cargo hub airports (e.g., Egelsbach (EDFE), Schoenhagen (EDAZ), Selma (0Q4), Houston SW (KAXH), Pearland (KLVJ), and Lancaster (KLNC)).

4.2.1. Analysis of Crewed Traffic Shares and Densities in TP Airspace

For UAS flight planning at non-towered airports, it is relevant to consider the share of flights that operate in different altitude bands of the TP airspace. Ideally, UAS want to minimize interaction with crewed traffic; thus, the holding stack should be placed at an altitude that is deconflicted from other traffic. This distinction by altitude bands helps to understand crewed traffic behavior in the TP airspace in order to minimize interaction of UAS with crewed aircraft when choosing a suitable UAS integration procedure and a location for the UAS holding stack. As discussed in Section 4.1.2, the vertical bound to the TP airspace was placed at 3000 ft (∼910 m) AGL. To provide a more detailed picture of traffic in the TP airspace, the flights found in the TP airspace are divided into three sets; see Figure 14.

$\mathbb{A}$: Set of flights from 0–1500 ft (∼460 m) AGL;

$\mathbb{B}$: Set of flights from 1500–3000 ft (∼460–910 m) AGL;

$\mathbb{X}$: Set of flights from 0–3000 ft (∼910 m) AGL.

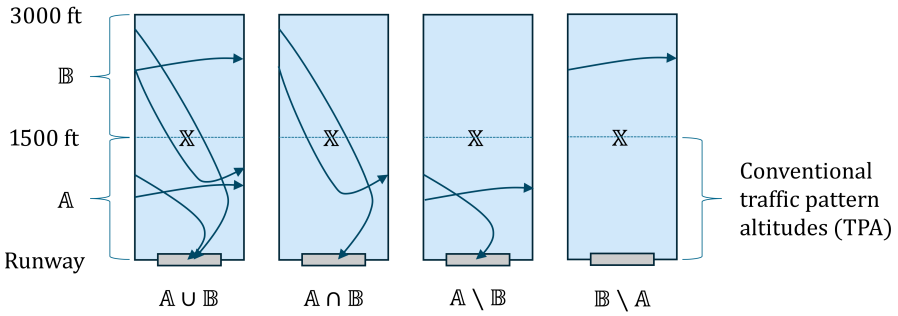

Figure 14. Visualization of different traffic behaviors in the TP airspace.

Here, $\mathbb{A} \subseteq \mathbb{X}$ and $\mathbb{B} \subseteq \mathbb{X}$. Airspace segment $\mathbb{X}$ contains the total number of flights in the defined TP airspace (i.e., flights in $\mathbb{A}$ or $\mathbb{B}$), which can be expressed by $\mathbb{A} \cup \mathbb{B}$. $\mathbb{A}$ is designed to cover the conventional TP integration altitudes. $\mathbb{B}$ covers all flights from the top of the conventional TPA to the top of the TP airspace. $\mathbb{A} \cap \mathbb{B}$ contains all flights that flew through both airspace segments (i.e., flights in $\mathbb{A}$ and $\mathbb{B}$), presumably landing at or departing from the airport. The total number of flights in $\mathbb{A}$ and in $\mathbb{B}$ may exceed the number in $\mathbb{X}$, as flights can transition and therefore be counted in both bands.

Next, the relative complement of $\mathbb{B}$ in $\mathbb{A}$, $\mathbb{A} \setminus \mathbb{B}$, is taken to describe those flights that were only present in $\mathbb{A}$. These flights only integrated into the TP airspace below 1500 ft (∼460 m) AGL and presumably landed at or departed from the airport or used airspace segment $\mathbb{A}$ to fly through the terminal airspace without landing. Finally, $\mathbb{B} \setminus \mathbb{A}$ describes

those flights that only integrated into the TP airspace from 1500–3000 ft (∼460–910 m) AGL, presumably overflying the airport.

By breaking down the traffic into altitude bands, deviations from convention can be identified. These deviations will be critical in determining UAS integration procedures and the feasibility of a holding stack at the airport of interest. It is clear from the data that a holding stack could not be placed at lower altitudes (i.e., below 1500 ft (∼460 m) AGL), due to the percentage of traffic operating at these altitudes at all airports investigated. If too much traffic is present at higher altitudes (i.e., $\mathbb{B}$), the holding stack will either need to occur at even higher altitudes (i.e., above 3000 ft (∼910 m) AGL), be located in an area away from the runway (defeating many of the advantages of placing the holding stack above the runway), or be deemed infeasible at the airport of interest.

Data for the twelve airports of interest are presented in Table 2. The background color is a gradient based on the assessment of the feasibility of UAS integration, with dark green being the most feasible and white being the least feasible airport. Each row is scaled only according to the values in that row. In general, UAS integration should be more feasible at an airport with more dark green. Airports with mixed green and white, e.g., Visalia (KVIS), are excellent candidates for future simulation studies to investigate and improve upon this proposed concept, as they are complex environments.

Table 2. Number (N) and share of flights (%) in different altitude bands in the TP airspace.

		EDWJ	EDWY	EDFE	EDAZ	KWVI	KOAR	KVIS	0Q4	KAXH	KLVJ	KLNC	KINJ
$N_{\mathbb{A}\cup\mathbb{B}}$ (in $\mathbb{A}$ or $\mathbb{B}$)	[flights]	7117	3495	15,719	6969	21,047	8783	25,273	4475	22,464	19,113	19,661	7287
$N_{\mathbb{A}}$		84.3	70.9	99.8	92.0	88.4	64.5	91.8	43.0	48.4	83.3	67.0	79.0
$N_{\mathbb{B}}$		32.0	37.3	0.5	26.0	63.2	62.4	58.2	62.1	62.2	31.1	51.9	48.9
$N_{\mathbb{A}\cap\mathbb{B}}$ (in $\mathbb{A}$ and $\mathbb{B}$)	[%]	17.3	10.4	0.5	20.0	51.6	26.9	50.0	5.2	10.6	14.4	18.9	27.8
$N_{\mathbb{A}\setminus\mathbb{B}}$ (only in $\mathbb{A}$)		67.6	62.3	99.4	73.8	36.8	37.6	41.8	37.8	37.8	68.9	48.1	51.2
$N_{\mathbb{B}\setminus\mathbb{A}}$ (only in $\mathbb{B}$)		15.1	27.3	0.1	6.2	11.6	35.5	8.2	57.0	51.6	16.7	33.0	21.0

Note to the table: The color gradient is an indicator for the feasibility of UAS integration, with dark green being the most feasible and white being the least feasible airport. Each row is scaled according to the values in that row.

Each individual airport will have its own distribution of traffic. However, the values in Table 2 can help to better understand how today's traffic integrates at these airports. If N is large, it is likely that the airport is consistently busy and thus may present additional integration difficulties to the UAS. Conversely, a small N indicates a less-busy airport, which may not merit a holding stack (e.g., Norderney (EDWY) and Selma (0Q4)).

Take, for example, Watsonville (KWVI) and Visalia (KVIS). At both airports, ∼50–52% of traffic integrates through both $\mathbb{A}$ and $\mathbb{B}$, meaning that a UAS aiming to integrate at these airports will likely need to contend with an aircraft transitioning altitudes, potentially increasing the difficulty of integration. Another ∼37–42% of flights at these two airports are integrated exclusively in $\mathbb{A}$, meaning that a UAS could likely stay clear of this traffic by remaining above 1500 ft (∼460 m) AGL, although the UAS would be flying among traffic in $\mathbb{B}$, unless it was flying above 3000 ft (∼910 m) AGL. However, at these airports, only a small percentage of traffic, ∼8–12%, is found only in $\mathbb{B}$, meaning that the traffic is likely overflying the airport and should have minimal impact on UAS integration and a UAS holding stack.

Putting these three percentages together, it is reasonable to assume that a holding stack at Watsonville (KWVI) and Visalia (KVIS) would need to be placed at higher altitudes, even above 3000 ft (∼910 m) AGL, to remain free of historical traffic. Conversely, Egelsbach (EDFE) and Pearland (KLVJ), which have a low percentage of overflight traffic (0.1% and 16.7%, respectively) and relatively little traffic with large altitude changes (0.5% and 14.4%), may present an easier integration opportunity to the UAS, as the traffic in the TP airspace might be more predictable. An airport like Marina (KOAR), on the other hand, with its more evenly distributed traffic, presents another type of integration hurdle.

To better understand and compare traffic activities at these airports, the analysis of the number of aircraft in Table 2 is supplemented by an assessment of traffic densities in different airspace segments, $\rho_{segment}$. By dividing the number of flights, N, by the volume of the airspace segment of interest in km^3, $V_{\mathbb{X}}$, $V_{\mathbb{A}}$, or $V_{\mathbb{B}}$, the density of aircraft can be found in Table 3. Note that $V_{\mathbb{A}}$ and $V_{\mathbb{B}}$ are half the volume of $V_{\mathbb{X}}$; see Figure 14.

Table 3. Annual traffic densities ($\rho_{segment}$) in different altitude bands in the TP airspace.

			EDWJ	EDWY	EDFE	EDAZ	KWVI	KOAR	KVIS	0Q4	KAXH	KLVJ	KLNC	KINJ
$V_{\mathbb{X}}$[1]:	Volume of $\mathbb{X}$	[km^3]	45.4	18.7	32.2	41.7	70.9	46.9	100.0	22.7	50.4	42.7	29.5	44.3
$\rho_{\mathbb{A}\cup\mathbb{B}}$:	$N_{\mathbb{A}\cup\mathbb{B}}$ per $V_{\mathbb{X}}$	$\left[\frac{\text{flights}}{\text{km}^3}\right]$	156.7	187.3	487.4	167.1	296.9	187.4	252.6	197.2	445.9	447.9	665.4	164.6
$\rho_{\mathbb{A}}$:	$N_{\mathbb{A}}$ per $V_{\mathbb{A}}$		264.3	265.7	972.6	307.6	524.9	241.8	463.7	169.7	431.7	746.5	891.2	259.9
$\rho_{\mathbb{B}}$:	$N_{\mathbb{B}}$ per $V_{\mathbb{B}}$		100.4	139.9	5.1	86.7	375.3	233.9	294.2	245.2	554.8	278.2	690.8	160.8
$\rho_{\mathbb{A}\cap\mathbb{B}}$:	$N_{\mathbb{A}\cap\mathbb{B}}$ per $V_{\mathbb{X}}$	$\left[\frac{\text{flights}}{\text{km}^3}\right]$	25.9	16.1	2.3	30.2	153.2	50.5	126.4	10.2	47.3	64.5	125.7	45.8
$\rho_{\mathbb{A}\setminus\mathbb{B}}$:	$N_{\mathbb{A}\setminus\mathbb{B}}$ per $V_{\mathbb{A}}$		212.5	233.6	969.2	247.2	218.5	140.9	211.0	149.3	337.0	617.6	639.9	168.4
$\rho_{\mathbb{B}\setminus\mathbb{A}}$:	$N_{\mathbb{B}\setminus\mathbb{A}}$ per $V_{\mathbb{B}}$		48.6	107.7	1.0	26.4	69.0	133.0	41.5	224.8	460.1	149.3	439.5	69.2

[1] $V_{\mathbb{A}}$ and $V_{\mathbb{B}}$ are half the volume of $V_{\mathbb{X}}$.

Note to the table: The color gradient is an indicator for the feasibility of UAS integration, with dark green being the most feasible and white being the least feasible airport; the gray color gradient has no implication. Each row is scaled according to the values in that row.

First, if $V_{\mathbb{X}}$ is large, that could indicate that larger aircraft (e.g., jet aircraft) are flying into that airport and/or that the TP is fairly spread out. A large $V_{\mathbb{X}}$ would also dictate a larger horizontal footprint for the holding stack. In general, the German airports exhibit more compact TP airspaces than their US counterparts. Second, $\rho_{\mathbb{A}\cup\mathbb{B}}$ gives an indication of the structure of the TP itself. A well-structured TP (i.e., the parts of the TP are clearly identified and the majority of traffic follows the pattern), such as that of Egelsbach (EDFE), will have a correspondingly high $\rho_{\mathbb{A}\cup\mathbb{B}}$. Conversely, a low $\rho_{\mathbb{A}\cup\mathbb{B}}$ could indicate that the TP is spread out or that, such as at Marina (KOAR), there are supplementary traffic maneuvers in the TP airspace. At Marina (KOAR), planes for skydiving will follow a circular or rounded quadrilateral pattern at altitudes separate from that of the TP; see Figure 13.

Investigating traffic densities is relevant to determining when an airspace segment is "too busy" for UAS integration. These traffic densities will impact the decision-making of UAS operators on how to plan the UAS flight and the UAS integration behavior; see Table 1. As discussed earlier in Section 2.4, safety thresholds need to be derived to distinguish between different levels of traffic (i.e., "minimal" and "saturated"; see Table 1) to determine safe UAS integration behaviors.

Airports with a high $\rho_{\mathbb{A}}$, such as Egelsbach (EDFE), Pearland (KLVJ), and Lancaster (KLNC), have dense TPs (see white or light green color gradient in Figure 13) and therefore a higher probability for UAS to interfere with crewed aircraft in the TP. On the other hand, data from these airports offer UAS more possibilities for predicting the intents of crewed aircraft when integrating into the TP. Additionally, Egelsbach (EDFE) has a relatively low $\rho_{\mathbb{B}}$, indicating that most aircraft in the TP airspace integrate into the TP via airspace segment $\mathbb{A}$. Overall, densities of aircraft that travel through both altitude bands $\mathbb{A}$ and $\mathbb{B}$ of the TP airspace, $\rho_{\mathbb{A}\cap\mathbb{B}}$, are relatively low for all airports. Due to their proximity to major airports, Houston SW (KAXH) and Lancaster (KLNC) have relatively high densities of aircraft that overfly the airports' TP; see white or light green color gradient of $\rho_{\mathbb{B}\setminus\mathbb{A}}$, without actually approaching the airport. A high $\rho_{\mathbb{B}\setminus\mathbb{A}}$ is an indicator for traffic streams that might interfere with a potential holding stack location for UAS. For better comparison, the visualization of traffic densities in different airspace segments of the TP airspace from Table 3 can be found in Appendix A in Figure A1.

4.2.2. Analysis of Crewed Flight Metrics in TP Airspace

In addition to traffic densities, which describe traffic activities on a broader level, nine crewed flight metrics are calculated for each airport of interest and are shown in Table 4 to better characterize individual traffic behaviors at each airport. These flight metrics are provided based on historical flights in the TP airspace, $V_{\mathbb{X}}$. As in the previous Tables 2 and 3, the color green indicates a value that implies greater feasibility for UAS integration.

Table 4. Calculated crewed flight metrics for TP airspace of interest ($V_{\mathbb{X}}$).

		EDWJ	EDWY	EDFE	EDAZ	KWVI	KOAR	KVIS	0Q4	KAXH	KLVJ	KLNC	KINJ
Overall norm. flight h $\mathbb{T}_{\text{overall,norm}}$	$\left[\frac{\text{flight h}}{\text{km}^3}\right]$	42.2	11.1	128.3	15.4	60.1	23.3	30.6	11.0	33.7	134.0	103.5	20.2
Overall norm. flight km $\mathbb{D}_{\text{overall,norm}}$	$\left[\frac{\text{flight km}}{\text{km}^3}\right]$	1937	840	6151	1296	5603	2417	3090	1151	3580	7317	7743	2029
Median flight time $\mathbb{T}_{\text{med}}$	[min]	2.6	1.4	1.9	1.6	3.6	2.2	2.5	1.2	1.3	3.0	1.7	2.8
Median norm. flight time $\mathbb{T}_{\text{med,norm}}$	$\left[\frac{\text{h}}{\text{km}^3}\right]$	0.0009	0.0013	0.0010	0.0006	0.0008	0.0008	0.0004	0.0009	0.0004	0.0012	0.0009	0.0010
Std. dev. norm. flight time $\sigma_{\mathbb{T}_{\text{norm}}}$	$\left[\frac{\text{h}}{\text{km}^3}\right]$	0.0114	0.0140	0.0177	0.0059	0.0049	0.0052	0.0024	0.0062	0.0046	0.0133	0.0125	0.0055
Median flight dist. $\mathbb{D}_{\text{med}}$	[km]	6.2	3.7	4.6	5.1	11.5	8.2	7.7	4.7	5.0	7.7	4.5	8.4
Median norm. flight dist. $\mathbb{D}_{\text{med,norm}}$	$\left[\frac{\text{km}}{\text{km}^3}\right]$	0.14	0.20	0.14	0.12	0.16	0.18	0.08	0.21	0.10	0.18	0.15	0.19
Std. dev. norm. flight dist. $\sigma_{\mathbb{D}_{\text{norm}}}$	$\left[\frac{\text{km}}{\text{km}^3}\right]$	0.38	0.25	0.65	0.27	0.32	0.46	0.15	0.36	0.28	0.54	0.71	0.34
Median flight speed $\mathbb{V}_{\text{med}}$	[kn]	78.5	85.1	76.8	102.8	103.5	121.6	99.5	122.4	124.1	82.7	87.2	97.9

Note to the table: The color gradient is an indicator for the feasibility of UAS integration, with dark green being the most feasible and white being the least feasible airport; the gray color gradient has no implication. Each row is scaled according to the values in that row.

Six of the nine metrics are normalized by the size of the TP airspace, $V_{\mathbb{X}}$, in km^3 (defined in Section 4.1) so as to better compare airports. Equation (4) shows the overall flight hours per km^3, $\mathbb{T}_{\text{overall,norm}}$. This metric is the normalized flight time in the TP airspace for each individual aircraft, t_i, in h, summed across all N flights that occurred during the period of study (i.e., one year). Equation (5) shows a similar metric, the overall

flight kilometers per km^3, $\mathbb{D}_{\text{overall,norm}}$. This metric describes the normalized flight distance in the TP airspace for each individual aircraft, d_i, in km, summed across all N flights.

$$\mathbb{T}_{\text{overall,norm}} = \frac{\sum_{i=1}^{N} t_i}{V_{\mathbb{X}}} \quad \text{in} \quad \frac{\text{flight h}}{\text{km}^3}. \tag{4}$$

$$\mathbb{D}_{\text{overall,norm}} = \frac{\sum_{i=1}^{N} d_i}{V_{\mathbb{X}}} \quad \text{in} \quad \frac{\text{flight km}}{\text{km}^3}. \tag{5}$$

Equations (6) and (7) show the median flight time per km^3, $\mathbb{T}_{\text{med,norm}}$, and the median flight distance per km^3, $\mathbb{D}_{\text{med,norm}}$. These two metrics provide insights about the common flight time and flight distance that a crewed aircraft historically needs in the TP airspace.

$$\mathbb{T}_{\text{med,norm}} = \frac{\text{median}\{t_1, t_2, \ldots, t_N\}}{V_{\mathbb{X}}} \quad \text{in} \quad \frac{\text{h}}{\text{km}^3} \quad \text{per flight.} \tag{6}$$

$$\mathbb{D}_{\text{med,norm}} = \frac{\text{median}\{d_1, d_2, \ldots, d_N\}}{V_{\mathbb{X}}} \quad \text{in} \quad \frac{\text{km}}{\text{km}^3} \quad \text{per flight.} \tag{7}$$

In addition to the median as a measure of central tendency being less sensitive to outliers, the standard deviation in Equations (8) and (9) is used to provide a measure of dispersion to describe the uncertainty that each airport represents in terms of its individual traffic behavior.

$$\sigma_{\mathbb{T}_{\text{norm}}} = \sqrt{\frac{1}{M-1}\sum_{j=1}^{M}\left(\mathbb{T}_{\text{norm, j}} - \overline{\mathbb{T}_{\text{norm}}}\right)^2} \quad \text{with} \quad \overline{\mathbb{T}_{\text{norm}}} = \frac{1}{M}\sum_{j=1}^{M}\mathbb{T}_{\text{norm, j}} \quad \text{in} \quad \frac{\text{h}}{\text{km}^3} \quad \text{per flight.} \tag{8}$$

$$\sigma_{\mathbb{D}_{\text{norm}}} = \sqrt{\frac{1}{M-1}\sum_{j=1}^{M}\left(\mathbb{D}_{\text{norm, j}} - \overline{\mathbb{D}_{norm}}\right)^2} \quad \text{with} \quad \overline{\mathbb{D}_{\text{norm}}} = \frac{1}{M}\sum_{j=1}^{M}\mathbb{D}_{\text{norm, j}} \quad \text{in} \quad \frac{\text{km}}{\text{km}^3} \quad \text{per flight.} \tag{9}$$

In Table 4, $\mathbb{T}_{\text{overall,norm}}$ and $\mathbb{D}_{\text{overall,norm}}$ can also be compared with $\rho_{\mathbb{A}\cup\mathbb{B}}$. These values can have a significant impact on the integration potential at an airport. If, for example, the UAS is in an LC2L state and is headed towards Egelsbach (EDFE), per Section 2.4, the UAS will be able to execute the IAP if there is no traffic (Scenario 4) or, if there is any traffic, will be forced to execute a holding maneuver (Scenario 5).

An airport with a high value of $\mathbb{T}_{\text{overall,norm}}$ indicates that the TP airspace at that airport is more likely to contain at least one aircraft per km^3. A high value of $\mathbb{D}_{\text{overall,norm}}$ indicates that traffic is likely to spatially utilize more of the TP airspace. Airports like Pearland (KLVJ) and Lancaster (KLNC) have a high value of $\mathbb{D}_{\text{overall,norm}}$ and show complete and dense TPs. Norderney (EDWY) and Selma (0Q4), on the other hand, exhibit lower values of $\mathbb{D}_{\text{overall,norm}}$, presumably because there is not much traffic and/or the traffic typically can simply utilize a straight-in approach.

Comparing $\mathbb{T}_{\text{med}}$ and $\mathbb{D}_{\text{med}}$ between different airports provides insights into individual traffic behaviors within the individual TP airspace. Figure 15 shows that a higher $\mathbb{D}_{\text{med}}$ corresponds to a higher $\mathbb{T}_{\text{med}}$ and vice versa. This correlation was expected since aircraft are anticipated to fly standard speeds in the TP, such as 70–90 kn as recommended by the FAA for single-engine airplanes [15]. Airports such as Juist (EDWJ), Norderney (EDWY), Egelsbach (EDFE), Pearland (KLVJ), and Lancaster (KLNC) match these standard speed assumptions, having $\mathbb{V}_{\text{med}}$ in the range of ~77–87 kn. In summary, a larger TP airspace, $V_{\mathbb{X}}$, likely results in a higher $\mathbb{T}_{\text{med}}$ and a higher $\mathbb{D}_{\text{med}}$; see Watsonville (KWVI) and Visalia (KVIS) compared to Norderney (EDWY) and Lancaster (KLNC) in Figure 15. Consequently, a larger TP airspace with a corresponding large historically operated TP is an indicator for higher performance aircraft flying at faster speeds compared to lower performance aircraft

flying lower speeds and therefore shorter TPs; see Watsonville (KWVI) and Visalia (KVIS) with a $\mathbb{V}_{\text{med}}$ of ∼100 kn compared to Norderney (EDWY) and Lancaster (KLNC) with a $\mathbb{V}_{\text{med}}$ of ∼79–87 kn in Figure 15.

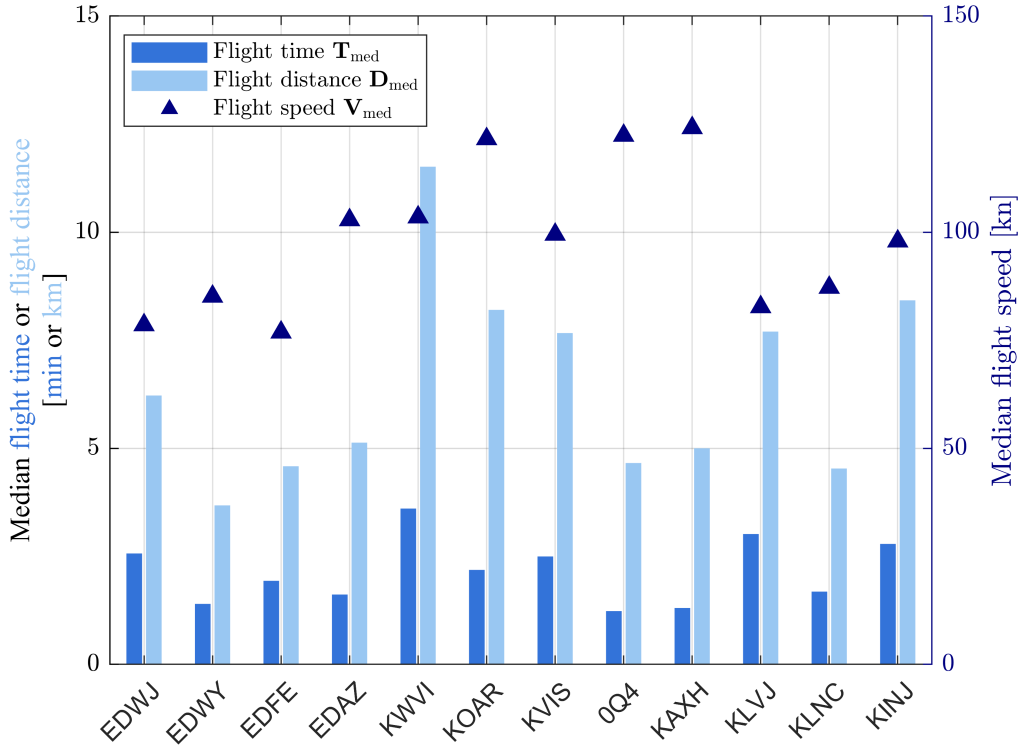

Figure 15. Crewed flight metrics for the TP airspace of interest.

Furthermore, Figure 15 shows that $\mathbb{T}_{\text{med}}$ and $\mathbb{D}_{\text{med}}$ are relatively low for airports such as Selma (0Q4) and Houston SW (KAXH), with $\mathbb{T}_{\text{med}}$ between 1.2 and 1.3 min and $\mathbb{D}_{\text{med}}$ between 4.7 and 5.0 km. Together with relatively high median flight speeds of $\mathbb{V}_{\text{med}} > 120$ kn, Table 2 and the analysis of individual flight trajectories show that these two airports have significant shares of overflying aircraft. At Selma (0Q4), a low-altitude Victor airway is passing right over the airport. Similarly, at Houston SW (KAXH), overflying arriving and/or departing aircraft to or from William P. Hobby (KHOU) airport, an international airport in Houston, Texas, operate at altitudes above 2000 ft AGL (∼610 m). These overflying traffic streams will likely need to be avoided by UAS when integrating into the TP airspace of Selma (0Q4) and Houston SW (KAXH), which also reduces the feasibility of a UAS holding stack at altitudes above conventional TPA.

Accordingly, Figures 16 and 17 provide insights into normalized crewed flight metrics $\mathbb{T}_{\text{med,norm}}$ and $\mathbb{D}_{\text{med,norm}}$. Take, for example, Juist (EDWJ) and Marina (KOAR), both airports have a similar analyzed airspace volume and traffic density in their TP airspace; see Table 3. Looking at their crewed flight metrics, Juist (EDWJ) has a higher $\mathbb{D}_{\text{med,norm}}$ than Marina (KOAR), 0.14 $\frac{\text{km}}{\text{km}^3}$ and 0.18 $\frac{\text{km}}{\text{km}^3}$, whereas both airports have similar values of $\mathbb{T}_{\text{med,norm}}$, 0.0009 $\frac{\text{h}}{\text{km}^3}$ compared to 0.0008 $\frac{\text{h}}{\text{km}^3}$. This implies that aircraft spend less time for the same distance flown in Marina (KOAR), indicating aircraft flying at higher median speeds in the TP airspace, which can be seen in Figure 15 with 78.5 kn for Juist (EDWJ) compared to 121.6 kn for Marina (KOAR). These data suggest that higher shares of aircraft cross the TP airspace without actually approaching Marina (KOAR) or that aircraft fly TPs at higher speeds, likely by aircraft with higher performances such as jet aircraft, compared to operations at Juist (EDWJ). At Marina (KOAR), the density of aircraft crossing the TP

airspace without integrating into conventional TPA, $\rho_{\mathbb{B}\setminus\mathbb{A}}$, is twice as high as in the TP airspace of Juist (EDWJ), 48.6 $\frac{\text{flights}}{\text{km}^3}$ compared to 133.0 $\frac{\text{flights}}{\text{km}^3}$.

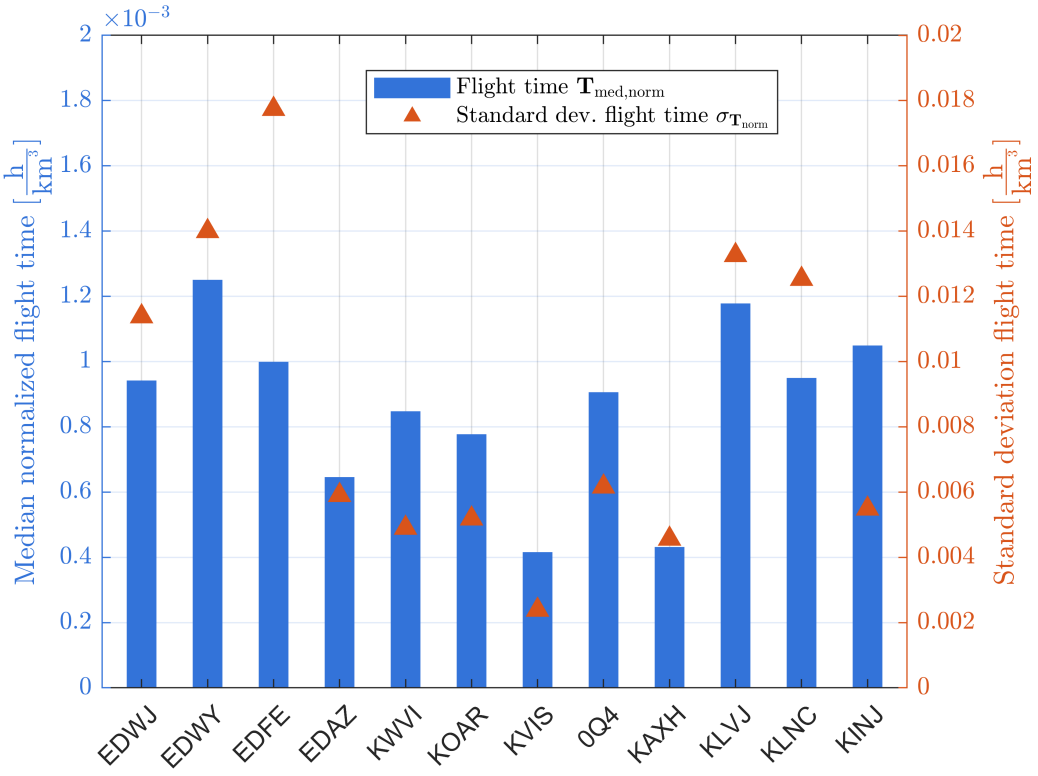

Figure 16. Normalized flight time and standard deviation for TP airspace of interest.

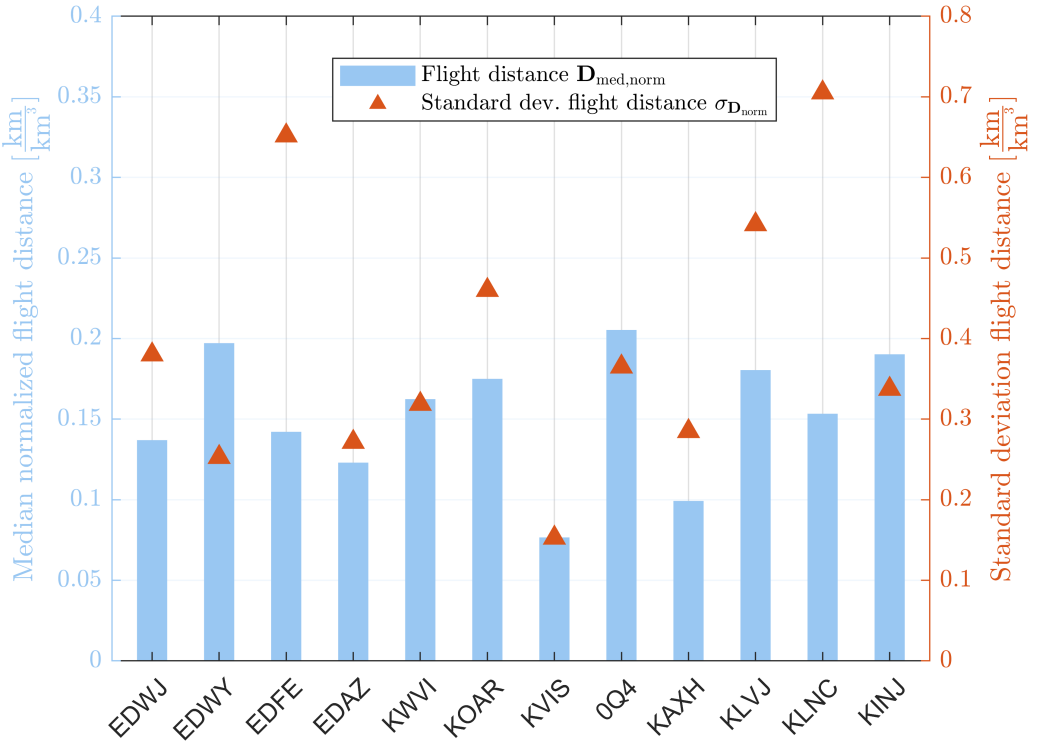

Figure 17. Normalized flight distance and standard deviation for TP airspace of interest.

For UAS integration, considering the number of aircraft in the vicinity of Juist (EDWJ) and Marina (KOAR) together with their $\mathbb{T}_{\text{med,norm}}$ and $\mathbb{D}_{\text{med,norm}}$ would imply similar

number and types of operations at first glance. However, a more in-depth analysis of the data suggests different results. A UAS holding stack at Marina (KOAR) will face traffic streams of crewed aircraft overflying the airport at relatively low altitudes in $V_{\mathbb{B}}$ compared to operations at Juist (EDWJ). This will likely increase the complexity of flight planning and traffic management of UAS transferring in and out of a holding stack located above the airport TP of Marina (KOAR).

Additionally, the standard deviation of flight time and flight distance indicates deviations from convention, which can be expressed in the uncertainty in predicting the flight intent of other aircraft in the TP airspace. Comparing the airports in Figure 16, Egelsbach (EDFE), Pearland (KLVJ), and Lancaster (KLNC), which are also among the airports with the highest traffic density in the TP airspace (see Table 2), have a relatively high standard deviation of their flight time. At first glance, it can be expected that UAS will interfere with a relatively high number of crewed aircraft in the TP airspace of these airports. On the one hand, a high number of historical aircraft will likely improve the prediction of the intent of crewed aircraft. On the other hand, given the data on the standard deviation, the integration of UAS at these three airports appears to be subject to relatively large uncertainties, as the standard deviation at these airports is relatively high, especially in terms of flight time.

Again, comparing traffic activities in the TP airspace of Juist (EDWJ) and Marina (KOAR), the standard deviation of their aircraft's flight distance ($\sigma_{\mathbb{D}_{\text{norm}}}$) is around the same level, 0.38 $\frac{\text{km}}{\text{km}^3}$ and 0.46 $\frac{\text{km}}{\text{km}^3}$. However, the standard deviation of their aircraft flight time ($\sigma_{\mathbb{T}_{\text{norm}}}$) differs significantly, 0.0114 $\frac{\text{h}}{\text{km}^3}$ at Juist (EDWJ) compared to 0.0052 $\frac{\text{h}}{\text{km}^3}$ at Marina (KOAR). One reason for this could be the higher number of overflying aircraft at Marina (KOAR), which, on average, have a lower but more similar flight time compared to aircraft at Juist (EDWJ). More flights at Juist (EDWJ) integrate into the TP of the airport, likely by using varying routes compared to approaching aircraft at Marina (KOAR), which are associated with higher uncertainties. Another probable reason for the comparatively low $\sigma_{\mathbb{T}_{\text{norm}}}$ is the skydiving activities at Marina (KOAR), which follow a predictable, prescribed circular or rounded quadrilateral pattern; see Figure 13.

It can be clearly seen that analyses of traffic densities and crewed flight metrics of aircraft in different altitude bands vary significantly by airport. This is caused by the topography of the airport's surroundings, flight restrictions due to different airspace classes in and around the terminal airspace, and the performance characteristics of landing and departing aircraft. At this point, it can be summarized that non-towered airports are complex environments for integrating UAS and that these airports can be susceptible to uncertainty when it comes to predicting aircraft intent. It is unlikely that a generic "one size fits all" approach for integrating UAS will be feasible for every non-towered airport environment. However, in order to determine if and in which airspace segments the proposed holding stack concept could work, the following section will investigate traffic activities more holistically by considering airspace segments above the TP airspace at the airports of interest, as well as airspace classes and different types of historical aircraft present at these airports.

4.3. Assessment of Locations for UAS Holding Stack in and Above TP Airspace

This section intends to identify locations for UAS holding stacks in and above the TP airspace, which refers to Scenarios 3 and 5 of Table 1. Recalling that a holding stack will likely not be placed below altitudes of 2500 ft (∼760 m) AGL due to altitudes where aircraft conventionally fly the TP (i.e., below 1500 ft (∼460 m) AGL), or in altitudes where aircraft integrate via overhead joins into the TP (i.e., 500 ft (∼150 m) above conventional TPA). Another 500 ft (∼150 m) above the altitudes that are used for overhead joins is reserved as a safety buffer before locating the holding stack. Therefore, for this conceptual approach,

the lowest possible layer of a holding stack for UAS is expected to be located at 2500 ft (∼760 m) AGL; see Figure 18.

In Table 5 and Figure 19, densities of aircraft in altitude bands of the TP airspace, segments $\mathbb{A}$ and $\mathbb{B}$, can be compared with densities above the TP airspace, segments $\mathbb{C}$ and $\mathbb{D}$. Note that $V_{\mathbb{A}}$, $V_{\mathbb{B}}$, $V_{\mathbb{C}}$ and $V_{\mathbb{D}}$ are a quarter of the volume of $V_{\mathbb{Y}}$ and that $V_{\mathbb{Y}}$ is twice the volume of $V_{\mathbb{X}}$; see Figures 14 and 18. Among all airports of interest, Juist (EDWJ), Norderney (EDWY), Egelsbach (EDFE), and Visalia (KVIS) have the lowest $\rho_{\mathbb{C}}$ and $\rho_{\mathbb{D}}$, likely presenting feasible airspace segments for installing a holding stack. Conversely, airports like Pearland (KLVJ) and Lancaster (KLNC) have comparatively high traffic densities above their TP airspace. The airspace of Lancaster (KLNC) has a density of 1177.7 $\frac{\text{flights}}{\text{km}^3}$ in segment $\mathbb{C}$, which is by far the highest value among all investigated airports. Airspace segment $\mathbb{D}$, however, only has a density of 177.9 $\frac{\text{flights}}{\text{km}^3}$, indicating that the segment $\mathbb{D}$ could be better suited to place a UAS holding stack at Lancaster (KLNC). For Pearland (KLVJ), a holding stack might be more feasible in segment $\mathbb{C}$, with a density of 378.8 $\frac{\text{flights}}{\text{km}^3}$ compared to segment $\mathbb{D}$, with a density of 858.8 $\frac{\text{flights}}{\text{km}^3}$.

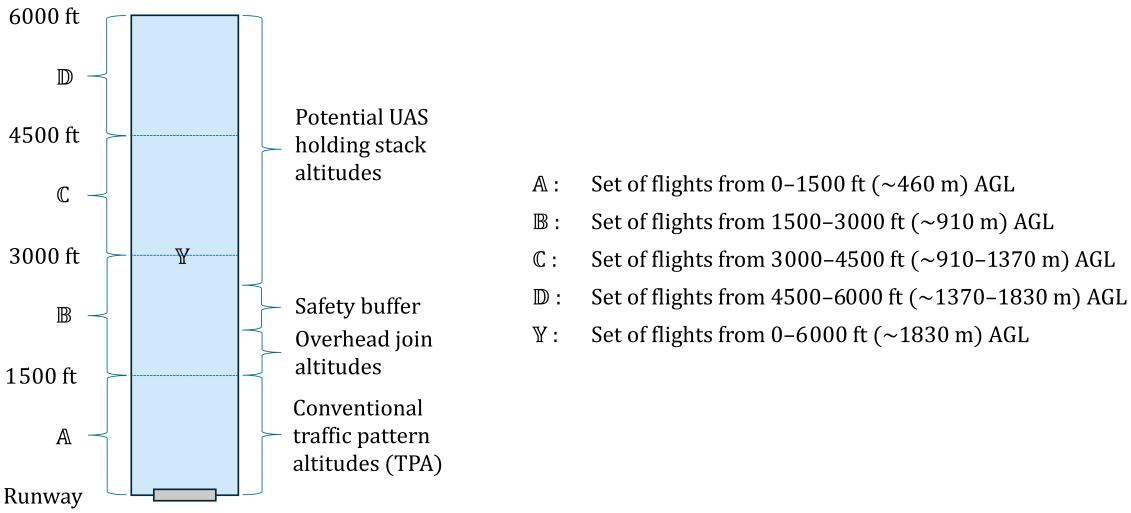

Figure 18. Description of airspace segments in and above the TP airspace.

To better understand individual traffic behaviors, Table 5 investigates average traffic densities, namely the annual median of daily medians of hourly density ($\rho^{\alpha}_{segment}$) for ten standard airport operating hours. Let D be the number of days in the year (i.e., $D = 365$) and $h \in \{8, 9, \ldots, 17\}$ be the airport operating hours considered each day from 8:00 AM to 6:00 PM local time. For each day, $d = 1, 2, \ldots, D$, the hourly flight counts are given by

$$\text{count}_{d,h} = \text{number of flights in hour } h \text{ on day } d.$$

The annual median density, $\rho^{\alpha}_{segment}$, for each airspace segment (V_{segment}: $V_{\mathbb{Y}}$ and $V_{\mathbb{A}}$–$V_{\mathbb{D}}$), see Equation (10), is compared with the total annual densities, $\rho_{\mathbb{Y}}$ and $\rho_{\mathbb{A}}$–$\rho_{\mathbb{D}}$, to assess correlations and deviations between both density metrics.

$$\rho^{\alpha}_{segment} = \frac{\text{median}\left(\left\{\text{median}\left(\text{count}_{d,8}, \ldots, \text{count}_{d,17}\right) \mid d = 1, \ldots, D\right\}\right)}{V_{\text{segment}}} \quad \text{in} \quad \frac{\text{flights}}{\text{km}^3}. \tag{10}$$

The total annual density, $\rho_{segment}$, provides an overall view of all traffic activities. $\rho_{segment}$ is, however, sensitive to peaks, for example, due to seasonal fluctuations. Another density metric, the annual median density, $\rho^{\alpha}_{segment}$, refers to the typical state of traffic at an airport and is insensitive to outliers (e.g., see many 0.00 values in Table 5).

Table 5. Total annual traffic densities ($\rho_{segment}$) and annual median traffic densities ($\rho^{\alpha}_{segment}$) in different altitude bands in and above the TP airspace.

			EDWJ	EDWY	EDFE	EDAZ	KWVI	KOAR	KVIS	0Q4	KAXH	KLVJ	KLNC	KINJ
$V_{\mathbb{X}}$[1,2]: Volume of $\mathbb{X}$		[km^3]	45.4	18.7	32.2	41.7	70.9	46.9	100.0	22.7	50.4	42.7	29.5	44.3
$\mathbb{Y}$	$\rho_{\mathbb{Y}}$: $N_{\mathbb{Y}}$ per $V_{\mathbb{Y}}$	$\left[\frac{\text{flights}}{\text{km}^3}\right]$	81.3	99.3	254.8	163.5	186.4	146.9	139.2	203.9	308.9	451.7	637.1	126.6
	$\rho^{\alpha}_{\mathbb{Y}}$		0.01	0.00	0.07	0.02	0.05	0.04	0.03	0.04	0.05	0.09	0.14	0.02
$\mathbb{A}$	$\rho_{\mathbb{A}}$: $N_{\mathbb{A}}$ per $V_{\mathbb{A}}$	$\left[\frac{\text{flights}}{\text{km}^3}\right]$	264.3	265.7	972.6	307.6	524.9	241.8	463.7	169.7	431.7	746.5	891.2	259.9
	$\rho^{\alpha}_{\mathbb{A}}$		0.02	0.00	0.25	0.07	0.14	0.04	0.11	0.00	0.10	0.21	0.20	0.05
$\mathbb{B}$	$\rho_{\mathbb{B}}$: $N_{\mathbb{B}}$ per $V_{\mathbb{B}}$	$\left[\frac{\text{flights}}{\text{km}^3}\right]$	100.4	139.9	5.1	86.7	375.3	233.9	294.2	245.2	554.8	278.2	690.8	160.8
	$\rho^{\alpha}_{\mathbb{B}}$		0.00	0.00	0.00	0.00	0.10	0.04	0.07	0.00	0.08	0.05	0.14	0.02
$\mathbb{C}$	$\rho_{\mathbb{C}}$: $N_{\mathbb{C}}$ per $V_{\mathbb{C}}$	$\left[\frac{\text{flights}}{\text{km}^3}\right]$	13.6	24.3	16.0	179.1	181.1	218.6	88.1	248.9	544.5	378.8	1177.7	103.1
	$\rho^{\alpha}_{\mathbb{C}}$		0.00	0.00	0.00	0.00	0.03	0.04	0.02	0.00	0.02	0.05	0.20	0.00
$\mathbb{D}$	$\rho_{\mathbb{D}}$: $N_{\mathbb{D}}$ per $V_{\mathbb{D}}$	$\left[\frac{\text{flights}}{\text{km}^3}\right]$	3.9	5.1	31.5	190.6	113.3	155.8	39.9	243.7	79.2	858.8	177.9	102.9
	$\rho^{\alpha}_{\mathbb{D}}$		0.00	0.00	0.00	0.00	0.03	0.04	0.00	0.00	0.00	0.00	0.00	0.00

[1] In this table, annual median densities are based on normalized flight counts over ten airport operating hours from 8:00 AM to 6:00 PM local time. The total annual densities, $\rho_{\mathbb{A}}$–$\rho_{\mathbb{D}}$ are based on flight counts over 24 h.
[2] $V_{\mathbb{A}}$, $V_{\mathbb{B}}$, $V_{\mathbb{C}}$ and $V_{\mathbb{D}}$ are a quarter of the volume of $V_{\mathbb{Y}}$ and $V_{\mathbb{X}}$ is half the volume of $V_{\mathbb{Y}}$.

Note to the table: The color gradient is an indicator for the feasibility of UAS integration, with dark green being the most feasible and white being the least feasible airport; the gray color gradient has no implication. Each row is scaled according to the values in that row.

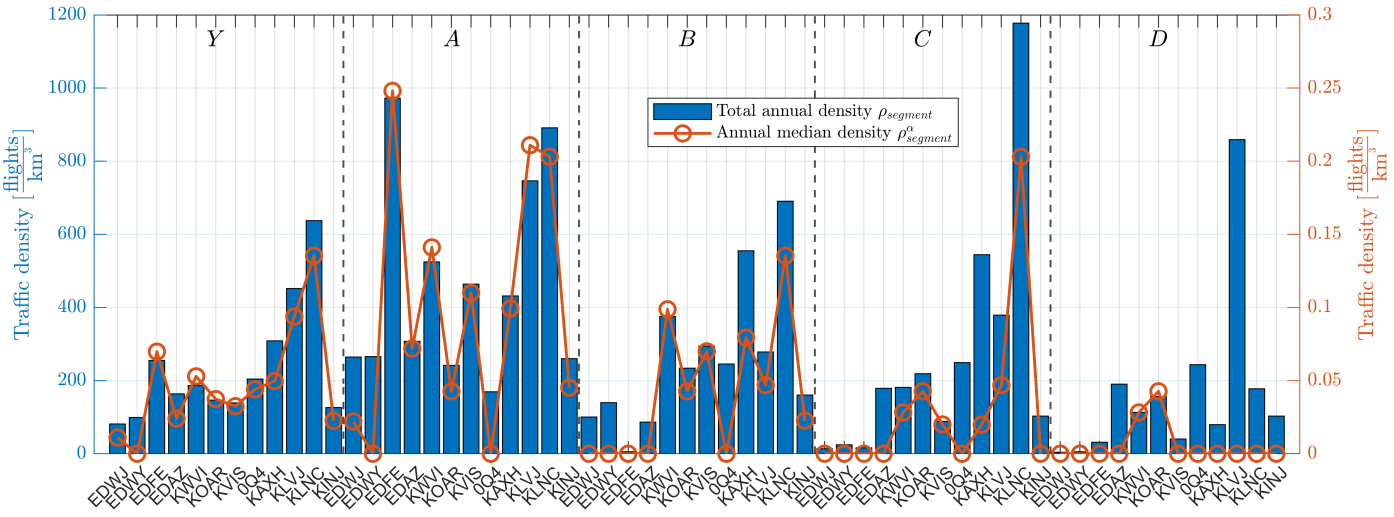

Figure 19. Visualization of total annual traffic densities and annual median traffic densities in different altitude bands in and above the TP airspace.

Generally, it can be assumed that an airport with a large number of total annual flights might have higher hourly medians. However, an airport with a lot of seasonal traffic during a few weeks has higher annual flight counts but lower hourly medians during that year. Conversely, an airport with lower steady traffic activities might have lower

overall annual flights but higher hourly medians over that year. To this end, individual metrics must be assessed and compared to provide a comprehensive view of the feasibility of UAS integration. Especially for initial UAS integration at non-towered airports, both density metrics, $\rho_{segment}$ and $\rho^{\alpha}_{segment}$, should be relatively low to enable safe and efficient integration procedures.

For most airports of interest, $\rho^{\alpha}_{segment}$ correlates with the total annual densities (blue bars); see Figure 19 or color gradients in Table 5. For airports where the correlation is relatively low, for example, $\rho_{\mathbb{C}}$ and $\rho^{\alpha}_{\mathbb{C}}$ at Houston SW (KAXH) and $\rho_{\mathbb{D}}$ and $\rho^{\alpha}_{\mathbb{D}}$ at Pearland (KLVJ), a significant increase in flight counts for individual operating hours of these airports can be observed, which are flattened by the median. See Appendix A Figure A2 for box plot charts visualizing lower and upper spreads and outliers of hourly flight counts at the airports of interest. In summary, the annual median density, $\rho^{\alpha}_{segment}$, provides a steadier picture of airport traffic densities, whereas the annual total density $\rho_{segment}$ provides an overall view of densities, which is not as conclusive when considering it without $\rho^{\alpha}_{segment}$. Therefore, both density metrics play an important role in determining traffic behaviors at non-towered airports. To get a more detailed view of total flights per airspace segment, Appendix A Figure A3 provides a visualization of flight counts similar to Figure 19.

In addition to the analysis of densities $\rho_{\mathbb{Y}}$ and $\rho_{\mathbb{A}}$–$\rho_{\mathbb{D}}$, individual aircraft types at the airports of interest are investigated in these airspace segments, with an overview of airspace classes provided in Tables 6 and 7. At all four non-towered German airports, the airport-specific TPA is surrounded by uncontrolled Class G airspace. At Juist (EDWJ) and Norderney (EDWY), Class G airspace extends from the ground up to 2500 ft (∼760 m) AGL; see Table 6. In Class G airspace, no aircraft receives ATC separation services and no clearance from ATC needs to be obtained prior to entering Class G airspace. Above Class G airspace at Juist (EDWJ) and Norderney (EDWY), controlled Class E airspace extends from the upper boundary of Class G to 10,000 ft MSL (approximately corresponding to Flight Level (FL)100 under standard pressure conditions). In Class E airspace, IFR aircraft get separated from other IFR aircraft and all IFR aircraft need a clearance before entering Class E airspace [14].

Table 6. Airspace classes and regulations around airports of interest in Germany.

				Juist (EDWJ)	**Norderney (EDWY)**	**Egelsbach (EDFE)**	**Schoenhagen (EDAZ)**
Airspace Class		**ATC Separation**	**ATC Clearance**				
Controlled airspace	Class C	IFR to V/IFR	V/IFR	>Class E	>Class E	>Class D	>Class E
	Class D	IFR to IFR	V/IFR	–	–	Class G to 2500 ft MSL	–
	Class E	IFR to IFR	IFR	Class G to FL100	Class G to FL100	–	Class G to Class C [1]
Uncontrolled airspace	Class G	No	No	Ground to 2500 ft AGL	Ground to 2500 ft AGL	Ground to 1500 ft MSL	Ground to 1000 ft AGL
Recommended TPA				600 ft MSL (592 ft AGL)	700 ft MSL (694 ft AGL)	1300 ft MSL (915 ft AGL)	1000 ft MSL (848 ft AGL)

[1] Class C airspace right above Schoenhagen (EDAZ) begins at 2500 ft (∼760 m) MSL. Note that another Class C airspace north of Schoenhagen (EDAZ) already begins at 1500 ft (∼460 m) MSL.

The surrounding airspace of Egelsbach (EDFE) and Schoenhagen (EDAZ) is more complex in terms of regulations. Egelsbach (EDFE) has the strictest airspace regulations

of all German non-towered airports, a designated ATZ, RMZ and TMZ (as explained in Section 2.1.1), which extend from the ground up to 1500 ft (∼460 m) MSL as part of Class G airspace. Note that the ATZ/RMZ/TMZ around Egelsbach (EDFE) is specified in MSL, whereas the uncontrolled airspace of the other German airports examined is specified in AGL. Above 1500 ft (∼460 m) MSL, controlled Class D airspace extends from 1500 ft (∼460 m) MSL to 2500 ft (∼760 m) MSL at Egelsbach (EDFE). Here, VFR aircraft in addition to IFR aircraft require an ATC clearance as well. Above 2500 ft (∼760 m) MSL, controlled Class C airspace extends up to FL100, where IFR aircraft are separated from VFR and IFR aircraft by ATC. Schoenhagen (EDAZ) has surrounding Class G airspace together with a designated RMZ from the ground up to 1000 ft (∼300 m) AGL. Above that, Class E extends up to controlled Class C airspace, which begins at 2500 ft (∼760 m) MSL [14].

Table 7. Airspace classes and regulations around airports of interest in California and Texas.

				Watsonville (KWVI)	**Marina (KOAR)**	**Visalia (KVIS)**	**Selma (0Q4)**
Airspace Class		**ATC Separation**	**ATC Clearance**				
Controlled airspace	Class B	V/IFR to V/IFR	V/IFR	–	–	–	–
	Class C	IFR to V/IFR	IFR [1]	–	1500 ft to 4200 ft MSL	–	–
	Class D	IFR to IFR	IFR [1]	–	–	–	–
	Class E	IFR to IFR	IFR	Class G to FL180	Class G to 1500 ft MSL; Class C to FL180	Ground to FL180	Class G to FL180
Uncontrolled airspace	Class G	No	No	Ground to 700 ft AGL	Ground to 700 ft AGL	–	Ground to 1200 ft AGL
Recommended TPA				1163 ft MSL (1000 ft AGL)	1137 ft MSL (1000 ft AGL)	1293 ft MSL (1000 ft AGL)	1105 ft MSL (800 ft AGL)

				Houston SW (KAXH)	**Pearland (KLVJ)**	**Lancaster (KLNC)**	**Hillsboro (KINJ)**
Airspace Class		**ATC Separation**	**ATC Clearance**				
Controlled airspace	Class B	V/IFR to V/IFR	V/IFR	2500 ft MSL to FL100	2000 ft MSL to FL100	4000 ft MSL to FL110	–
	Class C	IFR to V/IFR	IFR [1]	–	–	–	–
	Class D	IFR to IFR	IFR [1]	–	–	–	–
	Class E	IFR to IFR	IFR	Class G to 2500 ft MSL; Class B to FL180	Class G to 2000 ft MSL; Class B to FL180	Class G to 4000 ft MSL; Class B to FL180	Class G to FL180
Uncontrolled airspace	Class G	No	No	Ground to 700 ft AGL	Ground to 700 ft AGL	Ground to 700 ft AGL	Ground to 700 ft AGL
Recommended TPA				1070 ft MSL (1000 ft AGL)	1044 ft MSL (1000 ft AGL)	1501 ft MSL (1000 ft AGL)	1686 ft MSL (1000 ft AGL)

[1] Pilots flying VFR must establish a two-way radio communication with ATC.

Generally, the airspace classes around airports in California and Texas (Table 7) follow similar rules compared to Germany. In uncontrolled Class G airspace, aircraft are not subject to separation by ATC or need to receive a clearance prior to entry into terminal airspace. In airspace Classes D and C, however, only IFR aircraft require ATC clearance, but VFR aircraft are required to establish a two-way radio communication link. In the US, uncontrolled airspace Class G is commonly bounded at lower altitudes compared to Germany. Note that in the US, non-towered airports can also be located in controlled airspace Class E, such as Visalia (KVIS), whereas in Germany, Class E airspace is not dedicated to terminal airspaces. Houston SW (KAXH), Pearland (KLVJ) and Lancaster (KLNC) have a Class B airspace bordering their Class E airspace at relatively low altitudes (i.e., 2500 ft, 2000 ft, and 4000 ft MSL, respectively), which restricts all aircraft to ATC separation and clearances. In Germany, there is no Class B airspace.

In the US, when operating under IFR, ATC clearance "delivery" is needed before landing at or taking off from a non-towered airport, which would give the aircraft IFR clearance to arrive or depart. Note that this refers to an airport clearance, not an airspace clearance (referred to as ATC clearance in Tables 6 and 7). An IFR aircraft transitioning from Class E to Class G airspace does not need ATC clearance; it would normally only change airspace classes in this way if it intends to land at an airport that is located in Class G airspace, whereby the "one-in/one-out" paradigm still applies.

Since the lowest possible layer of a UAS holding stack is expected to be located at 2500 ft (∼760 m) AGL, see Figure 18, a holding above each of the airports of interest will take place in controlled airspace. A holding for UAS in controlled airspace, which are expected to fly under IFR as explained in Section 2.3.2, comes with advantages and disadvantages. On the one hand, in every controlled airspace, IFR aircraft get separated from other IFR aircraft, which enhances operational safety compared to IFR flights in uncontrolled airspace. On the other hand, introducing UAS operations at a larger scale will likely have a significant impact on ATC workloads and will increase the overall airspace complexity of the air traffic management (ATM) system. However, integrating crewed and uncrewed aircraft within one airspace environment could be managed by concepts such as U-space and dynamic airspace reconfiguration (DAR), for example, the latter aiming to enhance collaboration between ATC and digital USSP managing UAS traffic (currently subject to research in European U-space development) [45].

In addition to the traffic densities analyzed above, the following analysis intends to better explain and understand crewed traffic behaviors in altitude bands relevant for potential holding stack locations (i.e., above 2500 ft (∼760 m) AGL) by assessing different types of aircraft. Aircraft that operated in the TP airspace and above up to 6000 ft (∼1830 m) AGL are visualized and analyzed for the respective year according to different categories:

LA: "Light-weight" civilian fixed-wing aircraft with $<$ 2.0 t MTOW;
MA: "Medium-weight" civilian fixed-wing aircraft with 2.0–5.7 t MTOW;
HA: "Heavy-weight" civilian fixed-wing aircraft with $>$ 5.7 t MTOW;
GLI: Non-motor-driven civilian fixed-wing aircraft such as gliders;
HEL: Civilian rotary-wing aircraft such as helicopters;
MIL: Military fixed-wing and rotary-wing aircraft;
OTH: Other aircraft such as balloons or gyrocopters;
N/A: Aircraft with a missing type designator.

The following Figures 20 and 21 visualize arriving and departing flights over the course of a year (i.e., data for the latest available year, 2022 for German airports and 2023 for US airports). Each data point represents a flight, the y-axis indicates the altitude at which the flight initially integrated into the analyzed airspace, and the x-axis indicates the flight distance of each flight in and above TP airspace. The color of each data point

shows the aircraft type of each flight according to the above mentioned aircraft categories. Additionally, to better understand historical flight behaviors at the airports of interest, flight tracks for three different scenarios have been investigated:

1. Total annual flights in and above the TP airspace;
2. Annual flights integrating into the conventional TPA;
3. Annual flights overflying the conventional TPA.

The first scenario, "total annual flights in and above the TP airspace", provides data for all flights in the respective year, whereas the second and third scenarios focus on subsets of flights. The second scenario, "annual flights integrating into the conventional TPA", considers all flights that operated in conventional TPA (i.e., below 1500 ft (∼460 m) AGL) at any time during their flight and could therefore have flown above the TP airspace before integrating into conventional TPA, as indicated by the mapping of the data points to the *y*-axis. The third scenario, "annual flights overflying the conventional TPA", only considers flights that did not operate in conventional TPA and thus overflew the airport. Visualizations of the second flight track scenario (Figures A4 and A5) and third flight track scenario (Figures A6 and A7) can be found in Appendix A.

On the one hand, UA RPs want to avoid executing holding maneuvers at altitudes where traffic streams of aircraft fly before or while integrating into the TP (i.e., second flight track scenario). On the other hand, UA RPs also want to avoid executing holding maneuvers in altitudes where traffic streams of aircraft overfly conventional TPA (i.e., third flight track scenario). Looking at analyses of real airport environments, the following Figures 20 and 21 provide insights into different UAS integration problems.

Juist (EDWJ) has a total of 7385 annual flights in and above its TP airspace; see Figure 20a. Most flights are operated by the "LA" category (5954) followed by "HEL" flights (802), "MA" flights (232) and "GLI" flights (226). Flights in the "LA" category have a higher variation in their flight distance compared to the "HEL" category, indicating that "HEL" flights likely take similar approaches to the runway of Juist (EDWJ) or that they cross TP airspace altitudes on similar flight paths. Investigating individual "HEL" trajectories of the data sets, it can be seen that significant shares of "HEL" flights cross the TP airspace on their way to offshore wind parks located north of Juist (EDWJ); see Figure 12.

Furthermore, it can be seen that 226 "GLI" flights occur with 223 "GLI" flights landing and/or departing Juist (EDWJ) (see Figure A4a). At Juist (EDWJ), "GLI" flights have comparatively long flight distances and relatively low initial integration altitudes, probably due to leisure trips around the North Sea island, and departing "GLI" flights usually land back at Juist (EDWJ). For UAS integration, this implies that approaching UAS will be confronted with comparatively predictable "HEL" flights with short flight distances and less predictable "GLI" flights with relatively distributed, longer flight distances.

Considering less busy airspace segments for potential UAS holding stack locations above 2500 ft (∼760 m) AGL, it can be seen that the share of total annual historical flights significantly decreases at altitudes above 3500 ft (∼1070 m) AGL. Additionally, most aircraft integrate into conventional TPA at or below 1500 ft (∼460 m) AGL (see Figure A4a) and limited aircraft overfly the airport above 3500 ft (∼1070 m) AGL. Having similar distributions of flights at Norderney (EDWY), feasible multilayer holding locations for UAS above 3500 ft (∼1070 m) AGL can be suggested.

Historical flight activities at Egelsbach (EDFE), see Figure 20c, look different compared to Juist (EDWJ) and Norderney (EDWY). At Egelsbach (EDFE), significant shares of flights, except for "HA" flights, operate in conventional TPA up to 1500 ft (∼460 m) AGL and especially in uncontrolled Class G airspace. Smaller amounts of aircraft operate in controlled Class D airspace above Class G airspace, where every aircraft needs ATC clearance.

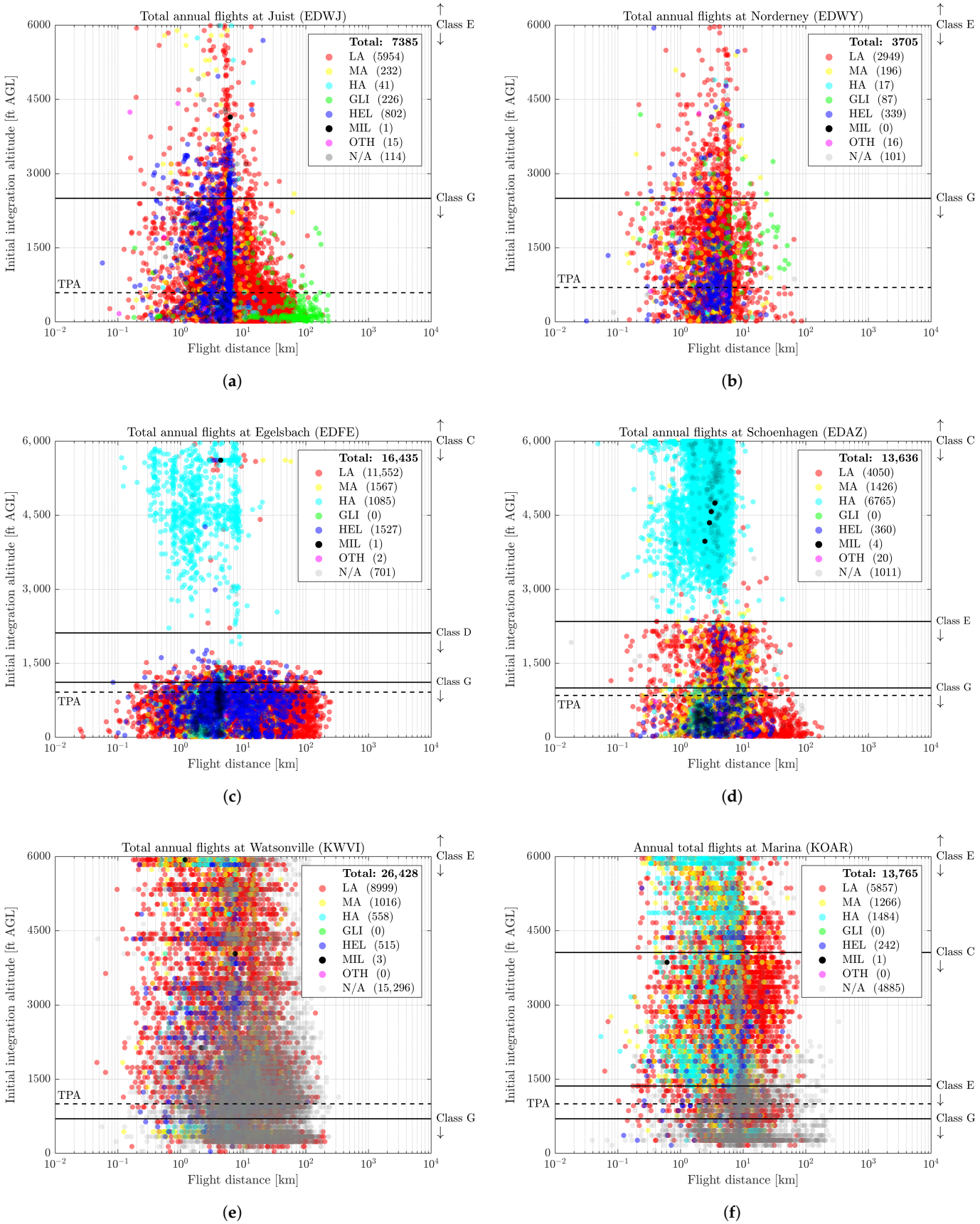

Figure 20. Scatter plots for airports of interest for total annual flights in the TP airspace and above up to 6000 ft (∼1830 m) AGL. Each data point indicates the initial airspace integration altitude (y-axis), the operated flight distance (x-axis), and the aircraft type (color): (**a**) Juist (EDWJ). (**b**) Norderney (EDWY). (**c**) Egelsbach (EDFE). (**d**) Schoenhagen (EDAZ). (**e**) Watsonville (KWVI). (**f**) Marina (KOAR).

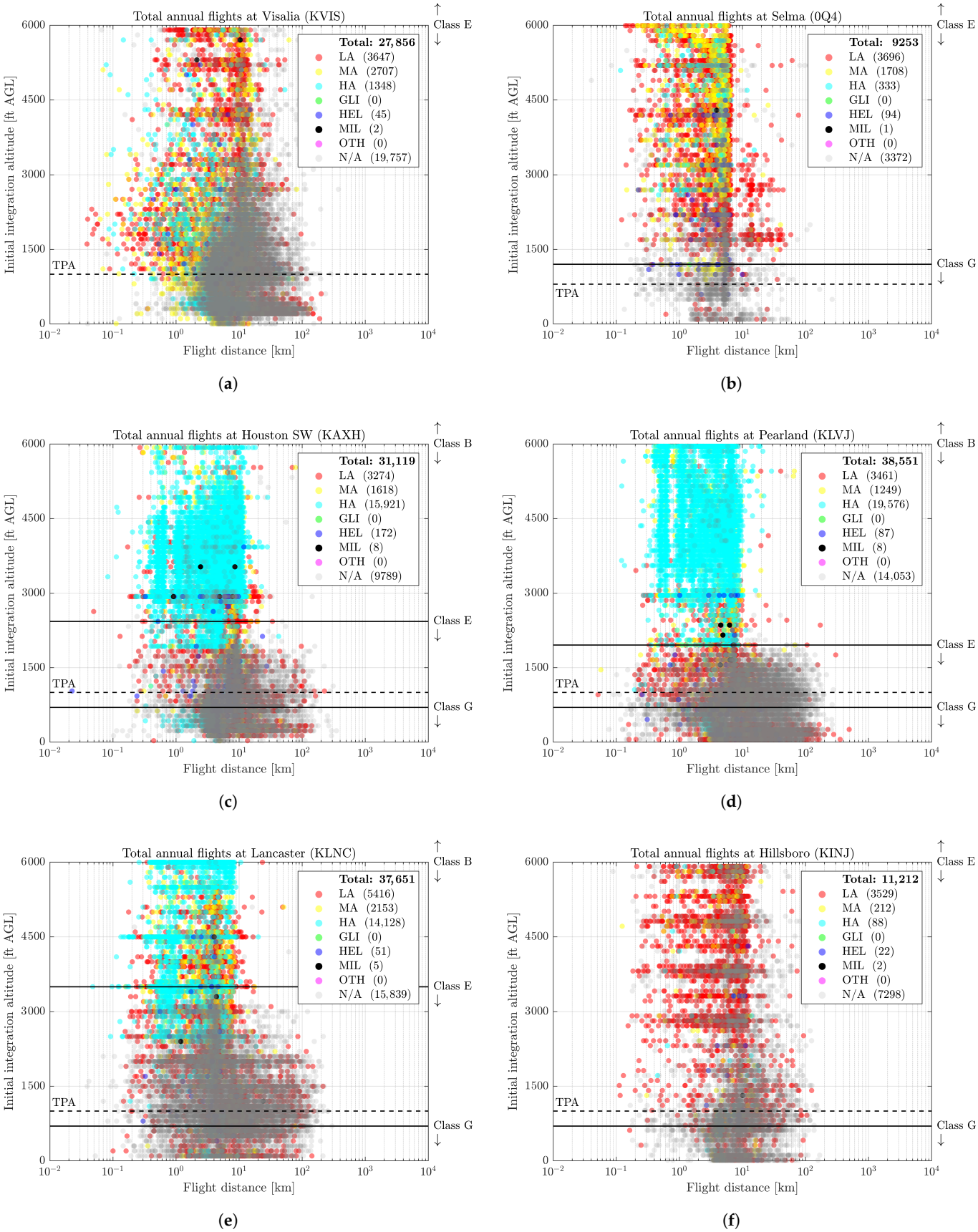

Figure 21. Scatter plots for airports of interest for total annual flights in the TP airspace and above up to 6000 ft (∼1830 m) AGL. Each data point indicates the initial airspace integration altitude (y-axis), the operated flight distance (x-axis), and the aircraft type (color): (**a**) Visalia (KVIS). (**b**) Selma (0Q4). (**c**) Houston SW (KAXH). (**d**) Pearland (KLVJ). (**e**) Lancaster (KLNC). (**f**) Hillsboro (KINJ).

Since Egelsbach (EDFE) is in close proximity to the busiest German airport, Frankfurt (EDDF), it can be seen that most flights, except for "HA" flights, integrate in Class G airspace, probably to reduce ATC workload and to separate VFR aircraft from traffic streams of "HA" flights. Traffic streams of "HA" flights increasingly overfly Egelsbach (EDFE) at altitudes above 4000 ft (∼1220 m) AGL (see Figure A6c), likely on their way to or from Frankfurt (EDDF). For Egelsbach (EDFE), holding altitudes between the defined minimum UAS holding altitude of 2500 ft (∼760 m) AGL and 4000 ft (∼1220 m) AGL could be ideal for a UAS holding stack. However, as mentioned earlier, ATC would need to provide clearances to UAS in case of a holding maneuver above 1500 ft (∼460 m) MSL.

Schoenhagen (EDAZ) provides another type of UAS integration hurdle. Significant shares of smaller aircraft operate in Class E airspace and below, see Figure 20d, while even more aircraft, especially "HA" flights, overfly the TP airspace (see Figure A6d). At Schoenhagen (EDAZ), an IAP from the south-east towards the capital airport of Germany, Berlin (EDDB), is located right above Schoenhagen (EDAZ), likely towards runway 07L or 07R. This implies that Schoenhagen (EDAZ) is potentially not a feasible candidate for a UAS holding stack above the TP airspace. However, a holding layer could be squeezed in between 2500 ft (∼760 m) and 3000 ft (∼910 m) AGL, which is the only low-traffic altitude band at Schoenhagen (EDAZ).

Watsonville (KWVI) and Marina (KOAR) are both relatively busy non-towered airports with varying types of aircraft increasingly distributed among all altitudes in and above their TP airspace. Note that comparatively high shares of flights at US airports do not have an aircraft type listed in their data sets and are therefore labeled "N/A" type aircraft. At first glance, it can be assumed that a multilayer holding stack for UAS might be more feasible next to the TP airspace of Watsonville (KWVI) and Marina (KOAR) instead of above. At both airports, significant shares of aircraft overfly conventional TPA (see Figure A6e,f) with fewer flights integrating into conventional TPA from above 3000 ft (∼910 m) AGL (see Figure A4e,f). Therefore, no specific recommendation for a UAS holding stack location is made for Watsonville (KWVI) and Marina (KOAR). However, flight track data imply that, if UAS were to integrate into the TP from above the airport, UAS would increasingly have to interact with overflying aircraft instead of TP-integrating aircraft, which are likely more predictable as they exhibit shorter flight distances compared to aircraft integrating into conventional TPA.

For the remaining US airports, it can be summarized that most flights integrated below 3000 ft (∼910 m) AGL into conventional TPA (see Figure A5a–f) and that Houston SW (KAXH), Pearland (KLVJ), and Lancaster (KLNC) have significant shares of "HA" flights overflying conventional TPA (see Figure A7c–e). It can also be seen that overflying "HA" flights exhibit shorter flight distances than flights in Class E airspace, which mostly integrate into conventional TPA, flying the TP or parts of the TP and therefore exhibit longer flight distances than overflying aircraft.

Most of the "HA" flights occur in controlled Class B airspace, where all aircraft need to receive ATC clearance and ATC separation services. Placing holding stacks in controlled airspace altitudes of these airports would significantly increase UAS interaction with overflying aircraft, as well as ATC workload. On the other hand, integrating UAS through controlled airspace Class B likely enhances operational safety for the UAS and surrounding traffic. For Houston SW (KAXH), a holding stack layer might be feasible above overflying traffic streams at 5500–6000 ft (∼1680–1830 m) AGL. However, a holding for UAS at such a high altitude would result in a long descent to conventional TPA, with a high proportion of overflying aircraft between the holding layer and conventional TPA, resulting in another UAS integration hurdle.

Both Visalia (KVIS) and Hillsboro (KINJ) have relatively high shares of flights integrating in conventional TPA below 3000 ft AGL (∼910 m) (see Figure A5a,f) and high shares of flights overflying the TP airspace (see Figure A7a,f). Additionally, historical traffic in the surrounding airspace of both airports can be seen to use flight paths at specific altitudes, which are likely based on dedicated VFR cruising altitudes or flight levels [55]. At Visalia (KVIS), traffic streams of flights occur between 4000–4500 ft (∼1220–1370 m) AGL and 5000–5500 ft (∼1520–1680 m) AGL. This implies that a holding stack layer might fit in altitude bands between each of these overflying traffic streams at 3500–4000 ft (∼1070–1220 m) AGL and at 4500–5000 ft (∼1370–1520 m) AGL. Similar observations can be made for Hillsboro (KINJ), traffic streams appear at 2500–3000 ft (∼760–910 m) AGL, 3500–4000 ft (∼1070–1220 m) AGL and 4500–5000 ft (∼1370–1520 m) AGL. Accordingly, one holding stack layer each might be feasible at altitudes between these overflying traffic streams. Finally, Selma (0Q4) has almost no flights integrating into conventional TPA below 1500 ft (∼460 m) AGL (see Figure A5b), but relatively distributed traffic activities between all other altitude bands. Therefore, no specific recommendations for UAS holding stack locations are made for Selma (0Q4).

In summary, most of the analyzed airports (except for Watsonville (KWVI), Marina (KOAR) and Visalia (KVIS)) have limited shares of historical flights that integrated into conventional TPA from above 3000 ft (∼910 m) AGL. Therefore, if airports have busier altitudes above 3000 ft (∼910 m) AGL, UAS and their holding stack locations will mostly interact with overflying aircraft, which might be more predictable due to shorter flight distances than aircraft that integrate at an airport by flying some or all parts of the TP, for example.

4.4. Determining UAS Behavior for TP Integration

This section summarizes the key findings for UAS integration and holding stack locations at the airports of interest, provided in Table 8, and discusses the TP integration cases for UAS, which have been proposed as part of the conceptual operating scheme in Figure 9. Implications are based on the discussed total and median traffic densities as well as crewed flight metrics. Along with providing a detailed picture of terminal airspace traffic activities and UAS integration hurdles, implications intend to help identify potential altitude bands for UAS holding stacks, the potential number of vertical layers of holding stacks and vertical flight distances that UAS need to cover to integrate from the lowest holding stack layer into the TPA.

Based on the analysis of the airports of interest, different UAS integration hurdles can be summarized based on the previous observations:

- **High variation of crewed aircraft performances**: High variations in crewed aircraft types with varying performances across altitude bands make it challenging to predict aircraft intent to determine safe and efficient flight paths for UAS.
- **High uncertainty of crewed flight intents**: High standard deviations of crewed flight metrics make state-based intent prediction of crewed aircraft more challenging.
- **Dense population across altitude bands**: A high number of flights across different altitude bands increases the risk of interaction between crewed and uncrewed aircraft. This reduces the number of potential holding stack layers in these altitude bands, making holdings for UAS above the TPA less feasible.
- **Long integration distances into the TP**: High vertical holding altitudes result in high vertical integration distances for UAS from their holding position into the TP. This could imply that a holding stack next to the TP airspace might be safer and more efficient for individual airports.

Table 8. Summary of key traffic activities and implications for UAS integration at airports of interest.

		Juist (EDWJ)	**Norderney (EDWY)**	**Egelsbach (EDFE)**	**Schoenhagen (EDAZ)**	**Watsonville (KWVI)**	**Marina (KOAR)**
$\mathbb{T}_{\text{med,norm}}$	$\left[\frac{\text{h}}{\text{km}^3}\right]$	0.0009	0.0013	0.0010	0.0006	0.0006	0.0006
$\sigma_{\mathbb{T}_{\text{norm}}}$	$\left[\frac{\text{h}}{\text{km}^3}\right]$	0.0114	0.0140	0.0177	0.0059	0.0046	0.0045
$\mathbb{D}_{\text{med,norm}}$	$\left[\frac{\text{km}}{\text{km}^3}\right]$	0.14	0.20	0.14	0.12	0.12	0.14
$\sigma_{\mathbb{D}_{\text{norm}}}$	$\left[\frac{\text{km}}{\text{km}^3}\right]$	0.38	0.25	0.65	0.27	0.28	0.38
Annual median densities[1]	$\left[\frac{\text{flights}}{\text{km}^3}\right]$	$\rho^\alpha_{\mathbb{A}}$ $\rho^\alpha_{\mathbb{B}}$ $\rho^\alpha_{\mathbb{C}}$ $\rho^\alpha_{\mathbb{D}}$	$\rho^\alpha_{\mathbb{A}}$ $\rho^\alpha_{\mathbb{B}}$ $\rho^\alpha_{\mathbb{C}}$ $\rho^\alpha_{\mathbb{D}}$	$\rho^\alpha_{\mathbb{A}}$ $\rho^\alpha_{\mathbb{B}}$ $\rho^\alpha_{\mathbb{C}}$ $\rho^\alpha_{\mathbb{D}}$	$\rho^\alpha_{\mathbb{A}}$ $\rho^\alpha_{\mathbb{B}}$ $\rho^\alpha_{\mathbb{C}}$ $\rho^\alpha_{\mathbb{D}}$	$\rho^\alpha_{\mathbb{A}}$ $\rho^\alpha_{\mathbb{B}}$ $\rho^\alpha_{\mathbb{C}}$ $\rho^\alpha_{\mathbb{D}}$	$\rho^\alpha_{\mathbb{A}}$ $\rho^\alpha_{\mathbb{B}}$ $\rho^\alpha_{\mathbb{C}}$ $\rho^\alpha_{\mathbb{D}}$
Total annual densities	$\left[\frac{\text{flights}}{\text{km}^3}\right]$	$\rho_{\mathbb{A}}$ $\rho_{\mathbb{B}}$ $\rho_{\mathbb{C}}$ $\rho_{\mathbb{D}}$	$\rho_{\mathbb{A}}$ $\rho_{\mathbb{B}}$ $\rho_{\mathbb{C}}$ $\rho_{\mathbb{D}}$	$\rho_{\mathbb{A}}$ $\rho_{\mathbb{B}}$ $\rho_{\mathbb{C}}$ $\rho_{\mathbb{D}}$	$\rho_{\mathbb{A}}$ $\rho_{\mathbb{B}}$ $\rho_{\mathbb{C}}$ $\rho_{\mathbb{D}}$	$\rho_{\mathbb{A}}$ $\rho_{\mathbb{B}}$ $\rho_{\mathbb{C}}$ $\rho_{\mathbb{D}}$	$\rho_{\mathbb{A}}$ $\rho_{\mathbb{B}}$ $\rho_{\mathbb{C}}$ $\rho_{\mathbb{D}}$
Potential less busy altitude bands for a holding stack[2]		> 3500 ft AGL	> 3500 ft AGL	2500 ft–4000 ft AGL	2500 ft–3000 ft AGL	No recommendation	No recommendation
Potential number of vertical holding stack layers[3,4]		5	5	3	1	-	-
Recommended TPA		600 ft MSL (592 ft AGL)	700 ft MSL (694 ft AGL)	1300 ft MSL (915 ft AGL)	1000 ft MSL (848 ft AGL)	1163 ft MSL (1000 ft AGL)	1137 ft MSL (1000 ft AGL)
Vertical distance from lowest holding layer into TPA		∼ 2400 ft	∼ 2800 ft	∼ 1600 ft	∼ 1650 ft	-	-

		Visalia (KVIS)	**Selma (0Q4)**	**Houston SW (KAXH)**	**Pearland (KLVJ)**	**Lancaster (KLNC)**	**Hillsboro (KINJ)**
$\mathbb{T}_{\text{med,norm}}$	$\left[\frac{\text{h}}{\text{km}^3}\right]$	0.0004	0.0008	0.0002	0.0003	0.0002	0.0007
$\sigma_{\mathbb{T}_{\text{norm}}}$	$\left[\frac{\text{h}}{\text{km}^3}\right]$	0.0024	0.0049	0.0039	0.0102	0.0094	0.0047
$\mathbb{D}_{\text{med,norm}}$	$\left[\frac{\text{km}}{\text{km}^3}\right]$	0.06	0.18	0.07	0.07	0.05	0.14
$\sigma_{\mathbb{D}_{\text{norm}}}$	$\left[\frac{\text{km}}{\text{km}^3}\right]$	0.16	0.29	0.25	0.41	0.54	0.28
Annual median densities[1]	$\left[\frac{\text{flights}}{\text{km}^3}\right]$	$\rho^\alpha_{\mathbb{A}}$ $\rho^\alpha_{\mathbb{B}}$ $\rho^\alpha_{\mathbb{C}}$ $\rho^\alpha_{\mathbb{D}}$	$\rho^\alpha_{\mathbb{A}}$ $\rho^\alpha_{\mathbb{B}}$ $\rho^\alpha_{\mathbb{C}}$ $\rho^\alpha_{\mathbb{D}}$	$\rho^\alpha_{\mathbb{A}}$ $\rho^\alpha_{\mathbb{B}}$ $\rho^\alpha_{\mathbb{C}}$ $\rho^\alpha_{\mathbb{D}}$	$\rho^\alpha_{\mathbb{A}}$ $\rho^\alpha_{\mathbb{B}}$ $\rho^\alpha_{\mathbb{C}}$ $\rho^\alpha_{\mathbb{D}}$	$\rho^\alpha_{\mathbb{A}}$ $\rho^\alpha_{\mathbb{B}}$ $\rho^\alpha_{\mathbb{C}}$ $\rho^\alpha_{\mathbb{D}}$	$\rho^\alpha_{\mathbb{A}}$ $\rho^\alpha_{\mathbb{B}}$ $\rho^\alpha_{\mathbb{C}}$ $\rho^\alpha_{\mathbb{D}}$
Total annual densities	$\left[\frac{\text{flights}}{\text{km}^3}\right]$	$\rho_{\mathbb{A}}$ $\rho_{\mathbb{B}}$ $\rho_{\mathbb{C}}$ $\rho_{\mathbb{D}}$	$\rho_{\mathbb{A}}$ $\rho_{\mathbb{B}}$ $\rho_{\mathbb{C}}$ $\rho_{\mathbb{D}}$	$\rho_{\mathbb{A}}$ $\rho_{\mathbb{B}}$ $\rho_{\mathbb{C}}$ $\rho_{\mathbb{D}}$	$\rho_{\mathbb{A}}$ $\rho_{\mathbb{B}}$ $\rho_{\mathbb{C}}$ $\rho_{\mathbb{D}}$	$\rho_{\mathbb{A}}$ $\rho_{\mathbb{B}}$ $\rho_{\mathbb{C}}$ $\rho_{\mathbb{D}}$	$\rho_{\mathbb{A}}$ $\rho_{\mathbb{B}}$ $\rho_{\mathbb{C}}$ $\rho_{\mathbb{D}}$
Potential less busy altitude bands for a holding stack[2]		> 3500 ft AGL	No recommendation	5500 ft–6000 ft AGL	No recommendation	No recommendation	> 3000 ft AGL
Potential number of vertical holding stack layers[3,4]		2–3	-	1	-	-	2–3
Recommended TPA		1293 ft MSL (1000 ft AGL)	1105 ft MSL (800 ft AGL)	1070 ft MSL (1000 ft AGL)	1044 ft MSL (1000 ft AGL)	1501 ft MSL (1000 ft AGL)	1686 ft MSL (1000 ft AGL)
Vertical distance from lowest holding layer into TPA		∼ 2500 ft	-	∼ 4500 ft	-	-	∼ 2000 ft

[1] Annual median of daily medians of hourly density.

[2] Potential altitude bands for UAS holding stack locations are not based on safety thresholds, whereas "ideal" locations would likely be determined based on numerical values and specific thresholds.

[3] The upper bound of the UAS holding stack is expected to be limited to 6000 ft (∼1830 m) AGL.

[4] Depends on the vertical space between individual overflying traffic streams.

When comparing the airports of interest with each other, fluctuations can be observed in the measured variables, presented in Table 8. Again, note that the color gradient is an indicator for the feasibility of UAS integration, with dark green being the most feasible and white being the least feasible airport. Each row is scaled according to the values of all twelve airports of interest. However, for annual median densities and total annual densities, the color gradient for $\rho^{\alpha}_{\mathbb{A}}$, for example, is based only on all $\rho^{\alpha}_{\mathbb{A}}$ values of the twelve airports.

Crewed flight metrics at Juist (EDWJ) and Schoenhagen (EDAZ) have average values between the investigated airports; however, total annual densities at Juist (EDWJ) are lower than at Schoenhagen (EDAZ), especially $\rho_{\mathbb{C}}$ and $\rho_{\mathbb{D}}$. At Juist (EDWJ), lower densities in higher altitudes likely result in more feasible holding layers. However, based on historical flight data, Schoenhagen (EDAZ) has a 500 ft ($\sim$150 m) altitude band with relatively few flights, potentially feasible for one holding layer, at a comparatively low altitude. This will likely result in a shorter vertical integration distance from holding into the TPA compared to the holding layers at Juist (EDWJ). Ideally, it can be expected that UAS holdings above the airport should be placed as low as possible to reduce the transition distance from holding into the TP.

On the other hand, Egelsbach (EDFE) also has low values of $\rho_{\mathbb{C}}$ and $\rho_{\mathbb{D}}$, but higher standard deviations for its crewed flight metrics. As a result, choosing the appropriate holding altitude or time window for TP integration might be subject to greater uncertainty.

Norderney (EDWY) exhibits high values for crewed flight metrics (i.e., $\mathbb{T}_{\text{med,norm}}$ and $\mathbb{D}_{\text{med,norm}}$), which probably affect efficient UAS integration into the TP airspace. As a result, statistically, UAS will have to interact with crewed aircraft, which spend more time and consume more space in the TP airspace compared to aircraft at other airports.

Airports like Watsonville (KWVI), Marina (KOAR) and Selma (0Q4) have fairly average values for their crewed flight metrics, standard deviations and densities in different altitude bands. Therefore, this paper does not provide specific recommendations for UAS integration and holding maneuvers, which likely makes these airports more difficult candidates for the initial integration of UAS.

Airports like Pearland (KLVJ) and Lancaster (KLNC) have comparatively low values of their crewed flight metrics and average standard deviations for flights in the TP airspace, but high total traffic densities (white color gradient) in and above their TP airspace. However, especially at Pearland (KLVJ), the annual median density is inversely correlated with the total annual density (dark green color gradient of $\rho^{\alpha}_{\mathbb{D}}$ compared to white color gradient of $\rho_{\mathbb{D}}$), which indicates a higher spread of flight counts (e.g., due to seasonal fluctuations) and/or higher shares of outliers. Even though UAS might be able to efficiently integrate into the airports TP due to fairly predictable flight intents (low expected crewed flight time and flight distance likely result in the same for UAS), traffic densities above the airport are probably too high for the placement of holding stacks. Here, airspace segments outside of the TP airspace should be investigated to determine airspace segments where a holding for UAS would be more feasible.

Houston SW (KAXH) exhibits low values for crewed flight metrics and standard deviations, but higher densities between its different airspace segments. The only less frequented altitude band is relatively high (i.e., green color gradient of $\rho^{\alpha}_{\mathbb{D}}$ and $\rho_{\mathbb{D}}$) and might only accommodate one holding layer. Therefore, UAS would have to fly a long distance from holding to the TPA with potentially loads of traffic in between. The long integration distance probably makes UAS integration from a holding rather inefficient. Identifying airspace segments outside the TP airspace might be more efficient and safe for UAS integration.

Considering the color gradient in Table 8 as an indicator for the feasibility of UAS integration, Visalia (KVIS) would be the "ideal" candidate among the airports of interest (followed by Hillsboro (KINJ) and Juist (EDWJ)). Similar to Houston SW (KAXH), Visalia (KVIS) has both comparatively low values for crewed flight metrics and standard deviations, but also exhibits relatively low densities relevant for determining holding stack locations, $\rho_{\mathbb{C}}$–$\rho_{\mathbb{D}}$ and $\rho^{\alpha}_{\mathbb{C}}$–$\rho^{\alpha}_{\mathbb{D}}$. However, Visalia (KVIS) appears to have traffic streams of overflying aircraft that span over two altitude bands of ∼500 ft (∼150 m); see Figure 21a between 4000–4500 ft (∼1220–1370 m) AGL and 5000–5500 ft (∼1520–1680 m) AGL, which would likely want to be avoided in the case of a planned UAS holding.

In summary, it is challenging to provide realistic recommendations for the feasibility of UAS holding stacks without numerical safety thresholds that describe whether it is safe to perform a holding pattern or not. As mentioned earlier, safety thresholds are needed to distinguish between different levels of traffic to determine safe UAS integration procedures. In particular, at selected US airports, higher shares of traffic are more evenly distributed across investigated altitude bands compared to their German counterparts. Therefore, in order to better determine holding locations and procedural integration options for UAS, more detailed analyses of risks of interaction, their potential impact, and safety thresholds to determine "minimal" and "saturated" levels of traffic for individual altitude bands will have to be investigated in the future.

Although the exact thresholds between the theoretical scenarios described in Section 2.4 are an area of future regulatory work, the metrics and variables presented herein can be used by authorities and rule makers as input parameters in simulation studies designed to establish those thresholds. Taking into account correlations and deviations between the different discussed quantitative measures, traffic activities need to be investigated from different angles to get a detailed picture of crewed flight behaviors at non-towered airports and to derive potential UAS integration options. As proposed in Figure 9, the following Figure 22 presents five potential integration designs for a UAS integrating into the TP of a non-towered airport, depending on whether a UAS holding stack is required or not.

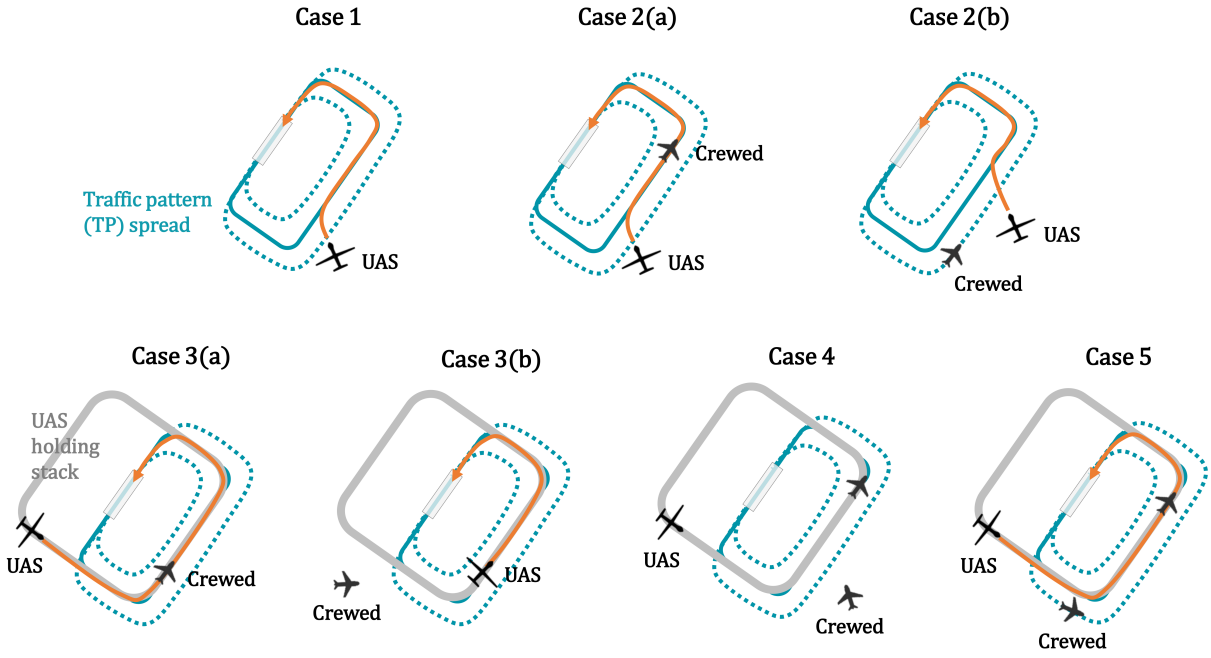

Figure 22. Different TP integration cases of UAS based on traffic densities and crewed flight metrics. Note that UAS are expected to transition via a standard overhead join approach from holding into the TP downwind leg. For simplicity, the overhead joins are not drawn in this figure.

Cases 1–3 present nominal flight situations, with Case 1 representing the simplest TP integration procedure. If there is no ongoing traffic in the terminal airspace, then the UAS can safely integrate into the TP without regard to other aircraft, for example, by performing a straight-in approach or by integrating into the downwind leg of the TP. Case 2 refers to "minimal" current traffic in the terminal airspace. Here, a threshold, called "minimal" traffic in this research, will determine that it is not required to transfer into holding. However, the UAS will have to interact with other aircraft in its vicinity while integrating into the downwind leg of the TP. Note that there are currently no regulatory-defined separation minima that would specify procedural spacing and merging of UAS with other traffic, especially in the terminal airspace. In addition to Case 2, Cases (a) and (b) determine when and how a UAS might integrate with current crewed traffic. Cases (a) and (b) use historical crewed flight metrics to determine the expected flight time and flight distance of current crewed aircraft. If historical flight data, ideally matching exactly the aircraft type of the current aircraft, have spent a lot of time in the TP airspace and have taken up a lot of airspace (i.e., high values for $\mathbb{T}_{\text{med,norm}}$ and $\mathbb{D}_{\text{med,norm}}$), then the UAS might want to integrate ahead of the other aircraft to increase efficiency. If the opposite is the case, the safest option would be to follow the preceding aircraft into the TP.

Case 3 involves "saturated" current traffic in the terminal airspace, which would now require the UAS to transfer into holding. Accordingly, the UAS will have to descend from holding into the TP. Again, Cases (a) and (b) determine when and how the integration with crewed aircraft in the vicinity of the airport should take place into the TP, but now from holding.

Cases 4–5 present off-nominal flight situations, such as during an LC2L, probably the most severe in-flight situation of a UAS. If any crewed aircraft is present in the terminal airspace, the UAS impaired by the LC2L will be required to transfer into holding. Accordingly, the UAS will have to stay in holding (Case 4) until all other aircraft have integrated into the TP. If that is the case, the UAS will descend from holding into the TP by following the preceding aircraft (Case 5).

5. Conclusions

To keep pace with ongoing advancements in aviation technologies and related air mobility concepts, this research provides implications for the design of terminal airspaces and procedures for how emerging UAS operations might integrate into today's non-towered airports. Considering terminal airspace and procedure design guidelines from ICAO and EUROCONTROL, this paper focuses on deriving design implications by assessing factors such as traffic density, flow complexity, type of aircraft operations, and local conditions and/or restrictions [43].

To date, there have been few studies analyzing terminal traffic data in the context of UAS airspace integration, especially in non-towered airport environments. There is a significant lack of data on existing and forecast crewed traffic activities to enable strategic and tactical air traffic flow management for safe and efficient UAS integration at non-towered airports.

This paper provides analyses of historical flight activities of crewed aircraft in terminal airspaces of non-towered airports and a methodology for UAS operators and regulators to quantify and better understand crewed traffic behaviors. Although unlikely that there will be a "one size fits all" approach for integrating UAS at non-towered airports, this research discusses historical crewed flight track data and their implications for efficient and safe terminal UAS airspace integration. To that end, a conceptual operating scheme for UAS at non-towered airports and different variables are derived, which quantitatively assess traffic activities in the terminal airspace and, more importantly, in the TP of non-towered

airports, which depend on the individual airport layout, environmental constraints, and the different types of aircraft that operate at these airports. Systematically identifying the TP airspace to assess traffic activities in the TP is intended to help determine where, when, and how UAS should integrate into the TP of a non-towered airport.

Furthermore, this paper proposes and discusses the feasibility of a holding stack concept for UAS in and above the TP airspace, using twelve real airport environments as examples. The proposed concept is designed to provide an internationally harmonized integration approach for UAS to safely separate from crewed aircraft around non-towered airports. A holding stack for UAS, which might be managed by concepts such as U-space, is intended to facilitate safe procedural TP integration of UAS, in addition to conflict resolution capabilities on board the UAS. Once the ongoing traffic activities of an individual airport exceed a certain safety threshold, the UAS is expected to transfer into holding in or above the TP airspace. Accordingly, if traffic uncertainty has been resolved and it is safe for the UAS to leave its holding position, the UAS is expected to integrate from holding via the overhead join approach into the TP.

Based on historical flight track analyses for the twelve airport environments, this paper provides implications on different UAS integration hurdles and on whether a holding in or above the TP airspace might be feasible. In the end, five different TP integration cases for UAS are discussed, which are likely to be impacted by the implications of historical traffic data presented in this paper. However, safe and efficient TP integration will require UAS to have robust merging and spacing integration capabilities, which have not yet been defined and standardized in regulations.

The approach presented in this paper can also help to inform decision-making processes for UAS contingency procedures. Assuming a UAS needs to divert from its flight plan due to an LC2L and has to approach the closest non-towered airport, assessing historical traffic activities helps to identify the risk of UAS interfering with crewed aircraft for different non-towered airports.

Due to a lack of standards and procedural contingency/emergency regulations, dynamic transitions between holding and missed approach under LC2L conditions will have to be investigated in more detail in the future and have not been discussed in-depth in this research. However, building on RTCA, Inc. DO–400, "Guidance Material: Standardized Lost C2 Link Procedures for Uncrewed Aircraft Systems", this paper provides insights into the need to define arrival, approach, and landing LC2L procedure guidelines and to "…investigate the potential need to separate UA holding patterns from traditionally piloted aircraft holding patterns" [37] (p. 52) such as mentioned in DO–400 Recommendations #13 and #14.

The proposed concept for UAS airspace integration at non-towered airports is based on a suite of metrics and variables against which that concept can be tested for different airport environments. Accordingly, this research is based on several operational assumptions, which are critical for concept implementation. First, it is expected that policy makers and regulators will certify onboard DAA functions for UAS to enable safe separation from VFR aircraft in terminal environments. Second, to enable VFR-like operational flexibility and IFR-like airspace accessibility, authorities will have to adapt current flight rules or introduce new sets of flight rules to enable highly automated UAS operations at scale, especially in uncontrolled airspace. Third, traffic management concepts such as U-space and respective digital services will have to be certified and implemented to enable increasingly automated and cooperative airspace interaction between traditional airspace users and new airspace entrants.

Furthermore, additional quantitative research is needed to algorithmically determine a standard decision-making process to derive "ideal" UAS holding altitudes and the

expected distribution of holding layers based on historical crewed and projected UAS traffic activities.

Additional research will have to be conducted to investigate integration potentials of UAS into TP airspaces by assessing performance-based separation minima between different categories of UAS and between UAS and crewed aircraft to determine airspace conflict risks. Using performance characteristics of individual UAS (e.g., uncrewed Cessna 208 Caravan), the maximum occupancies of terminal airspaces of non-towered airports can be algorithmically determined, based on historical traffic densities for an individual time interval (e.g., within the day or hour). This approach will help to tailor holding stacks to individual classes of terminal airspace conflict risks to perform simulations across a variety of representative non-towered airport environments.

Finally, future work will have to investigate communication mechanisms of multiple simultaneous UAS in the holding stack and their interface mechanisms with existing UAS traffic management concepts such as U-space to enable real-world flight tests.

Author Contributions: Conceptualization, T.F.S., J.S., H.I., N.P., V.B., E.N. and D.J.; methodology, T.F.S., J.S., H.I., N.P., V.B., E.N. and D.J.; software, T.F.S., J.S., N.P. and E.N.; validation, T.F.S., J.S., H.I., N.P., V.B., E.N. and D.J.; formal analysis, T.F.S. and J.S.; investigation, T.F.S. and J.S.; resources, T.F.S. and J.S.; data curation, T.F.S. and J.S.; writing—original draft preparation, T.F.S. and J.S.; writing—review and editing, T.F.S., J.S., N.P. and E.N.; visualization, T.F.S.; project administration, T.F.S. All authors have read and agreed to the published version of the manuscript.

Funding: This research received no external funding.

Data Availability Statement: Relevant data can be found in the manuscript. Restrictions apply to the availability of raw data sets used from Flightradar24. Raw data obtained from Flightradar24 are available at https://www.flightradar24.com (accessed on 21 June 2023) with the permission of Flightradar24. Raw data from Sherlock Data Warehouse are openly available from the NASA Technical Reports Server at https://www.nasa.gov/ames/aviationsystems/sherlock-data-warehouse (accessed on 13 August 2024). Selected processed data sets are available from the corresponding authors on reasonable request.

Acknowledgments: This work was conducted under the ATM-X cooperation agreement between NASA and DLR.

Conflicts of Interest: The authors declare no conflicts of interest.

Abbreviations

The following abbreviations are used in this manuscript:

ACAS	Airborne Collision Avoidance System
ADS-B	Automatic Dependent Surveillance-Broadcast
AGL	Above Ground Level
AMM	Airport Management Module
ASFK	Average Number of Simultaneous Flights per Square Kilometer
ATC	Air Traffic Control
ATM	Air Traffic Management
ATZ	Aerodrome Traffic Zone
C2	Command and Control
CA	Collision Avoidance
ConOps	Concept of Operations
DAA	Detect and Avoid
DAR	Dynamic Airspace Reconfiguration
DLR	German Aerospace Center
EASA	European Union Aviation Safety Agency

eVTOL	electric Vertical Takeoff and Landing
FAA	Federal Aviation Administration
FAF	Final Approach Fix
FL	Flight Level
HD	Horizontal Distance
IAF	Initial Approach Fix
IAP	Instrument Approach Procedure
ICAO	International Civil Aviation Organization
IF	Intermediate Fix
IFR	Instrument Flight Rules
IMC	Instrument Meteorological Condition
ILS	Instrument Landing System
GBSS	Ground-Based Surveillance System
LC2L	Lost Command and Control Link
MLAT	Multilateration
MSL	Mean Sea Level
MTOW	Maximum Takeoff Weight
NASA	National Aeronautics and Space Administration
RAM	Regional Air Mobility
RMZ	Radio Mandatory Zone
ROD	Rate of Descent
RP	Remote Pilot
SATS	Small Aircraft Transportation System
SCA	Self-Controlled Area
SID	Standard Instrument Departure Route
STAR	Standard Terminal Arrival Route
TCA	Terminal Control Area
TMA	Terminal Maneuvering Area
TMZ	Transponder Mandatory Zone
TP	Traffic Pattern
TPA	Traffic Pattern Altitude
UA	Uncrewed Aircraft
UAS	Uncrewed Aircraft System
US	United States
USSP	U-Space Service Provider
VD	Vertical Distance
VFR	Visual Flight Rules
VHF	Very High Frequency
VMC	Visual Meteorological Condition
VOC	Visual Operating Chart
WP	Waypoint

Appendix A

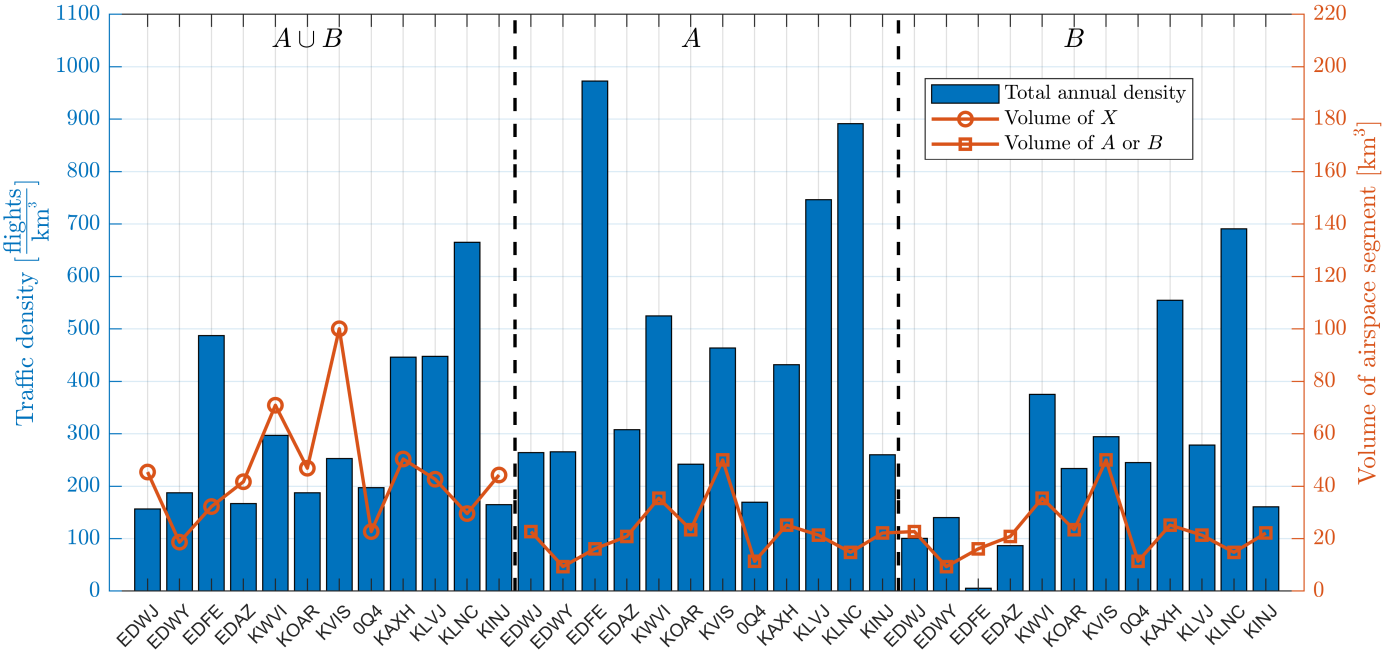

(**a**)

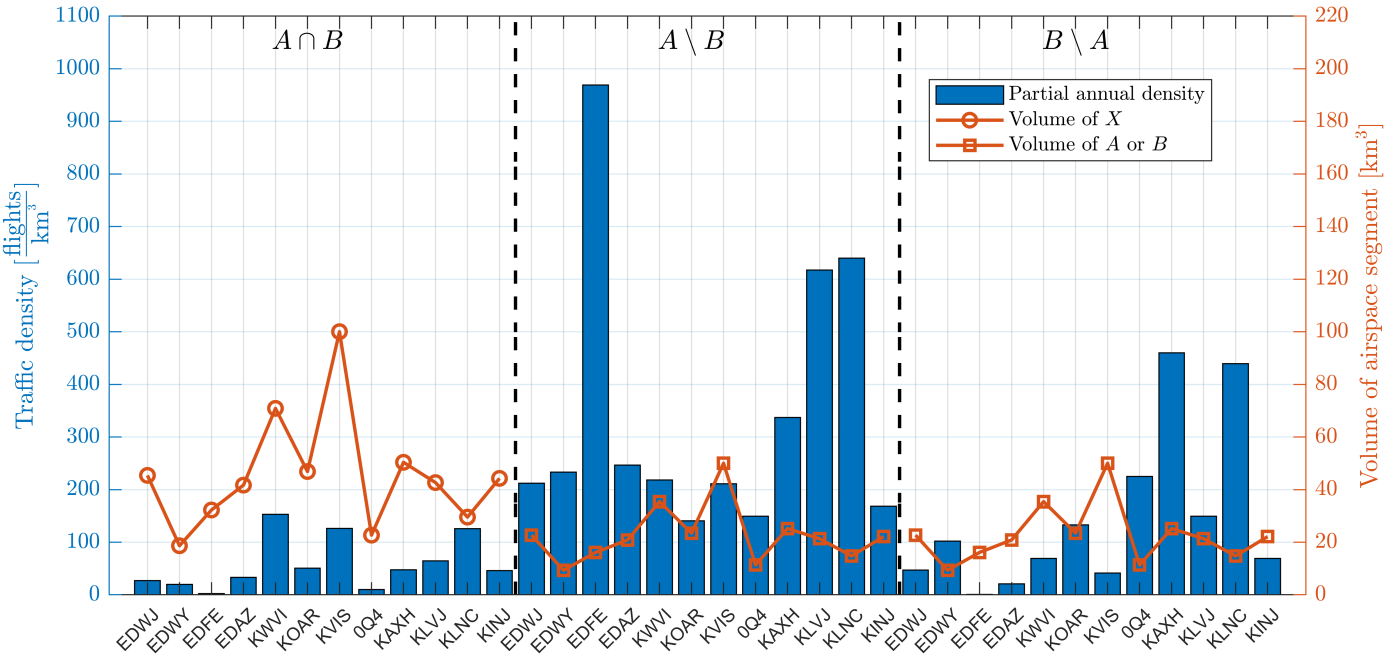

(**b**)

Figure A1. Sets of traffic densities in altitude bands of the TP airspace: (**a**) Visualization of total annual traffic densities in the TP airspace, in conventional TPA, and above conventional TPA. (**b**) Visualization of partial annual traffic densities in the TP airspace, in conventional TPA, and above conventional TPA.

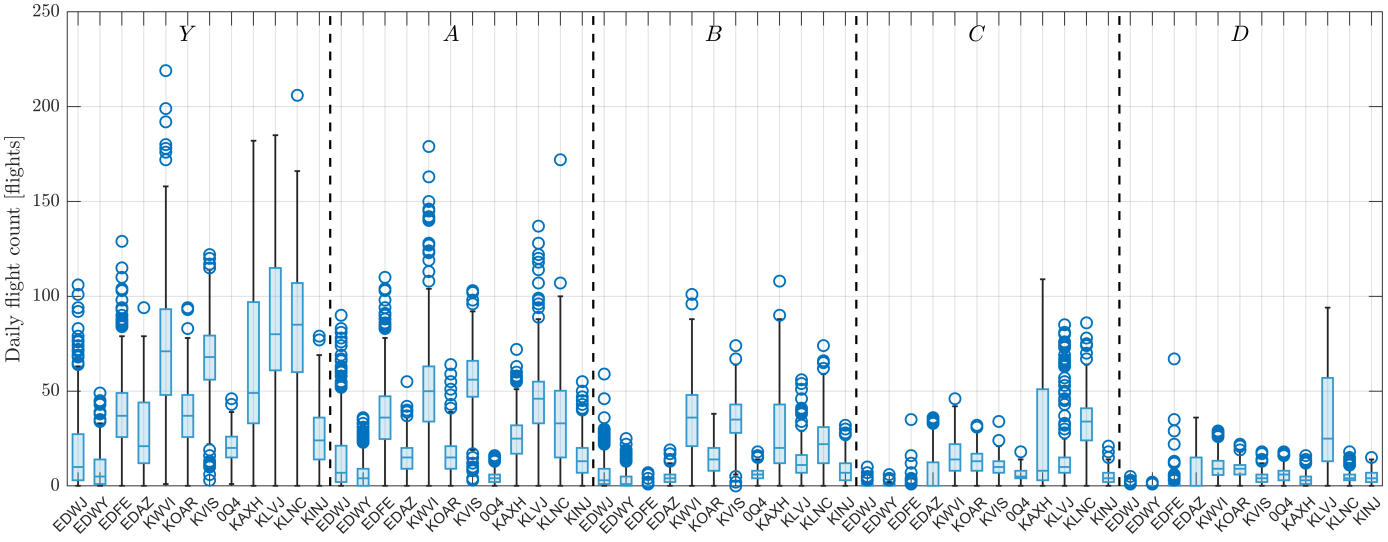

Figure A2. Box plot charts of daily flight counts in different altitude bands in and above the TP airspace over one year.

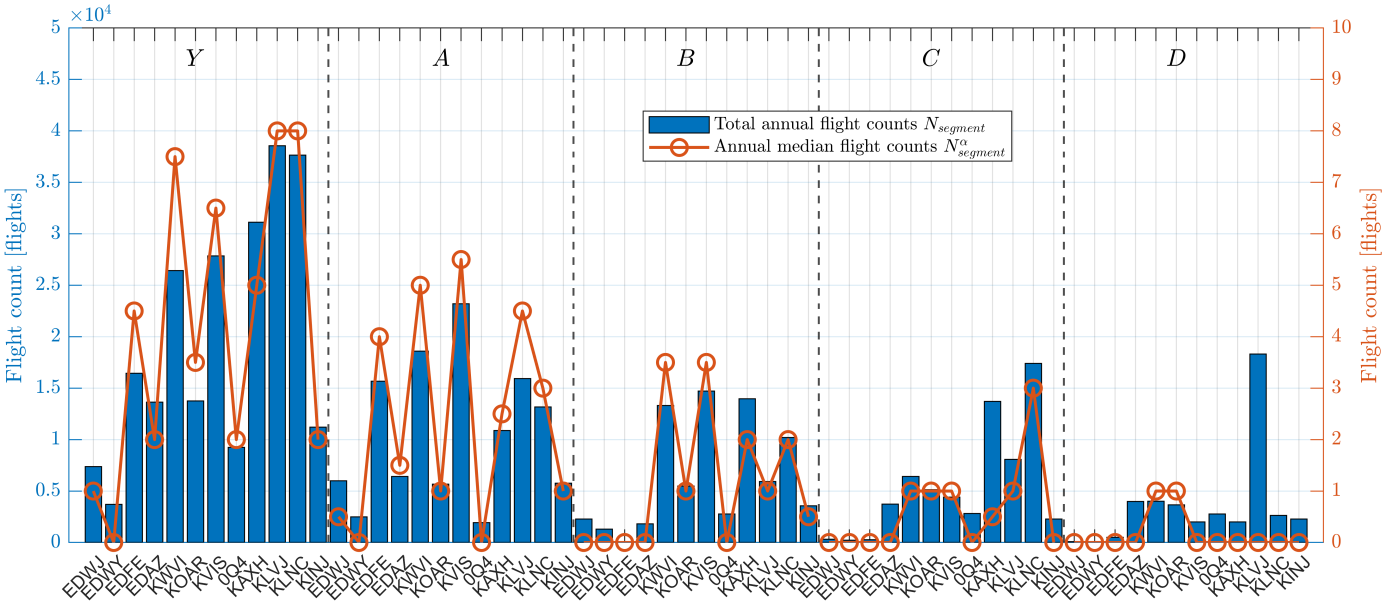

Figure A3. Visualization of total annual flight counts and annual average flight counts in different altitude bands in and above the TP airspace.

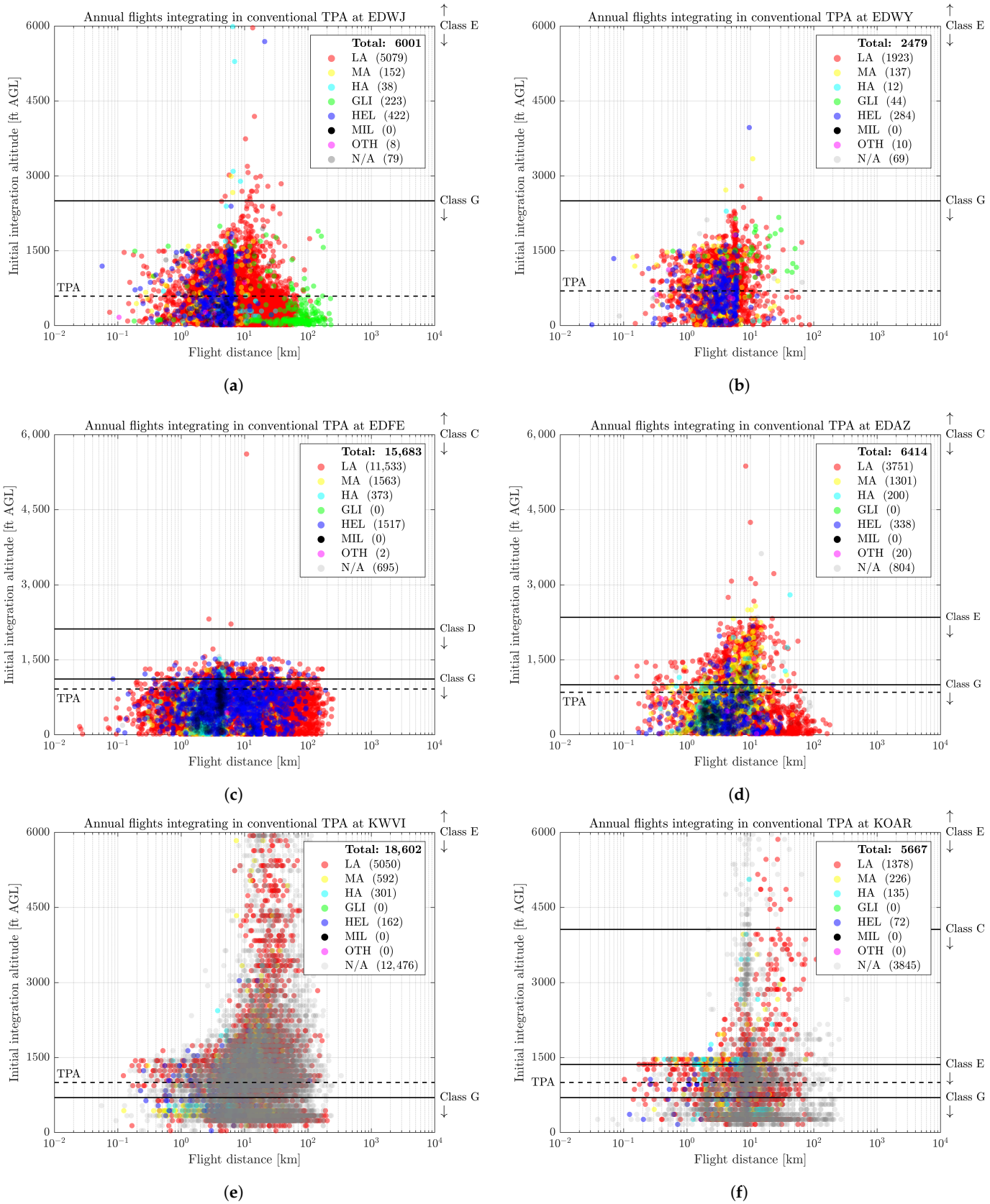

Figure A4. Scatter plots for airports of interest for annual flights in the TP airspace and above up to 6000 ft (∼1830 m) AGL integrating into conventional TPA (i.e., below 1500 ft (∼460 m) AGL). Each data point indicates the initial airspace integration altitude (*y*-axis), the operated flight distance (*x*-axis), and the aircraft type (color): (**a**) Juist (EDWJ). (**b**) Norderney (EDWY). (**c**) Egelsbach (EDFE). (**d**) Schoenhagen (EDAZ). (**e**) Watsonville (KWVI). (**f**) Marina (KOAR).

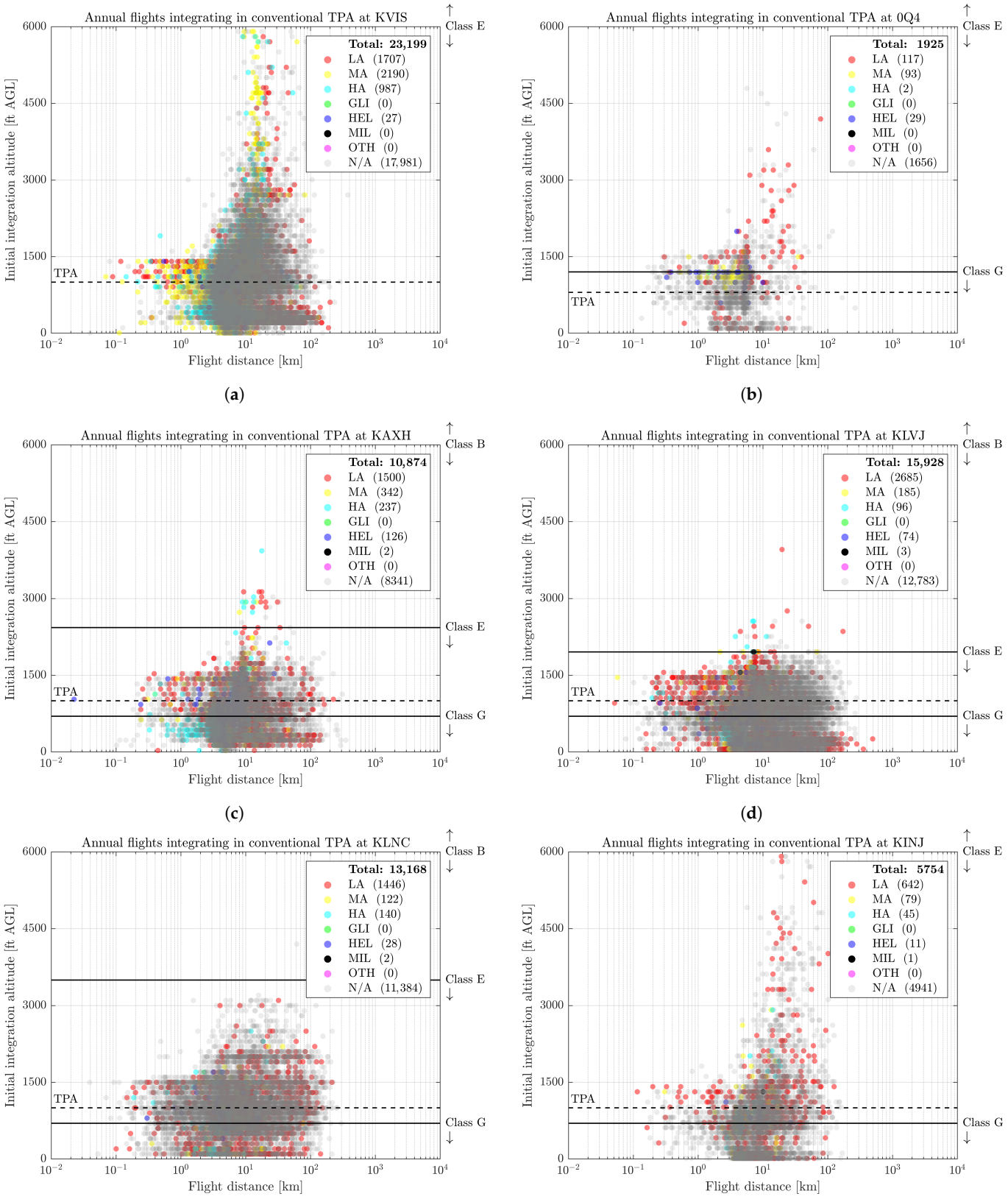

Figure A5. Scatter plots for airports of interest for annual flights in the TP airspace and above up to 6000 ft (∼1830 m) AGL integrating into conventional TPA (i.e., below 1500 ft (∼460 m) AGL). Each data point indicates the initial airspace integration altitude (*y*-axis), the operated flight distance (*x*-axis), and the aircraft type (color): (**a**) Visalia (KVIS). (**b**) Selma (0Q4). (**c**) Houston SW (KAXH). (**d**) Pearland (KLVJ). (**e**) Lancaster (KLNC). (**f**) Hillsboro (KINJ).

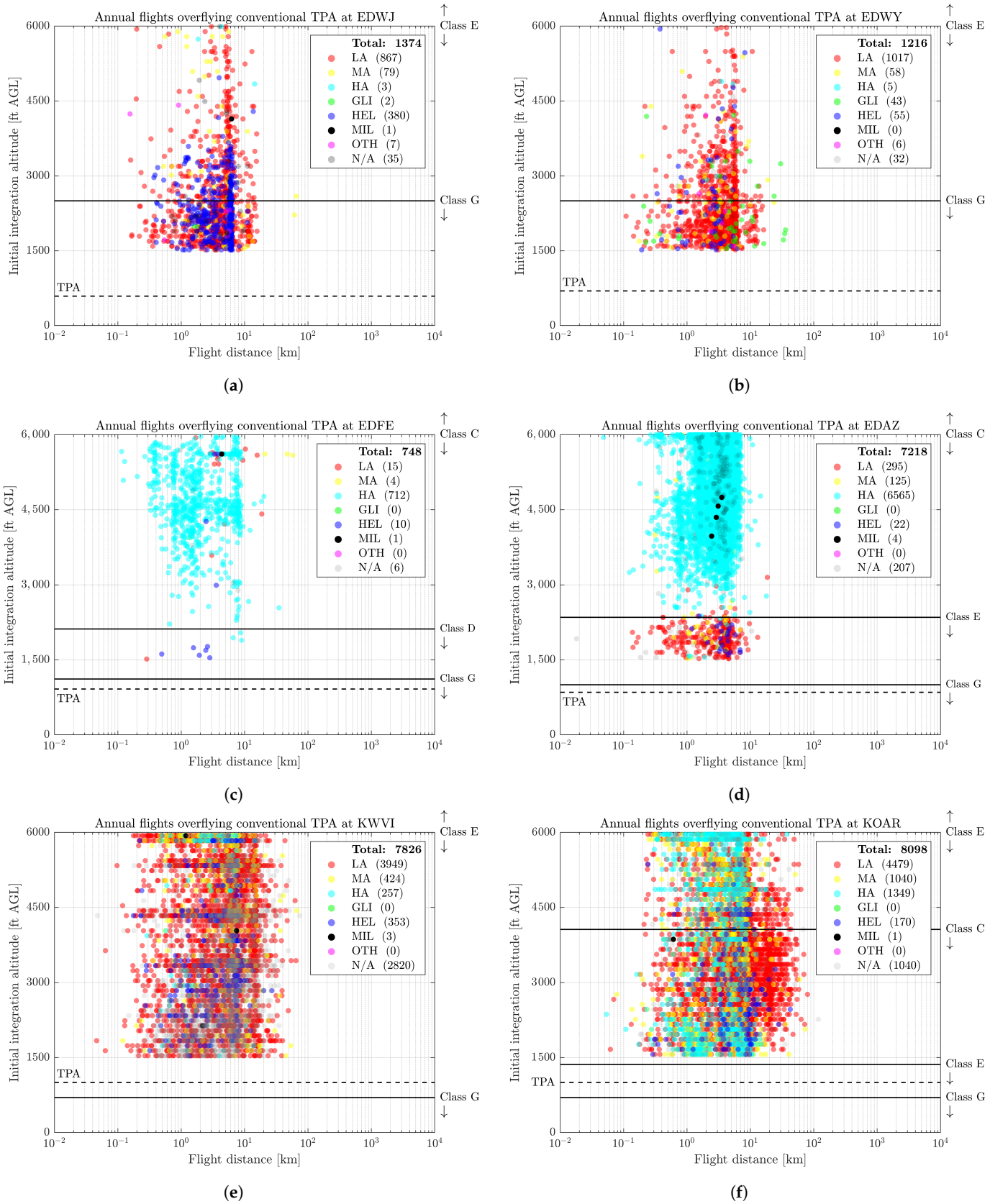

Figure A6. Scatter plots for airports of interest for annual flights in the TP airspace and above up to 6000 ft (∼1830 m) AGL overflying conventional TPA (i.e., above 1500 ft (∼460 m) AGL). Each data point indicates the initial airspace integration altitude (*y*-axis), the operated flight distance (*x*-axis), and the aircraft type (color): (**a**) Juist (EDWJ). (**b**) Norderney (EDWY). (**c**) Egelsbach (EDFE). (**d**) Schoenhagen (EDAZ). (**e**) Watsonville (KWVI). (**f**) Marina (KOAR).

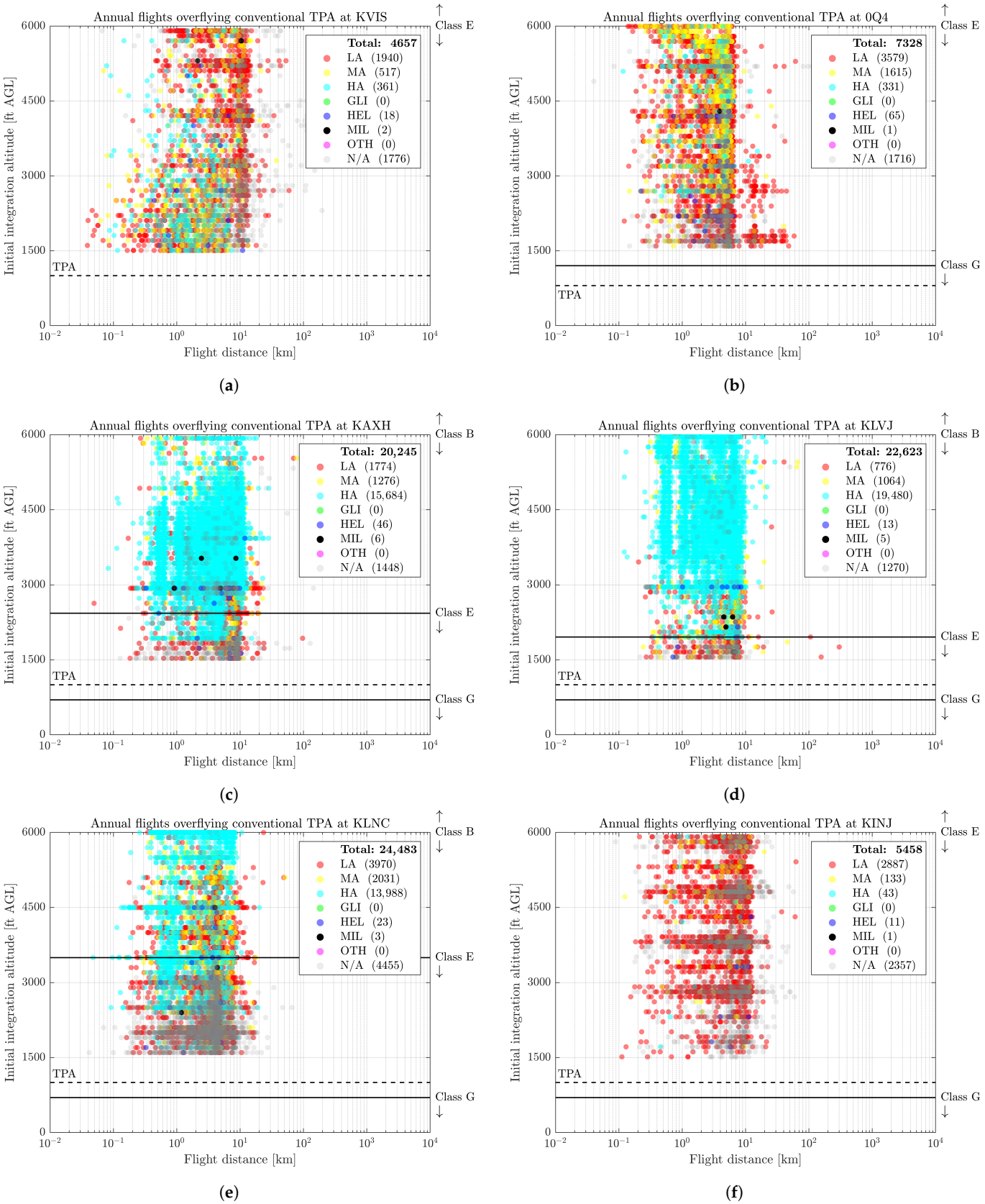

Figure A7. Scatter plots for airports of interest for annual flights in the TP airspace and above up to 6000 ft (∼1830 m) AGL overflying conventional TPA (i.e., above 1500 ft (∼460 m) AGL). Each data point indicates the initial airspace integration altitude (*y*-axis), the operated flight distance (*x*-axis), and the aircraft type (color): (**a**) Visalia (KVIS). (**b**) Selma (0Q4). (**c**) Houston SW (KAXH). (**d**) Pearland (KLVJ). (**e**) Lancaster (KLNC). (**f**) Hillsboro (KINJ).

Note that the sum of annual flights integrating in conventional TPA and annual flights overflying conventional TPA should add up to the value of total annual flights in and above TP airspace, which are visualized in Figures 20 and 21. For the German airports, however, a small number of flights are not counted in Figures A4–A7 (maximum ten flights) and therefore do not add up to the exact value of the total annual flights.

References

1. Andrews, J.; Lara, M.; Yon, R.; Del Rosario, R.; Block, J.; Davis, T.; Hasan, S.; Weingart, D.; Frankel, C.; Spitz, B.; et al. *LMI Automated Air Cargo Operations Market Research and Forecast*; NASA Contractor Report-20210015228; NASA Ames Research Center: Moffett Field, CA, USA, 2021.
2. Sievers, T.F.; Sakakeeny, J.; Dimitrova, N.; Idris, H. Operational integration potential of regional uncrewed aircraft systems into the airspace system. *CEAS Aeronaut. J.* **2025**, *16*, 1037–1059. [CrossRef]
3. Walsh, R. *Regional Air Mobility: Infrastructure Challenges, Passenger and Cargo Market Potential, and Sustainability Strategies for Underserved Airports*; NASA Technical Reports Server (NTRS) Document ID 20250002542; NASA Langley Research Center: Hampton, VA, USA, 2025.
4. Hayashi, M.; Idris, H.; Sakakeeny, J.; Jack, D. *PAAV Concept Document*; White Paper; NASA Ames Research Center: Moffett Field, CA, USA, 2022.
5. Antcliff, K.; Borer, N.; Sartorius, S.; Saleh, P.; Rose, R.; Gariel, M.; Oldham, J.; Courtin, C.; Bradley, M.; Roy, S.; et al. *Regional Air Mobility: Leveraging Our National Investments to Energize the American Travel Experience*; White Paper; NASA Langley Research Center: Hampton, VA, USA, 2021.
6. EUROCONTROL. Trends in Air Traffic—Volume 3. A Place to Stand: Airports in the European Air Network. Available online: https://www.eurocontrol.int/sites/default/files/publication/files/tat3-airports-in-european-air-network.pdf (accessed on 15 November 2024).
7. Bulusu, V.; Idris, H.; Chatterji, G. Analysis of VFR traffic uncertainty and its impact on uncrewed aircraft operational capacity at regional airports. In Proceedings of the AIAA Aviation 2023 Forum, San Diego, CA, USA, 12–16 June 2023; p. 3553. [CrossRef]
8. McMinn, J.D.; Patterson, A.; Gregory, I. Traffic Prediction for Uncommunicative Aircraft in Terminal Airspace: Development Framework and Performance Evaluations. In Proceedings of the 2025 AIAA SCITECH Forum, Orlando, FL, USA, 6–10 January 2025. [CrossRef]
9. Sievers, T.F.; Peinecke, N. Navigating the Uncertain: Integrating Uncrewed Aircraft Systems at Airports in Uncontrolled Airspace. In Proceedings of the 2024 Integrated Communications, Navigation and Surveillance Conference (ICNS), Herndon, VA, USA, 23–25 April 2024. [CrossRef]
10. Sievers, T.F.; Sakakeeny, J.; Idris, H.; Peinecke, N.; Bulusu, V.; Nagel, E.; Jack, D. A Concept for Procedural Terminal Area Airspace Integration of Large Uncrewed Aircraft Systems at Non-Towered Airports. In Proceedings of the First US-Europe Air Transportation Research & Development Symposium (ATRDS2025), Prague, Czech Republic, 24–27 June 2025. [CrossRef]
11. European Union Aviation Safety Agency (EASA). Certified Category—Civil Drones. Available online: https://www.easa.europa.eu/en/domains/drones-air-mobility/operating-drone/certified-category-civil-drones (accessed on 3 March 2025).
12. Federal Aviation Administration (FAA). Pilot/Controller Glossary. Available online: https://www.faa.gov/air_traffic/publications/atpubs/pcg_html/ (accessed on 27 March 2025).
13. US Government. 14 Code of Federal Regulations (CFR) Part 91.113. Available online: https://www.ecfr.gov/current/title-14/chapter-I/subchapter-F/part-91/subpart-B/subject-group-ECFRe4c59b5f5506932/section-91.113 (accessed on 5 January 2025).
14. DFS Deutsche Flugsicherung. Luftfahrthandbuch Deutschland. Available online: https://aip.dfs.de/basicAIP/ (accessed on 24 February 2025).
15. Federal Aviation Administration (FAA). Airplane Flying Handbook: FAA-H-8083-3C (2024). Available online: https://www.faa.gov/regulations_policies/handbooks_manuals/aviation/airplane_handbook (accessed on 24 March 2025).
16. Federal Aviation Administration (FAA). Aeronautical Information Manual (AIM). Official Guide to Basic Flight Information and ATC Procedures. Available online: https://www.faa.gov/air_traffic/publications/media/AIM-Basic-w-Chg1-and-Chg2-dtd-3-21-24.pdf (accessed on 27 March 2025).
17. DFS Deutsche Flugsicherung. Sichtflugkarte/Visual Operating Chart Juist EDWJ. Available online: https://aip.dfs.de/BasicVFR/ (accessed on 30 July 2025).
18. Holmes, B.J.; Durham, M.H.; Tarry, S.E. Small aircraft transportation system concept and technologies. *J. Aircr.* **2004**, *41*, 26–35. [CrossRef]
19. Viken, S.A.; Brooks, F.M.; Johnson, S.C. Overview of the small aircraft transportation system project four enabling operating capabilities. *J. Aircr.* **2006**, *43*, 1602–1612. [CrossRef]

20. Munoz, C.A. Hybrid verification of an air traffic operational concept. In Proceedings of the IEEE/NASA Workshop on Leveraging Applications of Formal Methods, Verification, and Validation, Columbia, MD, USA, 23–24 September 2005.
21. Consiglio, M.; Williams, D.; Murdoch, J.; Adams, C. SATS HVO concept validation experiment. In Proceedings of the AIAA 5th ATIO and 16th Lighter-Than-Air Systems Technology and Balloon Systems Conferences, Arlington, VA, USA, 26–28 September 2005; p. 7314. [CrossRef]
22. National Research Council (NRC) and Transportation Research Board and Committee. Future Flight: A Review of the Small Aircraft Transportation System Concept. Available online: https://onlinepubs.trb.org/onlinepubs/sr/sr263.pdf (accessed on 3 September 2024).
23. Geister, D.; Geister, R. Integrating unmanned aircraft efficiently into hub airport approach procedures. *J. Navig.* **2013**, *60*, 235–247. [CrossRef]
24. Pastor, E.; Prats, X.; Royo, P.; Delgado, L.; Santamaria, E. UAS pilot support for departure, approach and airfield operations. In Proceedings of the 2010 IEEE Aerospace Conference, Big Sky, MT, USA, 6–13 March 2010. [CrossRef]
25. Mahboubi, Z.; Kochenderfer, M.J. Autonomous Air Traffic Control for Non-Towered Airports. In Proceedings of the 11th USA/Europe Air Traffic Management Research and Development Seminar (ATM2015), Lisbon, Portugal, 23–26 June 2015.
26. Schwoch, G.; Geister, R.; Geister, D.; Sangermano, V.; Löhr, F.; Fas-Millán, M.; Gómez, M.; Sunil, E.; Reuber, E.; Rocchio, R.; et al. *INVIRCAT Final ConOps 'RPAS in the TMA'*; Final Report; SESAR Joint Undertaking: Brussels, Belgium, 2022.
27. Schwoch, G.; Duca, G.; Ferraiuolo, V.; Filippone, E.; Lanzi, P.; Petersen, C.; Rocchio, R.; Sangermano, V.; Teutsch, J. Preliminary validation results of a novel concept of operations for RPAS integration in TMA and at airports. *J. Phys. Conf. Ser.* **2023**, *2526*. [CrossRef]
28. Pastor, E.; Royo, P.; Delgado, L.; Perez, M.; Barrado, C.; Prats, X. Depart and approach procedures for UAS in a VFR environment. In Proceedings of the 1st International Conference on Applications and Theory of Automation in Command and Control Systems (ATACCS), Barcelona, Spain, 26–27 May 2011; pp. 27–37.
29. Federal Aviation Administration (FAA). Non-Towered Airport Flight Operations. 2023. Available online: https://www.faa.gov/documentlibrary/media/advisory_circular/ac_90-66c.pdf (accessed on 27 March 2025).
30. Garmin. Autonomi. Available online: https://discover.garmin.com/en-US/autonomi/#esp (accessed on 12 February 2025).
31. AIN. FAA Accepts Technical Requirements for Reliable Robotics' Navigation and Autopilot Systems. Available online: https://reliable.co/news (accessed on 13 December 2024).
32. Rorie, R.C.; Smith, C.L. Detect and Avoid and Collision Avoidance Flight Test Results with ACAS Xr. In Proceedings of the 43rd Digital Avionics Systems Conference (DASC), San Diego, CA, USA, 29–3 October 2024. [CrossRef]
33. RTCA, Inc. *DO-365B—Minimum Operational Performance Standards (MOPS) for Detect and Avoid (DAA) Systems, Minimum Performance Standards for Unmanned Aircraft System*; RTCA, Inc.: Washington, DC, USA, 2021.
34. European Union. *Commission Implementing Regulation (EU) 2021/664 of 22 April 2021 on a Regulatory Framework for the U-Space*; Implementing Regulation; European Union: Brussels, Belgium, 2021.
35. European Union Aviation Safety Agency (EASA). *AMC1 SERA.6005(c) Requirements for Communications, SSR Transponder and Electronic Conspicuity in U-Space Airspace*; EASA: Cologne, Germany, 2023.
36. German Aerospace Center (DLR). AREA U-Space (Air Space Research Area U-Space). Available online: https://www.dlr.de/en/uc/research-and-transfer/projects-and-missions/area-u-space (accessed on 9 January 2025).
37. RTCA, Inc. *DO-400 Guidance Material: Standardized Lost C2 Link Procedures for Uncrewed Aircraft Systems*; RTCA, Inc.: Washington, DC, USA, 2023.
38. Sievers, T.F.; Geister, D.; Schwoch, G.; Peinecke, N.; Schuchardt, B.I.; Volkert, A.; Lieb, J. *DLR Blueprint–Initial ConOps of U-Space Flight Rules (UFR). 2024*; Blueprint; DLR Institute of Flight Guidance: Braunschweig, Germany, 2024. [CrossRef]
39. Wing, D.; Lacher, A.; Ryan, W.; Cotton, W.; Stilwell, R.; John, M.; Vajda, P. *Digital Flight: A New Cooperative Operating Mode to Complement VFR and IFR*; Technical Memorandum (TM); NASA Langley Research Center: Hampton, VA, USA, 2022.
40. Clothier, R.A.; Williams, B.P.; Fulton, N.L. Structuring the safety Case for unmanned aircraft system operations in non-segregated airspace. *Saf. Sci.* **2015**, *79*, 213–228. [CrossRef]
41. ICAO. *ICAO Doc 8186: Aircraft Operations—Volume II Construction of Visual & Instrument Flight Procedures*, 16th ed.; ICAO: Montréal, QC, Canada, 2020.
42. Irvine, D.; Budd, L.; Ison, S.; Kitching, G. The environmental effects of peak hour air traffic congestion: The case of London Heathrow Airport. In Proceedings of the Research in Transportation Economics, Warsaw, Poland, 18–21 April 2016; Volume 55, pp. 67–73. [CrossRef]
43. EUROCONTROL. *Eurocontrol Manual for Airspace Planning*; Eurocontrol: Brussels, Belgium, 2003; Volume 2.
44. EUROCONTROL. *European Route Network Improvement Plan—Part 1: European Airspace Design Methodology-Guidelines*; Eurocontrol: Brussels, Belgium, 2019.
45. SESAR Joint Undertaking. *U-space ConOps and Architecture (Edition 4)*; SESAR Joint Undertaking: Brussels, Belgium, 2023.

46. International Civil Aviation Organization. *Annex 2 to the Convention on International Civil Aviation: Rules of the Air*, 10th ed.; ICAO: Montréal, QC, Canada, 2005.
47. Federal Aviation Administration (FAA). 13-01-262: Airport Facility Directory (AFD) Depiction of Traffic Pattern Altitudes. Available online: https://www.faa.gov/air_traffic/flight_info/aeronav/acf/media/Presentations/16-02-RD262_TPAs_Proposed_AIM_guidance_Boll.pdf (accessed on 14 June 2025).
48. Merlin Labs. Merlin-Home. Available online: https://merlinlabs.com/ (accessed on 21 January 2025).
49. Reliable Robotics Corporation. Reliable Robotics-Company. Available online: https://reliable.co/company (accessed on 21 January 2025).
50. Flightradar24. Flightradar24: Live Flight Tracker—Real-Time Flight Tracker Map. Available online: https://www.flightradar24.com/ (accessed on 21 June 2023).
51. NASA. Sherlock Data Warehouse. Available online: https://www.nasa.gov/ames/aviationsystems/sherlock-data-warehouse/ (accessed on 13 August 2024).
52. European Union Aviation Safety Agency (EASA). Horváth Second Workshop: Interoperability of E-Conspicuity Systems for GA. Available online: https://www.easa.europa.eu/en/downloads/139413/en (accessed on 24 May 2025).
53. Dahle, O.H.; Rydberg, J.; Dullweber, M.; Peinecke, N.; Bechina, A.A.A. A proposal for a common metric for drone traffic density. In Proceedings of the 2022 International Conference on Unmanned Aircraft Systems (ICUAS), Dubrovnik, Croatia, 21–24 June 2022. [CrossRef]
54. Federal Aviation Administration (FAA). *Federal Aviation Administration. United States Government Flight Information Publication. Chart Supplement Southwest U.S. 12 JUN 2025*; FAA: Washington, DC, USA, 2025.
55. National Archives and Records Administration (NARA). § 91.159 VFR Cruising Altitude or Flight Level. Available online: https://www.ecfr.gov/current/title-14/chapter-I/subchapter-F/part-91/subpart-B/subject-group-ECFR4d5279ba676bedc/section-91.159 (accessed on 2 September 2025).